GEORGIA DOT RESEARCH PROJECT 18-23

Final Report

DEVELOPMENT OF TOOLS TO MODEL DRIVER BEHAVIOR IN A COOPERATIVE AND DRIVERLESS VEHICLE MIXED ROADWAY ENVIRONMENT

Office of Performance-based Management and Research
600 West Peachtree Street NW | Atlanta, GA 30308

January 2022

TECHNICAL REPORT DOCUMENTATION PAGE

1. Report No.: FHWA-GA-22-18-23	2. Government Accession No.: N/A	3. Recipient's Catalog No.: N/A
4. Title and Subtitle: Development of Tools to Model Driver Behavior in a Cooperative and Driverless Vehicle Mixed Roadway Environment		5. Report Date: January 2022
		6. Performing Organization Code: N/A
7. Author(s): Michael Hunter (PI), Ph.D. (https://orcid.org/ 0000-0002-0307-9127); Angshuman Guin (coPI), Ph.D. (https://orcid.org/ 0000-0001-6949-5126); Abhilasha Saroj, Ph.D.; Jong In Bae		8. Performing Organization Report No.: 18-23
9. Performing Organization Name and Address: Georgia Tech Research Corp. 505 Tenth St. Atlanta, GA 30318		10. Work Unit No.: N/A
		11. Contract or Grant No.: PI#0015718
12. Sponsoring Agency Name and Address: Georgia Department of Transportation Office of Performance-based Management and Research 600 West Peachtree St. NW Atlanta, GA 30308		13. Type of Report and Period Covered: Final; March 2019 – January 2022
		14. Sponsoring Agency Code: N/A
15. Supplementary Notes: Prepared in cooperation with the U.S. Department of Transportation, Federal Highway Administration.		
16. Abstract: Promising advances in autonomous vehicle (AV) technology have fueled industry and research fields to dedicate significant efforts to the study of the integration of AVs into the traffic network. While most studies anticipate a beneficial role of AVs, contributing to improved traffic efficiency and roadway safety, the underlying assumptions on the interactions between AVs and human-driven vehicles (HDVs) are often cooperative in nature. The first portion of this study investigates the impact of aggressive human-driven vehicles' (AHDVs) merging behaviors on traffic performance in a mixed environment that includes three vehicle types: AVs, HDVs, and AHDVs. This study is undertaken in an open-source microscopic traffic simulation model, Simulation of Urban Mobility (SUMO). AHDVs have been modeled in this study to show aggressive merging behaviors at a merge section of a freeway exit ramp by targeting the farthest reachable AV for lane change as well as forcing a merge immediately in front of the AV. Results show that the travel-time gains achieved by AHDVs were at the expense of AVs and HDVs, and the interaction of aggressive HDVs with cooperative AVs could negatively impact overall capacity. The second portion of this study developed an Excel-based tool exploring the impact of AVs on departure capacity from a signalized intersection. Through both portions of this study, it was seen that critical indicators of the impact of AVs on traffic performance are: (1) Is a rise in aggressive interactions witnessed? (2) What are the headways being adopted by AVs? And (3) What are the spacing and maximum-length platooning characteristics?		
17. Keywords: Autonomous Vehicles, Mixed Traffic Simulation, Aggressive Behavior, Queue-Jump	18. Distribution Statement: No Restriction	

19. Security Classification (of this report): Unclassified	20. Security Classification (of this page): Unclassified	21. No. of Pages: 167	22. Price: Free

Form DOT 1700.7 (8-72) Reproduction of completed page authorized

GDOT Research Project 18-23

Final Report

DEVELOPMENT OF TOOLS TO MODEL DRIVER BEHAVIOR IN A COOPERATIVE AND DRIVERLESS VEHICLE MIXED ROADWAY ENVIRONMENT

By
Michael Hunter, Ph.D.
Principal Investigator

Angshuman Guin, Ph.D.
co-Principal Investigator

Abhilasha Saroj, Ph.D.
Researcher

Jong In Bae
Graduate Research Assistant

Georgia Tech Research Corporation

Contract with
Georgia Department of Transportation

In cooperation with
U.S. Department of Transportation
Federal Highway Administration

January 2022

SI* (MODERN METRIC) CONVERSION FACTORS

APPROXIMATE CONVERSIONS TO SI UNITS

Symbol	When You Know	Multiply By	To Find	Symbol
		LENGTH		
in	inches	25.4	millimeters	mm
ft	feet	0.305	meters	m
yd	yards	0.914	meters	m
mi	miles	1.61	kilometers	km
		AREA		
in^2	square inches	645.2	square millimeters	mm^2
ft^2	square feet	0.093	square meters	m^2
yd^2	square yard	0.836	square meters	m^2
ac	acres	0.405	hectares	ha
mi^2	square miles	2.59	square kilometers	km^2
		VOLUME		
fl oz	fluid ounces	29.57	milliliters	mL
gal	gallons	3.785	liters	L
ft^3	cubic feet	0.028	cubic meters	m^3
yd^3	cubic yards	0.765	cubic meters	m^3
		NOTE: volumes greater than 1000 L shall be shown in m^3		
		MASS		
oz	ounces	28.35	grams	g
lb	pounds	0.454	kilograms	kg
T	short tons (2000 lb)	0.907	megagrams (or "metric ton")	Mg (or "t")
		TEMPERATURE (exact degrees)		
^oF	Fahrenheit	5 (F-32)/9 or (F-32)/1.8	Celsius	^oC
		ILLUMINATION		
fc	foot-candles	10.76	lux	lx
fl	foot-Lamberts	3.426	candela/m^2	cd/m^2
		FORCE and PRESSURE or STRESS		
lbf	poundforce	4.45	newtons	N
lbf/in^2	poundforce per square inch	6.89	kilopascals	kPa

APPROXIMATE CONVERSIONS FROM SI UNITS

Symbol	When You Know	Multiply By	To Find	Symbol
		LENGTH		
mm	millimeters	0.039	inches	in
m	meters	3.28	feet	ft
m	meters	1.09	yards	yd
km	kilometers	0.621	miles	mi
		AREA		
mm^2	square millimeters	0.0016	square inches	in^2
m^2	square meters	10.764	square feet	ft^2
m^2	square meters	1.195	square yards	yd^2
ha	hectares	2.47	acres	ac
km^2	square kilometers	0.386	square miles	mi^2
		VOLUME		
mL	milliliters	0.034	fluid ounces	fl oz
L	liters	0.264	gallons	gal
m^3	cubic meters	35.314	cubic feet	ft^3
m^3	cubic meters	1.307	cubic yards	yd^3
		MASS		
g	grams	0.035	ounces	oz
kg	kilograms	2.202	pounds	lb
Mg (or "t")	megagrams (or "metric ton")	1.103	short tons (2000 lb)	T
		TEMPERATURE (exact degrees)		
^oC	Celsius	1.8C+32	Fahrenheit	^oF
		ILLUMINATION		
lx	lux	0.0929	foot-candles	fc
cd/m^2	candela/m^2	0.2919	foot-Lamberts	fl
		FORCE and PRESSURE or STRESS		
N	newtons	0.225	poundforce	lbf
kPa	kilopascals	0.145	poundforce per square inch	lbf/in^2

* SI is the symbol for the International System of Units. Appropriate rounding should be made to comply with Section 4 of ASTM E380. (Revised March 2003)

TABLE OF CONTENTS

LIST OF FIGURES

LIST OF TABLES

LIST OF ACRONYMS/ABBREVIATIONS

ACC	Adaptive Cruise Control
AHDV	Aggressive Human-Driven Vehicle
AV	Autonomous Vehicle
CACC	Cooperative Adaptive Cruise Control
CAV	Connected and Autonomous Vehicle
CV	Connected Vehicle
HCM	Highway Capacity Manual
HDV	Human-Driven Vehicle
IDM	Intelligent Driver Model
LMRS	Lane Change Model with Relaxation and Synchronization
LOS	Level of Service
PIB	Peachtree Industrial Boulevard
SCAT	Simplified Capacity Analysis Tool
SUMO	Simulation of Urban Mobility
TraCI	Traffic Control Interface
TSD	Time–Space Diagram
TwB	Travel while Braking
VAD	Vehicle Awareness Device

EXECUTIVE SUMMARY

OVERVIEW

Many studies that support an optimistic outlook on the traffic flow impacts of autonomous vehicles (AVs) limit modeled driving behavior modifications to the cooperative actions of the AVs. However, these studies have not considered the impacts on traffic performance of potential aggressive interactions of human-driven vehicles (HDVs) with AVs in a mixed environment (AVs and HDVs). Considering that AVs will not retaliate when they are the target of an aggressive action, it is not hard to postulate that some human drivers may display aggressive behaviors toward AVs, taking advantage of the AVs' collision-avoidance features. Given these potential behaviors, the objective of this effort is to develop and test models of AV interaction with aggressive human drivers.

To aid in understanding the potential impact of aggressive HDV (AHDV) interactions with AVs, this effort has investigated a merging situation at an off-ramp. Three classes of vehicles are simulated: AVs, HDVs, and AHDVs. AHDVs represent human-driven vehicles with aggressive merging-behavior characteristics. To perform this study, AHDV behavior at a merge section of a freeway exit ramp, in a mixed-traffic environment, is simulated using the open-source traffic simulation package SUMO (Simulation of Urban Mobility). Two types of potential AHDV merging behavior when interacting with an AV are modeled: (1) aggressive merge with maximum advancement, and (2) aggressive merge with zipper. The aggressive merge with maximum advancement represents the highest level of aggressive behavior. The AHDVs with this behavior target the farthest

reachable AV on the deceleration lane to act as the following vehicle in the receiving lane, i.e., the AHDV will lane change in front of the AV, essentially without regard for the available gap. In the second type, the aggressive merge with zipper, the AHDVs continue to target downstream AVs in the exit lane, but avoid the scenario where the same AV is targeted by multiple AHDVs.

The impacts of the AHDVs' aggressive behaviors in a mixed-traffic environment (i.e., AVs, HDVs, and AHDVs) on different network traffic characteristics, such as travel time and capacity, is demonstrated. Four experiments are conducted to explore the impact of the AHDV behavior on traffic operations. The first experiment observes the change in speed of the target AV, as well as the following traffic, when a platoon of 10 AHDVs merges in front of the AV near a freeway exit. The second and third experiments observe the travel times of exiting AHDVs and other vehicles when AHDVs are randomly distributed throughout the traffic stream with varying percentages of AVs and AHDVs in the traffic composition. The fourth experiment considers the impact on capacity in a similar merging situation where vehicle behavior is set as cooperative or noncooperative utilizing SUMO driver-behavior parameters.

Experiments 1 through 3 showed that the presence of human drivers' aggressive merging behaviors had adverse effects on AVs and HDVs. The adverse effects were more significant in high congestion, when there is a queue on the deceleration lane. The impacts of AHDVs' aggressive merges were muted by the larger headways between vehicles in low congestion when there is no queue on the deceleration lane. Based on the experiment 2 and experiment 3 results, AHDVs had a higher travel-time gain with higher level of aggressive behaviors, which in return had greater adverse effects on the AVs'

and the HDVs' travel times. Throughout the experiments, the system-wide travel time tended to be relatively stable, indicating that the AHDV travel-time improvements came at the expense of AVs' and other vehicles' travel times.

Experiment 4 took a closer look at the impact of cooperative behavior–induced aggressive merges on capacity. It was seen that when most vehicles are either fully cooperative or noncooperative, similar capacities are obtained; however, where a higher percentage of cooperative vehicles are positioned to be targeted by more aggressive vehicles, this aggressive-to-non-aggressive interaction can significantly reduce capacity. In addition, it was seen, similar to experiments 1 through 3, that AHDV gains were achieved at the expense of AVs. Finally, even in those scenarios where the overall capacity was not significantly changed in response to the variation in the percentage of cooperative vehicles in the traffic, increased fluctuations in the flow may potentially negatively impact operations as well as the safety conditions in the upstream traffic.

As a final component of this research, an Excel-based Simplified Capacity Analysis Tool (SCAT) is developed. This tool draws predicted saturation flow rates, at various connected and autonomous vehicle (CAV) market penetration rates, from the literature and a simulation experiment. These saturation flow rates are utilized to determine potential phase capacities at a signalized intersection. While the freeway SUMO experiments focused on the impact of lane changing, SCAT explores the impact of CAV car-following and platooning behaviors. It is seen that a wide variation in capacity predictions may be found throughout the literature, from slight reductions to significant increases in capacity as AV market penetration increases. Across the literature, when considering the car-following aspect of AV operations, it is clear that two key sets of

assumptions are driving the predictions: the first is the headways selected by the AVs in a mixed-traffic environment, and the second is the characteristics of AV platoons, i.e., platooned vehicle spacing and maximum platoon length.

The findings of this study suggest that despite the general belief in the benefits of autonomous vehicles, there may be adverse impacts on the non-aggressive vehicle travel times in the presence of human drivers' aggressive merging behaviors in a mixed-traffic environment, especially in congested conditions. Thus, when the potential benefits of the AV are most needed, i.e., at or near capacity, it is possible that human interaction may negate many of the potential savings.

Report Organization

Chapter 2 presents efforts found in the literature on AV modeling, such as assumptions made, frequently adjusted parameters, and common characteristics of AVs. Chapter 3 presents a comparison between the PTV VISSIM and SUMO simulation modeling platforms and discusses the selection of SUMO for the merge modeling efforts. Chapter 4 presents how the two aggressive merging models were developed, as well as the four different experiments that investigate the impacts of the aggressive merging models in a mixed traffic environment. Chapter 5 highlights the data collection conducted for the headway utilized to calibrate the model in chapter 6. Finally, chapter 6 presents the Simplified Capacity Analysis Tool.

Recommendations

As seen in the report, the high state of uncertainty in AV driving-behavior characteristics and a similar level of uncertainty in the behavior of human-driven vehicles when

interacting with AVs, makes it extremely difficult to incorporate AVs into current planning and design processes with any sense of assuredness. However, based on this project, Georgia Department of Transportation (GDOT) can likely achieve an early sense of the ultimate operational impacts of AVs by tracking three primary leading indicators:

1. As AV tests continue, or low market penetration occurs, is a rise in aggressive interactions witnessed?
2. What are the headways being adopted by AV manufacturers, and what are the potential regulatory requirements?
3. Are platoons implemented in AVs, and, if so, what are the spacing requirements and maximum length restrictions, which are again potentially manufacturer and/or regulatory-agency driven?

As the direction of each of these indicators becomes clearer, GDOT will be able to select the more likely futures from the many potential predicted futures, with a higher level of confidence. This would allow AV penetration to begin to influence policy decisions and design decisions, such as queue management at ramp junctions, HV/AVs lane-usage restrictions, optimizing signalized intersections to process AV platoons, etc., in a more informed manner.

CHAPTER 1. INTRODUCTION

Many studies that support an optimistic outlook on the traffic-flow impacts of autonomous vehicles (AVs) limit modeled driving behavior modifications to the cooperative actions of the AVs, such as slowing down for merging vehicles. Similarly, lane changes to advance the AV position in the traffic stream relative to other vehicles receive low priority (Aria et al. 2016, Rahman and Abdel-Aty 2018, Stanek et al. 2017).

However, these and similar studies have not considered the impacts on traffic performance of potential aggressive interactions of human-driven vehicles (HDVs) with AVs in a mixed environment (i.e., AVs and HDVs), although such behaviors are likely to occur. For instance, mobility service companies have observed aggressive human driver behaviors directed at their AV test fleets, such as abrupt merging, tailgating, and hostile verbal and hand gestures (Randazzo 2018, Hamilton 2019). Even without AVs in the fleet, aggressive behavior has been observed at merge locations with heavy queuing. For example, within the last few hundred feet of a merge section an aggressive driver may take advantage of the slower acceleration and larger headways of heavy vehicles (Toth 2014). By extension, considering that AVs will not retaliate when they are the target of an aggressive action, it is not hard to postulate that some human drivers may display aggressive behaviors toward AVs, taking advantage of the AVs' collision-avoidance features. Even drivers that do not typically display such behavior may be more aggressive, or ignore common courtesies in vehicle interactions, when interacting with AVs. Given these potential behaviors, the objective of this effort is to develop and test models of aggressive merging behaviors, targeted toward AVs by a subset of human-driven vehicles, in a mixed environment.

To this end, the potential impact of merging behaviors on traffic performance is explored in a simulation environment. Three classes of vehicles are simulated: AVs, HDVs, and aggressive human-driven vehicles (AHDVs). AHDVs represent human-driven vehicles with aggressive merging-behavior characteristics. To perform this study, AHDV behavior at a merge section of a freeway exit ramp, in a mixed traffic environment, is simulated using the open-source traffic simulation package SUMO (Simulation of Urban Mobility) (Eclipse Foundation 2020). Two types of potential AHDV merging behavior when interacting with an AV are modeled: (1) aggressive merge with maximum advancement, and (2) aggressive merge with zipper. The aggressive merge with maximum advancement represents the highest level of aggressive behavior. The AHDVs with this behavior target the farthest reachable AV on the deceleration lane to act as the following vehicle in the receiving lane, i.e., the AHDV will lane change in front of the AV, essentially without regard for the available gap. In the second type, the aggressive merge with zipper, the AHDVs continue to target downstream AVs in the exit lane, but avoid the scenario where the same AV is targeted by multiple AHDVs. If an AV has already participated in a targeted merge with an AHDV, then the next AHDV will target the next AV upstream of that AV. Where an AV is not present, the AHDV will select and merge in front of an HDV in a non-aggressive manner, similar to HDVs.

Using simulation experiments, the impacts of the AHDVs' aggressive behaviors in a mixed-traffic environment (i.e., AVs, HDVs, and AHDVs) on different network traffic characteristics, such as travel time, is demonstrated. Three experiments are conducted to explore the impact of the AHDV behavior on traffic operations. The first experiment observes the change in speed of the target AV, as well as the following traffic, when a

platoon of 10 AHDVs merges in front of the AV near a freeway exit. The second and third experiments observe the travel times of exiting AHDVs and other vehicles when AHDVs are randomly distributed throughout the traffic stream with varying percentages of AVs and AHDVs in the traffic composition. The results of the three experiments show that the presence of AHDVs' aggressive behaviors lead to increased travel times, indicating higher levels of interruption in the traffic flow in a congested condition.

As a final component of this research, an Excel-based Simplified Capacity Analysis Tool (SCAT) is developed. This tool draws predicted saturation flow rates, at various connected and autonomous vehicle (CAV) market penetration rates, from the literature and a simulation experiment. These saturation flow rates are utilized to determine potential phase capacities at a signalized intersection. While the freeway SUMO experiment focused on the impact of lane changing, SCAT explores the impact of CAV car-following and platooning behaviors.

The remainder of this report is organized as follows. Chapter 2 provides background information on AV driving behaviors, the interaction between AV and human-driven vehicles, and modeling of aggressive AVs. Chapter 3 presents the process for the selection of the simulation modeling platform. Chapter 4 reviews the development of the selected simulation. Chapter 5 presents the results. Chapter 6 presents the Simplified Capacity Analysis Tool. Finally, chapter 7 summarizes the findings.

CHAPTER 2. BACKGROUND

UNCERTAINTY IN INTERACTIONS BETWEEN AUTONOMOUS VEHICLES AND HUMAN ROAD USERS

Over the past decade, the rapid advancement in autonomous driving technology in research and in industry has led several automobile manufacturers to develop and deploy various levels of autonomous vehicles. Numerous studies present optimistic roadway performance outlooks given the deployment of autonomous vehicles. However, there is a gap in the understanding of the impacts of the autonomous vehicles' interactions with human drivers, which is crucial for reliably modeling the impacts of AV implementation. This is particularly relevant in the transition phase where roadways are expected to consist of a mixed fleet of AVs and HDVs. Such a mixed fleet may result in significant changes to roadway safety, operational, environmental, and other performance metrics.

A significant source of the current uncertainty stems from the lack of standardization in autonomous vehicles' driving behaviors (National Highway Traffic Safety Administration [NHTSA] 2017, Zhao et al. 2019). However, human drivers' actions toward AVs are also a significant source of uncertainty. For instance, the trends in people's perception and behavior toward AVs are captured in several recent studies. Results of a survey conducted in 2016 indicated that the majority of the respondents would feel uncomfortable driving alongside an AV (Tennant et al. 2016). It has been suggested that given such concerns, AV and HDV interaction behaviors may contribute to traffic disturbances, particularly under low AV market penetration levels (Nishimura et al. 2019). An intersection field study by Rothenbucher et al. (2016) observed changes in pedestrian's and bicyclist's behavior in the presence of AVs. The pedestrians and

bicyclists acted in a conservative manner, which is hypothesized to be due to their uncertainty in potential AV behaviors. Further, in a few studies, field experts have shared concerns on the possibility of human drivers displaying aggressive behaviors toward AVs, taking advantages of AVs' conservative behaviors (Müller et al. 2016, Hedlund 2017). These concerns on human drivers' aggressive behaviors targeted to AVs have been observed on real-world roadways. News articles have reported that mobility service companies such as Uber and Waymo have been observing human drivers' behaviors such as aggressive merging, tailgating, and hostile verbal and hand gestures directed toward their autonomous vehicles (Randazzo 2018, Hamilton 2019).

PREVIOUS RESEARCH ON MODELING AUTONOMOUS VEHICLE BEHAVIORS

As stated previously, one of the key common challenges experienced in modeling AV behavior is the lack of standardization in driving behavior parameters (NHTSA 2017, General Motors 2015, National Academies of Sciences, Engineering, and Medicine 2017). While it is challenging to anticipate and model AV driving behaviors, the ability to utilize current human driving-behavior models with minimal modifications to model AV driving behaviors has been explored by numerous researchers (Stanek et al. 2017, Wagner 2016). Most studies model AV driving behaviors using traditional car-following models and lane-changing models with customized decision-making processes and modified parameter values that assign certain characteristics to the AVs. The following list provides the frequently assumed behavioral modifications from human driver-behavior models to AV/CAV models.

Frequently assumed behavioral modifications for AV/CAV vehicles include the following:

- Lower headways.
- Lower deviation or zero randomness in speed variation from speed limit.
- Lower reaction time.
- Slows down for merging vehicles (cooperative lane change).
- Higher acceleration rate.

Table 1 summarizes AV/CAV behavior assumptions and parameter adjustments for a sample of roadway application studies drawn from the literature. A more detailed discussion of several of these studies may be found in chapter 6.

Table 1. Summary of AV/CAV behavior assumptions and parameters employed.

Author(s), Year	AV/ CAV	Simulation Software	Scenario Roadway	Anticipated AV/CAV Behaviors	Adjusted Parameters (Parameter Name)
Freeway					
Aria et al., 2016	AV	VISSIM	Segment of an autobahn with weaving area, on-ramp, and off-ramp	• Lower headways • Fixed range in scanning surroundings • Lower speed deviation from the speed limit • Earlier decision point in lane change • Cooperative lane change	• Lower headway time (CC1) • Higher look ahead (and back) distance • Lower speed dependency of oscillation (CC6) • Advanced merging • Cooperative lane change
Stanek et al., 2017	AV	VISSIM 9	Two freeway segments in California	• Lower headways • Higher acceleration rate • Lower reaction time to green light • Cooperative lane change	• Lower standstill distance (CC0) • Lower headway time (CC1), • Higher threshold for entering following (CC3) • Lower negative and positive following threshold (CC4, CC5)
Mesionis et al., 2020	AV	AIMSUN	20-mile stretch of 3-lane freeway	• Earlier lane change for turns • Not accepting lower gap for merge • Less likely to overtake other vehicles • Lower reaction time • Lower headway	• Advanced merging • Disabled lower gap acceptance for merge • Lower probability in overtaking other vehicles • Lower reaction time • Lower standstill distance (CC0)
Richter et al., 2019	AV	SUMO	Freeway segment with an on- ramp and an acceleration lane	• Lower headway • Lower reaction time • No randomness in speed • Earlier lane change for merging • Slow down for merging vehicle	• Lower time headway (tau) • Smaller simulation length • Removed randomness in speed (SpeedFactor) • Zero driver imperfection (sigma) • Earlier merging decision point • Higher cooperation to merging vehicles
Yu et al., 2019	AV	AIMSUN	3-lane freeway segment with on-ramp and off-ramp	• Lower headways • Lower acceleration rate	• Lower time headways • Lower minimum gap • Lower acceleration rate
Seth et al., 2019	AV	VISSIM	Highway section with on-ramp and off-ramp	• Lower standstill distance • Lower headways • Lower reaction time • Smaller oscillation in speed • Smaller oscillation during acceleration • Cooperative to merging vehicles	• Lower standstill distance (CC0) • Lower headway time (CC1) • Lower negative and positive following threshold (CC4, CC5) • No speed dependency of oscillation (CC6) • Lower oscillation acceleration (CC7) • Lower lane changing minimum headway (LC4) • Cooperative lane change

Author(s), Year	AV/ CAV	Simulation Software	Scenario Roadway	Anticipated AV/CAV Behaviors	Adjusted Parameters (Parameter Name)
Liu, P. and Fan, W. 2020	CAV	VISSIM	4-lane freeway segment	• Higher acceleration rate • Lower car following distance • Lower desired headway	• Higher acceleration rate • Lower headway (even lower headway for between two CAVs) (CC0, CC1)
Papadoulis et al., 2019	CAV	VISSIM 7	3-lane freeway segment with two on-ramps and two off-ramps	• Lower time gaps • Higher distance in observing surrounding vehicles	• Lower headway time (CC1) • Lower minimum time gap in lane changing (MG1) • Higher look ahead (and back) distance
Li and Wagner, 2019	AV	SUMO	3-lane freeway with two on-ramps and an off-ramp	• Lower time-gap • Lower driver imperfection • Higher compliance rate to speed limits • Slows down for merging vehicles	• Lower time gap (tau) • Zero driver imperfection (sigma) • Lower deviation from speed limit (SpeedFactor) • Higher cooperative behavior (lcCooperative)
Tomás et al., 2019	AV	VISSIM 9	3-lane freeway segment for 9 km	• Lower headway • Higher acceleration rate • Lower variation in acceleration • Greater acceptable merging gap	• Lower standstill distance (CC0) • Lower headway time (CC1) • Lower threshold for entering following (CC3) • Lower negative and positive following thresholds (CC4/CC5) • Lower oscillation acceleration (CC7) • Higher standstill acceleration (CC8) • Higher acceleration at 80 km/hr (CC9) • Higher lane changing minimum headway (LC4) • Lower safety distance reduction factor (LC5)
Sukennik et al., 2018	AV	VISSIM 10	Urban roads and freeway	• Lower headway	• Lower standstill distance (CC0) • Lower headway time (CC1) • Lower following variation (CC2) • Lower threshold for entering following (CC3)
Martin-Gasulla et al., 2019	CAV	VISSIM 11	Straight single-lane freeway	• Higher speed stability and headway to leading vehicle • Lower headway when following CAVs • Higher headways when following conventional vehicles (compared to headways of human drivers)	• Lower headway when CAV following another CAV • Higher headway CAV following conventional vehicle (higher than conventional vehicles' headway)

Author(s), Year	AV/ CAV	Simulation Software	Scenario Roadway	Anticipated AV/CAV Behaviors	Adjusted Parameters (Parameter Name)
Roundabout					
Tiblijaš et al., 2018	AV	VISSIM 11	Single-lane roundabout with 3 or 4 approaches	• Lower headways • Lower reaction time • Lower speed instability • Higher acceleration rates	• Lower standstill distance (CC0), • Lower headway time (CC1), • Lower following variation (CC2) • Lower negative and positive following threshold (CC4, CC5) • Lower speed dependency of oscillation (CC6) • Lower oscillation acceleration (CC7) • Higher standstill acceleration (CC8) • Higher acceleration at 80 km/hr (CC9)
Morando et al., 2018	AV	VISSIM 9	Single-lane roundabout with 4 approaches	• Shorter gap • No randomness in speed • Higher acceleration rate • Higher capability in observing vehicles ahead	• Lower standstill distance (CC0) • Lower headway time (CC1) • Lower following variation (CC2) • Lower negative and positive following threshold (CC4, CC5) • Zero speed dependency of oscillation (CC6) • Higher acceleration rate • Higher look-ahead distance
Atkins, 2016	CAV	VISSIM 8	Roundabout	• Lower headway • Lower variation in acceleration rate • Lower safety distance • Higher acceleration rate	• Lower standstill distance (CC0) • Lower headway time (CC1) • Lower oscillation acceleration (CC7) • Lower safety distance, higher standstill acceleration (CC8) • Lower minimum time gap in lane changing (MG1) • Lower minimum headway in lane changing (MG2)
Anagnostopoulos and Kehagia, 2019	CAV	VISSIM 11	Double lane roundabout	• Lower headways • Zero speed oscillation • Lower acceleration rates • Higher look ahead distance • Slow down for merging vehicles	• Lower standstill distance (CC0) • Lower headway time (CC1) • Zero following variation (CC2) • Zero negative and positive following threshold (CC4, CC5) • Zero speed dependency of oscillation (CC6) • Higher acceleration rates (CC7, CC8, CC9) • Higher look ahead distance • Cooperative lane change
Single Lane Roadway					
Wang and Wang, 2017	AV	VISSIM 7	4 km single-lane roadway	• Lower reaction time, lower headways • No speeding	• Lower standstill distance (CC0) • Lower headway time (CC1) • Tighter bounds on speed distribution

Author(s), Year	AV/ CAV	Simulation Software	Scenario Roadway	Anticipated AV/CAV Behaviors	Adjusted Parameters (Parameter Name)
Lu et al., 2018	AV	SUMO	Single-lane roadway	• Lower headways • Higher acceleration rate • Zero driver imperfection	• Lower minimum gap when standing (minGap) • Lower time headway (tau) • Higher acceleration rate • Zero driver imperfection (sigma)
Atkins, 2016	CAV	VISSIM 8	Single-lane link	• Lower headway • Lower variation in acceleration rate • Lower safety distance	• Lower standstill distance (CC0) • Lower headway time (CC1) • Lower oscillation acceleration (CC7) • Lower safety distance reduction factor (LC5)
Multilane Roadway					
Lu et al., 2020	AV	SUMO	2-lane roadway in a grid network	• Lower headways • Higher acceleration rate	• Lower offset to the leading vehicle when standing (minGap) • Higher acceleration rate • Lower time headway (tau) • Zero driver imperfection (sigma)
Atkins, 2016	CAV	VISSIM 8	Multi-lane link	• Lower headway • Lower variation in acceleration rate • Lower safety distance • Greater acceptable merging gap	• Lower standstill distance (CC0) • Lower headway time (CC1) • Lower oscillation acceleration (CC7) • Lower lane changing min. headway (LC4) • Lower safety distance reduction factor (LC5)
Atkins, 2016	CAV	VISSIM 8	Multi-lane link with merge	• Lower headway • Lower variation in acceleration rate • Lower safety distance • Higher acceleration rate	• Lower standstill distance (CC0) • Lower headway time (CC1) • Lower oscillation acceleration (CC7) • Higher standstill acceleration (CC8) • Higher acceleration rate at 80 km/hr (CC9) • Lower minimum time gap in lane changing (MG1) • Lower minimum headway in lane changing (MG2)
Signalized Intersection					
Wang and Wang, 2017	AV	VISSIM 7	1 km single-lane signalized intersection	• Lower reaction time • Lower headways • No speeding	• Lower reaction time • Lower standstill distance (CC0) • Lower headway time (CC1) • Tighter bounds on speed distribution
Elvarsson, 2017	AV	VISSIM 9	Main arterial roadway with two signalized intersections	• Lower acceleration rate • Lower deceleration rate • Tighter bound on speed distribution • Lower headway	• Lower acceleration rate • Lower deceleration rate • Tighter bound on speed distribution • Lower standstill distance (CC0)

Author(s), Year	AV/ CAV	Simulation Software	Scenario Roadway	Anticipated AV/CAV Behaviors	Adjusted Parameters (Parameter Name)
Atkins, 2016	CAV	VISSIM 8	Signalized junction	• Lower headway • Lower variation in acceleration rate • Lower safety distance • Higher acceleration rate	• Lower standstill distance (CC0) • Lower headway time (CC1) • Lower oscillation acceleration (CC7) • Higher standstill acceleration (CC8)
Espinosa, 2015	AV	VISSIM 8	6-lane signalized intersection	• Increased range in distance and in number of surrounding vehicles to observe surrounding conditions • Lower headway • Slow down for merging vehicle • Earlier decision point for merge	• Higher look ahead (and back) distance • Lower headway time (CC1), • Cooperative lane change • Advanced merging
Morando et al., 2017	AV	VISSIM 9	3-lane signalized intersection	• Lower headways • Zero speed oscillation • Higher acceleration rate • Greater look ahead distance	• Lower standstill distance (CC0) • Lower headway time (CC1) • Lower following variation (CC2) • Lower negative and positive following threshold (CC4, CC5) • Zero speed dependency of oscillation (CC6) • Higher acceleration rates (CC8, CC9) • Higher look ahead distance

A common simulation platform utilized for modeling AVs is VISSIM. Table 2 summarizes the list of frequently and infrequently used modified VISSIM parameters.

Table 2. List of frequently and infrequently used VISSIM parameters.

Frequently Used VISSIM Parameters	Studies That Used Parameter
Standstill Distance (CC0)	Stanek et al. 2017, Mesionis et al. 2020, Seth et al. 2019, Liu and Fan 2020, Tomás et al. 2019, Sukennik et al. 2018, Tiblijaš et al. 2018, Morando et al. 2018, Atkins 2016, Anagnostopoulos and Kehagia 2019, Wang and Wang 2017, Elvarsson 2017, Morando et al. 2017
Headway Time (CC1)	Aria et al. 2016, Stanek et al. 2017, Seth et al. 2019, Liu and Fan 2020, Tomás et al. 2019, Sukennik et al. 2018, Tiblijaš et al. 2018, Morando et al. 2018, Atkins 2016, Anagnostopoulos and Kehagia 2019, Wang and Wang 2017, Espinosa 2015, Morando et al. 2017
Following Variation (CC2)	Stanek et al. 2017, Sukennik et al. 2018, Tiblijaš et al. 2018, Morando et al. 2018, Anagnostopoulos and Kehagia 2019, Morando et al. 2017
Negative Following Threshold (CC4)	Stanek et al. 2017, Seth et al. 2019, Tomás et al. 2019, Tiblijaš et al. 2018, Morando et al. 2018, Anagnostopoulos and Kehagia 2019, Morando et al. 2017
Positive Following Threshold (CC5)	Seth et al. 2019, Tomás et al. 2019, Tiblijaš et al. 2018, Morando et al. 2018, Anagnostopoulos and Kehagia 2019, Morando et al. 2017
Speed Dependency of Oscillation (CC6)	Aria et al. 2016, Seth et al. 2019, Tiblijaš et al. 2018, Morando et al. 2018, Anagnostopoulos and Kehagia 2019, Morando et al. 2017
Oscillation Acceleration (CC7)	Seth et al. 2019, Tomás et al. 2019, Tiblijaš et al. 2018, Atkins 2016, Anagnostopoulos and Kehagia 2019, Morando et al. 2017
Standstill Acceleration (CC8)	Tomás et al. 2019, Tiblijaš et al. 2018, Atkins 2016, Anagnostopoulos and Kehagia 2019, Morando et al. 2017
Acceleration at 80km/hr (CC9)	Tomás et al. 2019, Tiblijaš et al. 2018, Atkins 2016, Anagnostopoulos and Kehagia 2019

Frequently Used VISSIM Parameters	**Studies That Used Parameter**
Look Ahead (and Back) Distance	Aria et al. 2016, Morando et al. 2018, Espinosa 2015, Morando et al. 2017
Cooperative Lane Change	Aria et al. 2016, Seth et al. 2019, Morando et al. 2018, Espinosa 2015
Infrequently Used VISSIM Parameters	**Studies Used Parameter**
Threshold for Entering Following (CC3)	Stanek et al. 2017, Tomás et al. 2019, Sukennik et al. 2018
Advanced Merging	Aria et al. 2016, Mesionis et al. 2020, Espinosa 2015
Minimum Time Gap in Lane Changing (MG1)	Mesionis et al. 2020, Atkins 2016
Lane Changing Minimum Headway (LC4/MG2)	Tomás et al. 2019, Atkins 2016
Lower Safety Distance Reduction Factor (LC5)	Tomás et al. 2019, Atkins 2016, Elvarsson 2017

The two most common customizations to model AV driving behaviors are: (1) cooperative responses to other road users, and (2) conservative driving behavior. Examples of cooperative responses and conservative driving behaviors include AVs slowing down to allow vehicles to merge in front of them and AVs not changing lanes for speed gain, respectively (Nishimura et al. 2019, Liu et al. 2017, Hua et al. 2020).

AV–HUMAN INTERACTION MODELING

Models of AV driving commonly assume conservative behaviors where AVs interact with pedestrians, such as AVs responding to pedestrians much earlier relative to human perception (Kapania et al. 2019); or when interacting with HDVs, AVs reduce speed or change lanes to allow the HDV to merge (Stanek et al. 2017; Liu et al. 2018b). Additionally, in a few studies, AVs are modeled to adjust their driving behaviors and decision-making process based on the observed or predicted behaviors of human drivers (Wei et al. 2013, Tian et al. 2018). Despite differences in

approaches to modeling AV driving behaviors, there is a common goal of determining AV driving decisions based on cooperative behavior with neighboring road users (Schwarting et al. 2018). The customizations of AV characteristics are based on the common view of conservative and cooperative AV driving behaviors (Müller et al. 2016). Table 3 presents a summary of AV-and-human-driver interaction modeling approaches reviewed in the literature survey. In the table, the discussed car-following models and the corresponding modifications are used to model vehicles' longitudinal movement, as the car-following models govern the speed and headway controls. Similarly, the discussed lane-changing models and the corresponding modifications are used to model vehicles' lateral movements, as the lane-changing models govern the decision-making process in vehicle merges. The following abbreviations are used in the table; CV – Connected Vehicle, CACC – Cooperative Adaptive Cruise Control, and ACC – Adaptive Cruise Control. The 'Additional Modification' column refers to any additional change that was made by the author(s) to the adopted car-following model or lane-changing model.

Two key observations from the table below are: (1) VISSIM and SUMO are the dominant simulation platforms that were utilized among the reviewed studies, and (2) studies that utilized SUMO used SUMO's default lane-changing model without any additional modification. The absence of additional modification on lane-changing model suggests aggressive lane changing behaviors were not considered.

Table 3. Summary of AV – Human interaction modeling approaches.

	Scenario Settings				Longitudinal Movement		Lateral Movement	
Author(s)	**Simulation Tool**	**Scenario Layout**	**Mixed Traffic**	**AV-HDV Interaction**	**Use of Existing Car-following Model**	**Additional Modification**	**Use of Existing Lane-changing Model**	**Additional Modification**
Rahman and Abdel-Aty 2018	VISSIM	3-lane Freeway	Yes (CV Platoon and Human Vehicles)	Yes	Wiedemann 99 / IDM[1]	Gap Control	VISSIM Default	Merge Control
Liu et al. 2018b	AIMSUM	4-lane Freeway Mainline & Single-lane On-ramp	Yes (ACC/CACC Platoon and Human Vehicles)	Yes	Multiple Sources (IDM, Gipps, Newell, and Shladover)	-	Lateral Movement Logics Developed by Shladover	CACC Operation Rules
Nishimura et al. 2019	Scenargie	3-lane Straight Roadway	Yes (AV and Human Vehicles)	Yes	IDM	Acceleration Control	LMRS[2]	Merge Control
Stanek et al. 2017	VISSIM	20 Freeway Miles, 15 Freeway Interchanges, 3 Parallel Arterial Corridors, 32 Intersections	Yes (AV and Human Vehicles)	Yes	Wiedemann 74	Acceleration and Gap Control	VISSIM Default	Merge Control
Tian et al. 2018	-	Single-lane Roundabout	Yes (1 AV and 1 Human Vehicle)	Yes	Discrete-time Model	-	Game Theoretic Decision-making Model	Driver Type Estimation
Wagner 2016	SUMO	City Network	Yes (AV and Human Vehicles)	No	Helly's Model	-	SUMO Default	-
Wei et al. 2013	-	2-lane Freeway Mainline and Single-lane On-ramp	Yes (AV and Human Vehicle)	Yes	Markov Decision Process	Speed Control	Lateral decision made in the developed algorithm	-
Zhao et al. 2019	Driving Simulator (Scenario Built with MATLAB and PreScan)	3-lane Roadway	Yes (AV and Human Vehicles)	Yes	Default Car-following Model	Speed Control	Default Lane-change Model	-
Zhou et al. 2017	-	3-lane Freeway	Yes (AVs and Human Vehicles)	Yes	CIDM[3]	-	CIDM	Merge Control

	Scenario Settings				Longitudinal Movement		Lateral Movement	
Author(s)	**Simulation Tool**	**Scenario Layout**	**Mixed Traffic**	**AV-HDV Interaction**	**Use of Existing Car-following Model**	**Additional Modification**	**Use of Existing Lane-changing Model**	**Additional Modification**
Aria et al. 2016	VISSIM	3-lane Freeway / 4-lane Freeway	Yes (AVs and Human Vehicles)	Yes	Wiedemann 99	Gap Control	Wiedemann 99	Merge Control
Tiblijaš et al. 2018	VISSIM	Various Sizes of Roundabouts	Yes (AVs and Human Vehicles)	Yes	Wiedemann 74	Gap Control	Wiedemann 74	-
Hua et al. 2020	Cellular Automata	2-lane Freeway / 3-lane Freeway	Yes (CAVs and Human Vehicles)	Yes	TS Model[4]	Gap and Speed Control	TS Model	Lane Selection
Guo et al. 2020	Python-based Simulation	3-lane Freeway with On-ramp and Off-ramp	Yes (CAVs and Human Vehicles)	Yes	Enhanced Q-learning Algorithm	Trajectory Planning	Enhanced Q-learning[5] Algorithm	Merge Control
Liu et al. 2017	Cellular Automata	3-lane Freeway	Yes (AVs and Human Vehicles)	Yes	Rules from NaSch[6] Model	-	STCA[7] Model	Merge Control

[1] Intelligent driver model.
[2] Lane-change model with relaxation and synchronization.
[3] Cooperative intelligent driver model.
[4] Takagi–Sugeno fuzzy model.
[5] Quality or value-based learning algorithm.
[6] Nagel–Schreckenberg model.
[7] Symmetric two-lane cellular automaton model.

AGGRESSIVE BEHAVIOR MODELING APPROACH

To model different levels of aggressive behaviors between AVs and HDVs, Liu et al. (2017) developed different levels of aggressive lane-changing modes. In their effort, HDVs are assigned to the higher aggressive lane-changing mode (Liu et al. 2017). In another study, aggressive behavior in AV and HDV interaction is introduced by allowing HDVs to force lane changes that caused the following AVs to slow down to create a sufficient gap for the merge (Liu et al. 2018a). Studies that allowed HDVs to behave aggressively toward AVs observed greater traffic-flow instability with increased penetration levels of AVs (Liu et al. 2018a) or a higher number of incomplete trips with AVs traveling at extremely low or high speed (Nishimura et al. 2019). These results are drastically different from findings of improved safety and reduced travel times in other AV studies that did not consider aggressive behaviors (Rahman and Abdel-Aty 2018, Aria et al. 2016). The possibility of such behaviors targeted at a given vehicle type is not without precedence. For example, mobility service companies such as Uber or Lyft reported that HDVs will exhibit aggressive behaviors specifically toward AVs (Randazzo 2018, Hamilton 2019).

Most current studies allow the HDVs to increase aggressiveness based on the availability of gap distance, regardless of the type of the following vehicle type in the target lane (Nishimura et al. 2019; Liu et al. 2018a). In order to investigate the interaction impacts of HDVs' biased aggressive behaviors toward AVs, the levels of aggressive driving behaviors of the HDVs should vary based on the target vehicle type. Modeling different aggressive driving behaviors based on vehicle type requires flexible simulation models that allow for real-time adjustments of driving behavior characteristics and parameters based on vehicle types.

CHAPTER 3. SELECTION OF SIMULATION MODEL APPROACH

INTRODUCTION

A key objective of this study is to model the interaction between aggressive human-driven vehicles and AVs. Modeling AV and aggressive human-driven vehicle driving behaviors, and developing various fleet-penetration scenarios, requires simulation software capabilities such as flexibility in driving models and real-time interaction with agents during simulation run-time. This section presents the evaluation criteria utilized for simulation software selection. Two software packages are considered, SUMO and VISSIM (Eclipse Foundation 2020, PTV Group 2021). Table 4 lists the key evaluation criteria identified for AV modeling. The following sections explain the reasoning for each of the criteria and the capabilities of the two software packages – SUMO and VISSIM – corresponding to each evaluation criterion.

KEY EVALUATION CRITERIA

General Information

Both software packages have interfaces that enable run-time communication with agents, such as vehicles and signal control systems. SUMO's source code is publicly available and accessible as an open-source platform, whereas VISSIM offers source codes on AddIns.

Availability of Driving Models

Different car-following models or lane-changing models may be more appropriate to model the AV characteristics based on the given scenario. For example, an area with higher interaction with other vehicles, such as a roundabout, may require a different modeling complexity than a signal-controlled intersection with protected-only

movements. SUMO offers a higher number of car-following and lane-changing models compared to VISSIM. However, both software packages offer significant flexibility by allowing users to modify existing models or import customized models. Critically, such capabilities allow users to assign variations in vehicle behaviors by vehicle types.

Driver Behavior Model Parameters

Through the literature survey it is seen that due to the lack of standards in AV driving behaviors many AV modeling approaches rely on assumptions and expectations of AVs' anticipated behaviors. As a result, studies that simulate AVs may share certain characteristics such as conservative, cooperative, or cautious; however, they differ in the driving-behavior models and the parameter values utilized. SUMO's driving-behavior models have an arguably higher level of flexibility given a higher number of model parameters and the open-source nature of the software. However, as stated, both software packages allow the control of parameters during run-time. Such capability is particularly critical in AV modeling as it allows the AV model to adapt to different roadway conditions.

Data Export

The outputs that record the states of the simulation agents, such as vehicles, lanes, and signal control systems, are used to measure key performance indices to test the study hypothesis. Both software packages allow the user to extract various outputs that can be used to measure model performance. Critically, both models allow for the output of vehicle trajectory data, from which numerous other measures may be derived.

User Contribution

VISSIM has been widely used in the public and private sectors as well as academic and research settings, while SUMO has been primarily used for academic and research efforts. A large user community may be helpful in determining experimental designs and model development as previous similar efforts may be used for reference. Efficiency may also be gained through the adoption of previously developed models or findings. For example, a previously developed driving-behavior model can be imported to SUMO or VISSIM for AV modeling.

SUMO has an online community in which users exchange knowledge and contribute to improve SUMO functionality. SUMO's ACC and CACC car-following models are developed by a research team (Lopez et al. 2018). Such interactions among users and between users and developers help enable referencing and learning from previous studies.

Signal Control System

Signal control systems are often used to simulate different traffic patterns and flow rates. Complex traffic control systems can be established via the respective interface in SUMO and VISSIM, such as the vehicle preemption signal control system. VISSIM offers more variations of signal control systems that are readily available to users.

Overall Comments

Each software package has advantages and disadvantages that can be weighted differently based on the study objective. Based on the identified criteria for modeling AV driving behavior, SUMO's key advantages include the source code availability and the number of driving-behavior models and parameters. These enable the

identification of key parameters to model AV characteristics and provide significant flexibility for modeling AV behavior. VISSIM's key advantages include a larger user base and greater variety of signal control systems that can aid in more efficient implementations of complex traffic control systems.

The research team selected SUMO for this study because SUMO's key advantages were critical in modeling aggressive human driving behavior and the subsequent AV response. Additionally, being able to access the driver behavior model and parameters via the source code helped the team to identify key parameters to control to model the aggressive merging behaviors as well as the AV response.

Table 4. Evaluation criteria summary on simulation tools.

Evaluation Criteria	SUMO (Lopez et al. 2018)	VISSIM (PTV Group 2021)
1. General Information		
Compatibility with Operating Systems	Windows, Linux, macOS	Windows, Linux
Source Code	Written in C++	Written in C++
Source Code Availability	Yes; online source code library publicly accessible	AddIn source codes available
Interface	TraCI	COM & EDM
Programming Language Compatible with Interface	Compatible with Python, C++, MATLAB, Java	Compatible with Python, C++, MATLAB, Java
Accessibility	Open Source (publicly accessible)	Commercial
2. Availability of Driver Models		
Car-following Models	14 car-following models imported	2 car-following models imported
Lane-changing Models	3 lane-changing models imported	2 lane-changing models imported
Import-customized Models	Yes	Yes
Modification on Existing Models	Yes	Yes
3. Driver Behavior Model Parameters		
Vehicle Attribute Parameters	38 parameters	10 parameters
Lane-changing Model Parameters	23 parameters	14 parameters
Parameters Adjustable in Simulation?	Yes	Yes
4. Data Export		
Export File Format	xml	Various Types
Output Data Type	Vehicle-based, detector-based, simulation-based, traffic light-based, lane-based	Vehicle-based, pedestrian-based, traffic light-based, lane-based, detector-based
5. User Contribution		
User Base	Academic/Research Sector	Academic/Research Sector, Private Sector, Public Sector
Allows External Contribution?	Yes; online discussion forum, imported a user-developed car-following model	No
6. Traffic Light System		
Fixed Time Method	Yes	Yes
Coordinated Method	Yes	Yes
Actuation Method	Yes	Yes
Ring-Barrier Sequence	No	Yes
Optimization	No	Yes

CHAPTER 4. SIMULATION MODELING OF DRIVER BEHAVIOR

AGGRESSIVE MERGE BEHAVIOR MODEL DEVELOPMENT

Simulation Tool

For this study, SUMO (version 1.6.0) is used to simulate the merging behavior scenarios. The SUMO's Traffic Control Interface (TraCI) is utilized for modeling vehicle interaction behaviors. TraCI provides access to the values of the simulation objects during run-time, enabling customization of vehicle behaviors (Eclipse Foundation 2020). In the current application, to model aggressive AHDV merge behaviors, TraCI is used to retrieve the real-time speed of target vehicles, control the AHDVs' speed for overtaking the AV, and force the merge in front of the target AV by accepting low front and rear gaps. In this study, Python (Python) is used for developing the TraCI scripts.

Network Layout

Figure 1Figure 1. Diagram. Roadway layout on merging zone, highlighted in yellow.

shows the modeled network layout. It consists of two through lanes with a 600 ft deceleration lane to an exit ramp. The aggressive merge behavior occurs in the area near the freeway exit ramp, i.e., the merging zone. The two-lane freeway extends for 1 mile upstream of the beginning of the merge zone, allowing for sufficient space for vehicles to queue during congestion without spilling out of the network. The outflow from the ramp is controlled by a simple two-phase, pretimed traffic signal, with the splits and cycle length set dependent on the modeled scenario; they are specified in each experiment. The ramp junction with the cross street is 1,500 ft downstream from the ramp gore. Figure 2. Diagram. Speed by lane.

shows the simulated speed for each lane and the lane labels used in the study.

Figure 1. Diagram. Roadway layout on merging zone, highlighted in yellow.

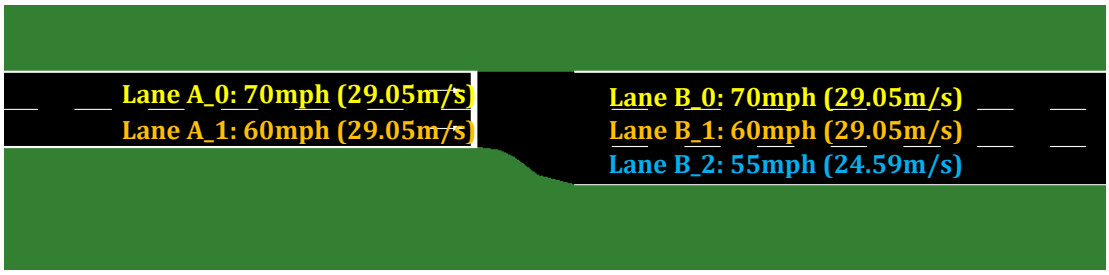

Figure 2. Diagram. Speed by lane.

Vehicle Classification and Characteristics

To study the interactions between the different vehicle types, three vehicle classes are defined based on driving behaviors, as follows:

1. AVs: Exhibit cooperative driving behaviors; i.e., AVs slow to extend the leading gap, allowing merging vehicles to more easily enter their lane. When AVs exit the freeway, they will change lanes at the start of the deceleration lane. AV behavior is fully controlled by SUMO.
2. AHDVs: Travel on a high-speed lane (Lane B_1, figure 2) until they merge into the deceleration lane. These vehicles exhibit aggressive merge behavior toward AVs by accepting smaller gaps (minimum half-vehicle in length to begin a merge) in front of the AV compared to a merge in front of an HDV. AHDVs will always seek to merge in front of the farthest reachable downstream AV in the deceleration lane. When making an aggressive merge, the AHDV behavior is controlled through TraCI. When an AV is not

reachable, the AHDV merge behavior will be non-aggressive and controlled by SUMO.

3. HDVs: Exhibit the same cooperative driving behaviors as that of AVs but are not targeted by AHDVs. HDV behavior is fully controlled by SUMO.

Aggressive Behavior Model

The objective of the aggressive merging behavior is to perform an aggressive lane change in front of a target vehicle. AHDVs' aggressive merge behaviors consist of customizing two key behaviors of AHDVs—target selection behavior and merging behavior. The objective of the target selection behavior is to identify the optimal target vehicle. When queueing occurs on the deceleration lane, the targeting behavior allows AHDVs to travel on the higher-speed lane (Lane B_1) until merging in front of target vehicles in Lane B_2, thus allowing AHDVs to make queue-jumps. After a target is selected, the AHDVs adjust their speed, within the constraints of the presence of other vehicles in front of them on the same lane, and seek to merge in front of the target vehicle.

As mentioned in chapter 1, two merge types are considered in the study based on the levels of aggressiveness in the targeting behavior: (1) aggressive merge with maximum advancement, representing the highest level of aggressive merge; and (2) aggressive merge with "zipper" action, representing a moderate level of aggressive merge. The merging behavior process is similar for these two merge types; however, they differ from each other in their target behavior process. The next section describes the target behavior process for these two types of aggressive merges.

Aggressive Merge Behavior Model: Target Selection Process

Aggressive Merge with Maximum Advancement

The objective of the target selection behavior in the aggressive merge with maximum advancement is to identify the optimal target vehicle, which in this study is considered the AV farthest downstream in the deceleration lane. When queueing occurs on the deceleration lane (Lane B_2), this targeting behavior allows AHDVs to travel on the higher-speed adjacent lane (Lane B_1) until merging in front of target vehicles in the deceleration lane, thus allowing AHDVs to queue-jump. To implement this behavior, an AHDV's initial target is the closest AV on the target lane. After a target is selected, the AHDV adjusts its speed to overtake the AV, within the constraints of the speed of the leading vehicle in the same lane (if one is present) or the lane speed. Once the AHDV is in the vicinity (to be defined subsequently) of the target vehicle, the AHDV checks if the next downstream AV is reachable prior to the end of the deceleration lane. By repeating this process, the AHDV merges in front of the farthest reachable downstream AV. As every AHDV targets the farthest AV, this behavior often results in multiple AHDVs merging in front of the same AV, as shown in figure **3**Figure 3. Diagram. Aggressive merge behavior of AHDVs toward AVs..

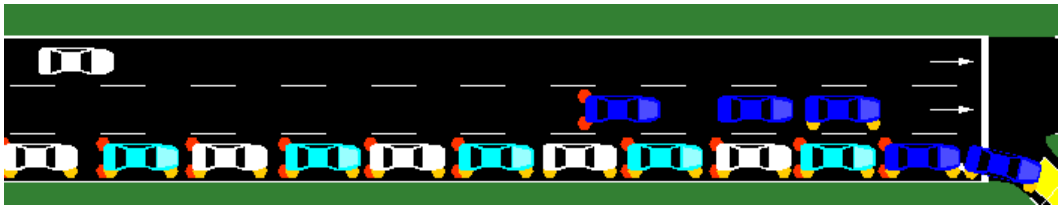

Figure 3**. Diagram. Aggressive merge behavior of AHDVs toward AVs. (AHDV – deep blue vehicles, AV – light blue vehicles, and HDV – white vehicles)**

If an AHDV's target AV becomes no longer reachable due to a speed change or interference from other vehicles in the AHDV's lane, then the AHDV seeks to merge in front of an HDV. However, the merge in front of the HDV no longer uses

aggressive gap selection; rather, it is fully controlled by SUMO. If SUMO is unable to successfully complete the merge and an AV from upstream on the deceleration lane begins to overtake the AHDV (which may occur when congestion results in a lower speed on the mainline lane than that on the deceleration lane), the AHDV returns to its aggressive behavior and merges in front of the approaching AV.

Aggressive Merge with Zipper

In the aggressive merge with zipper case, to target a vehicle for merge, AHDVs first check whether there is an AHDV merge occurring downstream. If there is an aggressive merge downstream, the AHDVs do not target the same AV affected by the previous merge but rather target any following AV behind the last merge's target AV, as shown in figure 4. This selection of a new target vehicle, different from the last merge's target vehicle, makes this aggressive merge with zipper case less aggressive compared to the aggressive merge with maximum advancement case. Targeting the following vehicle of the last merge results in shorter queue-jumping distance than the queue-jumping distance in the aggressive merge with maximum advancement case. If there is no relevant merge downstream or AHDVs cannot reach the optimal target vehicle, AHDVs target the farthest reachable AV by going through the same target selection process as the aggressive merge with maximum advancement case. The aggressive merge with zipper case represents a moderate level of aggressive behaviors in AHDVs.

Figure 4**. Diagram. Aggressive merge with zipper.**
(AHDV – deep blue vehicles, AV – light blue vehicles, and HDV – white vehicles)

There are three essential computations used to model the targeting behavior—*position check, can catch,* and *merge position check*. These three functions are executed every time step to update the target vehicle based on the position and speed changes in AHDVs and their target vehicles.

Position Check

To merge into the deceleration lane, the AHDV must decrease to the speed of the vehicle in front of the target AV, as the target AV and its leading vehicle represent the lagging and leading vehicles, respectively, for the gap that will be entered by the AHDV. The objective of *position check* is to determine if the AHDV has reached the position where it must decide whether to target the next downstream AV or keep the current target and start braking to prepare for the merge. Figure 5Figure 5. Diagram. Illustration of AHDV's decision point.

(AHDV – deep blue vehicles, AV – light blue vehicles, and HDV – white vehicles)

shows an illustration of this decision point position check process. The braking distance is the distance the AHDV will travel to reduce its speed to the merge speed by the time it is one vehicle length downstream of the AV. Travel while Braking (TwB), is the distance that the target vehicle travels while the AHDV travels the braking distance. When the braking distance is equal to or less than the sum of TwB

and vehicle length, the *position check* function returns ‘true’ and the target vehicle ID is sent to the *can catch* function to determine whether the next potential target vehicle is reachable. If the *position check* function returns ‘false’, it indicates that the AHDV has not yet reached the decision point position and, thus, continues to travel at its current speed.

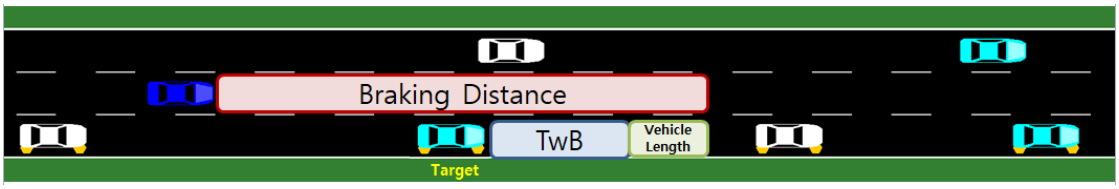

Figure 5. Diagram. Illustration of AHDV’s decision point.
(AHDV – deep blue vehicles, AV – light blue vehicles, and HDV – white vehicles)

Can Catch

The objective of the *can catch* function is to determine if the AHDV can reach the front of the target vehicle, to allow for a merge, before the deceleration lane-end point. This is determined by evaluating the current position and speed conditions, and comparing the travel time of the AHDV and target vehicles to the end of the lane. *Can catch* is applied at every time step to confirm that the current target vehicle may still be reached, allowing for potential changing conditions due to congestion. In addition, *can catch* is utilized when the AHDV evaluates if it will switch from its current target to the next downstream AV.

The travel-time comparison between AHDV and the target vehicle is based on the current position and speed data, as shown in the equations below. The AHDV must be able to reach the lane endpoint before the potential target vehicle. The travel time of the target vehicle can be calculated by dividing the remaining distance until the lane end by the current speed.

$$\text{Target Vehicle Travel Time} = \frac{Lane\ Length - Target\ Vehicle\ Position}{Target\ Vehicle\ Speed} \quad (1)$$

Calculating the travel time of an AHDV depends on its current position. As shown in figure 6, the remaining distance is divided into two regions.

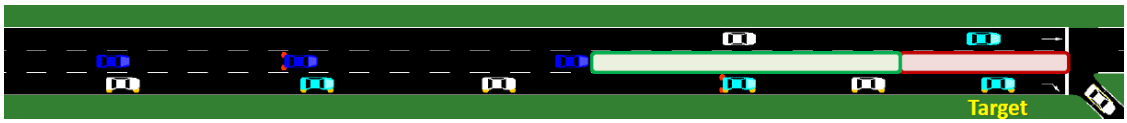

Figure 6. Diagram. AHDV travel-time calculation.
(AHDV – deep blue vehicles, AV – light blue vehicles, and HDV – white vehicles)

The distance in red indicates the braking distance from the AHDV's current speed to the target speed (equation 2), with the merge occurring at the end of the deceleration lane. The distance in green indicates the distance that the AHDV needs to travel at its current speed until it starts braking (equation 3). Thus, the AHDV's travel time (equation 4) is the sum of the travel time over the fixed-speed distance (indicated in green in figure 5) and the travel time over the braking distance (indicated in red in figure 5). If the AHDV's travel time is less than the target vehicle's travel time, the *can catch* function returns 'true'.

$$\text{Braking Distance} = \frac{Target\ Speed^2 - AHDV\ Current\ Speed^2}{2 * Deceleration\ Rate} \quad (2)$$

$$\text{Distance to Start Braking} = \text{Lane Length} - \text{AHDV}'\text{s Current Position} - \text{Braking Dist.} \quad (3)$$

$$\text{Braking Time} = \frac{(Target\ Speed - AHDV\ Current\ Speed)}{Deceleration\ Rate} \quad (4)$$

$$\text{AHDV Travel Time} = \frac{Distance\ to\ Start\ of\ Braking}{AHDV's\ Current\ Speed} + Braking\ Time \quad (5)$$

As stated, *can catch* is executed every time step for the current target AV. If the *can catch* function returns 'false', it indicates the AHDV is no longer able to catch the current target AV vehicle. When this occurs, merge control is released to SUMO, which will execute a non-aggressive merge maneuver into the deceleration lane as soon as possible. However, while SUMO is seeking a merge opportunity, the AHDV continues to search for an AV within 20 ft downstream, or approaching from the upstream if the deceleration lane is moving faster than the mainline lane. If an AV is identified, the TraCI logic will be reinitiated.

Merge Position

This function checks whether an AHDV is within the position to initiate an aggressive merge. Once the AHDV is in position, the merge process initiates. As shown in figure 7, an AHDV executes the merge process if its front bumper is anywhere between the center of the target vehicle and the head of the leading vehicle to the target vehicle (red region in figure 7).

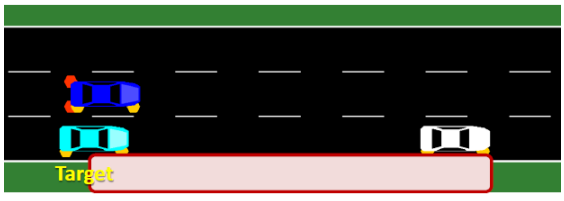

Figure 7. Diagram. Illustration of merge position. (AHDV – deep blue vehicles, AV – light blue vehicles, and HDV – white vehicles)

Target AV Selection Process in Aggressive Merge with Maximum Advancement Case

The flowchart of the AHDV's target AV selection process is shown in figure 8 and figure 9. The target selection process is undertaken every time step. The following steps are the general procedure:

1. Vehicle ID list is updated to contain the IDs for all AHDVs currently in the merging zone. Vehicles entering the merging zone are added and vehicles that have merged into the deceleration lane are removed.
2. When an AHDV first arrives at the upstream start of the merging zone, the deceleration lane condition is reviewed. If the deceleration lane is empty, the AHDV changes lane without any further consideration.
3. If the deceleration lane is not empty, the AHDV checks for the presence of any AV.
4. If there is no AV, the AHDV continues to search for any AV upstream and downstream of its current location while allowing SUMO to execute a merge whenever it is possible. This process continues until either SUMO executes the merge or the AHDV finds an AV in the traffic.
5. If there is more than one AV in the deceleration lane, the AHDV initially identifies the nearest downstream AV.
6. Next, using the *can catch* function, the merge feasibility of the AHDV with the nearest AV is checked. If the AHDV cannot merge in front of the nearest AV, it indicates that there is no AV that the AHDV can catch. The process returns to step 4.
7. If the AHDV can catch the nearest AV, the position of the AHDV is checked (using the *position check* function) to determine whether the AHDV is ready

to search for the next AV downstream. If the AHDV is not in such position, it continues to travel until being checked again in the next time step.

8. If the AHDV is in such position, the next AV downstream is identified and checked for merge feasibility using the *can catch* function.
9. If the AHDV can catch the next AV in downstream, the target AV is updated. If not, the current target AV is maintained.
10. In every time step, the *can catch* function is used to determine if the AHDV can still catch the current target AV.
11. If the AHDV can no longer catch the current target AV, the AHDV first searches to check whether the nearest reachable AV is downstream. If there is one, the AHDV updates its target.
12. If there is no reachable downstream AV, the AHDV searches for the nearest reachable AV that is upstream. If there is one, the AHDV updates its target. If there is no such AV, the process returns to step 4.
13. The process continues until all AHDVs have been checked; then the simulation time advances.

Target Selection Process in Aggressive Merge with Zipper Case

The flowchart of the target selection process in the aggressive merge with zipper case is shown in figure 10 and figure 11. The first four steps in the target selection process are the same as the maximum advancement case. The following steps are a divergence from the maximum advancement case at step 5:

5. If there is more than one AV, the AHDV searches for any previous merge. If there is no previous merge, the AHDV finds the nearest AV and follows

the same steps in the aggressive merge with maximum advancement case (step 8).

6. If there is a previous merge, the AHDV searches for the follower AV of the previous merge. If there is no follower vehicle, it indicates that the lane behind the merge is empty. Thus, the a AHDV allows SUMO to execute a lane change whenever possible.
7. If the AHDV finds a follower AV to the previous merge, the merge feasibility is checked with the ‘can catch’ function. If the AHDV can catch the follower AV, the follower AV is selected as the target vehicle.
8. If the AHDV cannot catch the follower AV, the AHDV searches for the nearest AV and the same steps are followed as in the aggressive merge with maximum advancement case. However, if the AHDV is ahead of an HDV, the AHDV allows SUMO to merge it in front of the HDV.

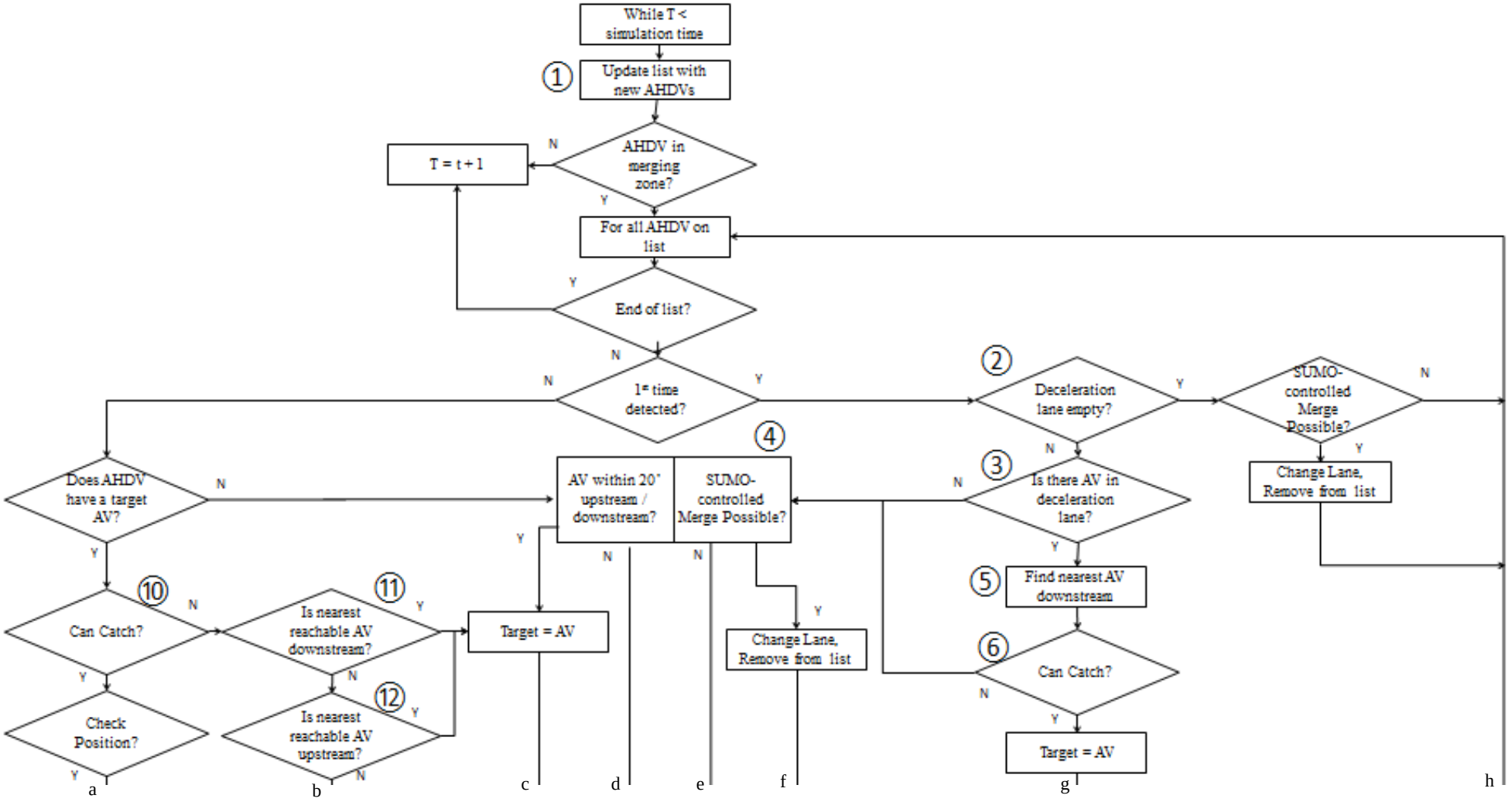

Figure 8. Flowchart. Target AV selection process with step numbers in the process description marked (top).

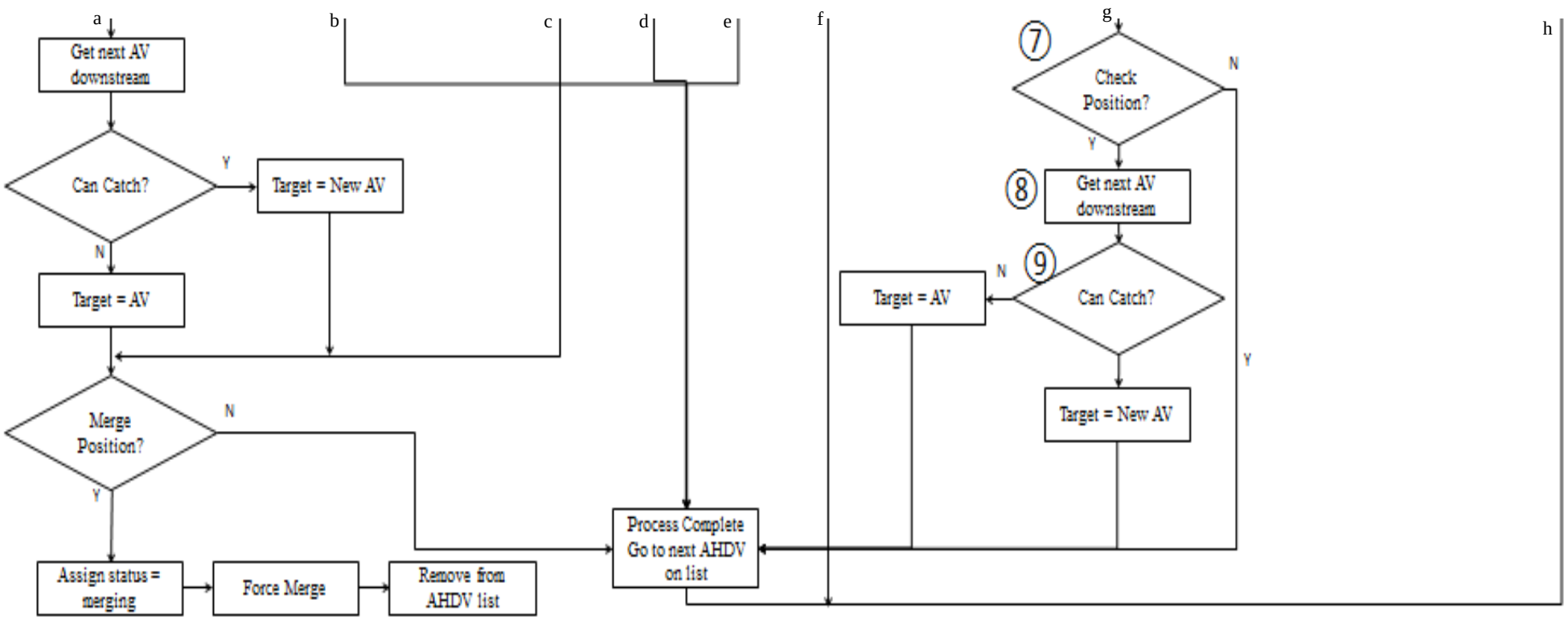

Figure 9. Flowchart. Target AV selection process with step numbers in the process description marked (bottom).

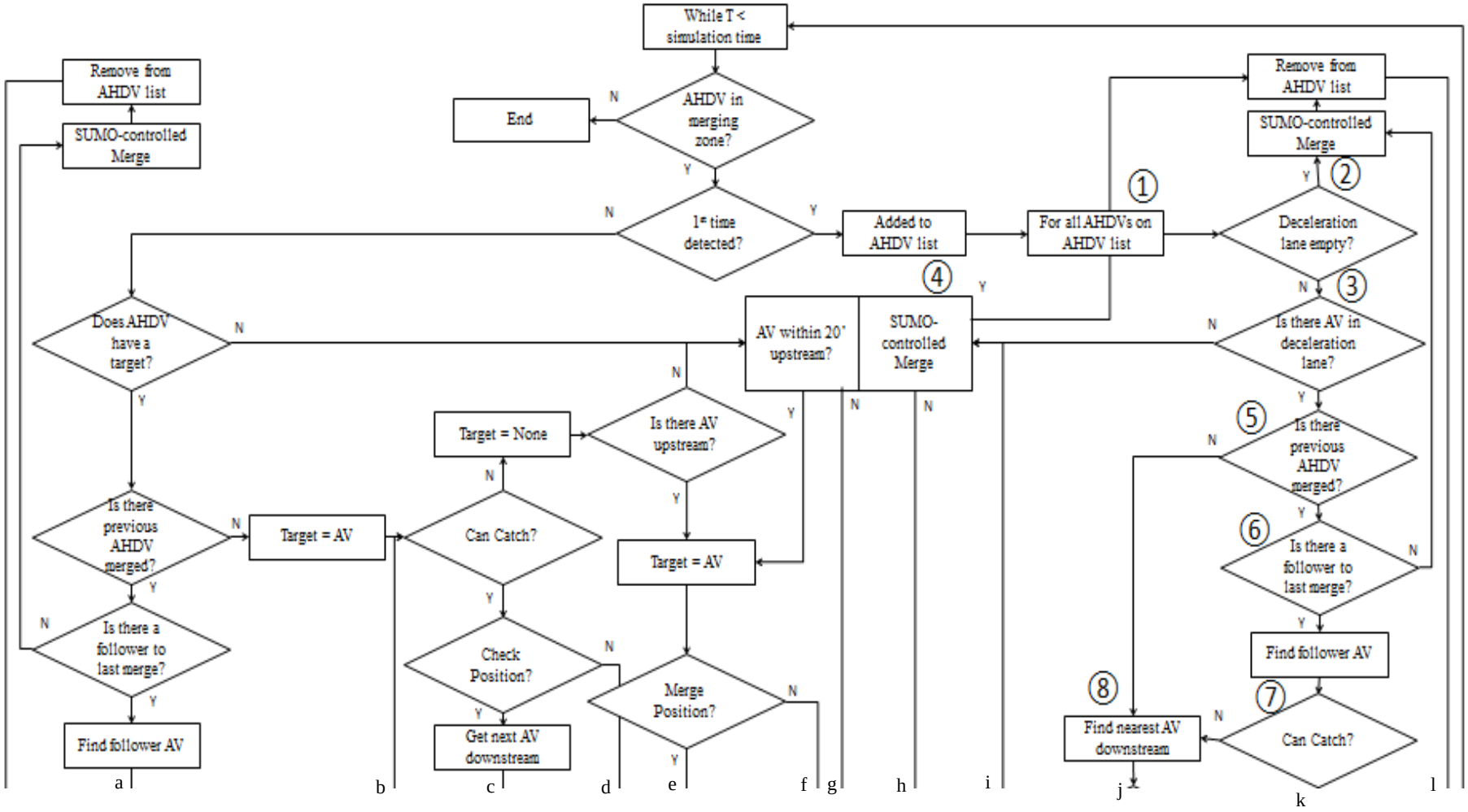

Figure 10. Flowchart. Target selection process in aggressive merge with zipper (top).

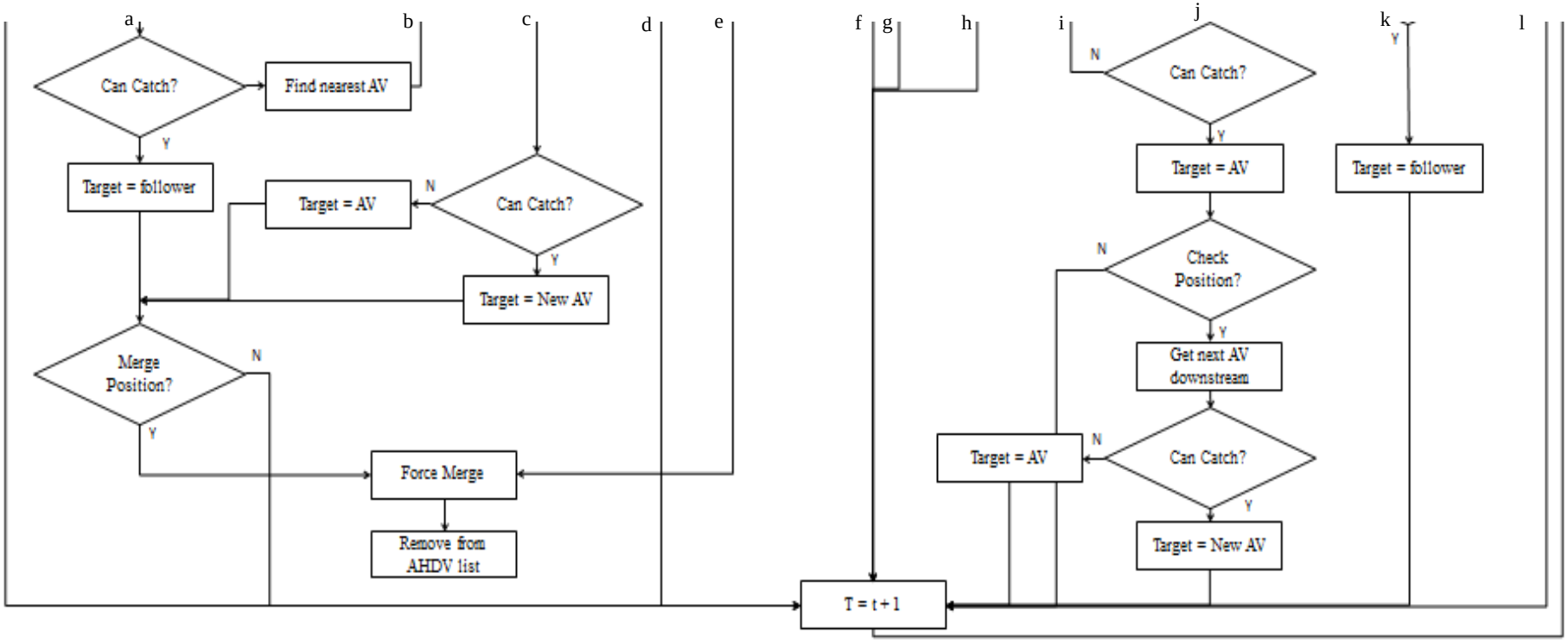

Figure 11. Flowchart. Target selection process in aggressive merge with zipper (bottom).

Aggressive Merge Behavior Model: Lane Changing

After the targeting process is complete and the AHDV is positioned next to the target AV, the lane change process is initiated. As shown in figure 12, AHDVs merge in front of the target AV as soon as the AHDV's rear bumper crosses the front bumper of the AV, forcing the AV to decelerate to meet its desired spacing. For this aggressive merge, the TraCI *moveTo* command is utilized. The *moveTo* command in SUMO manually moves the position of a vehicle by the specified coordinate shift and, critically, it does not require the vehicle to satisfy any gap requirements.

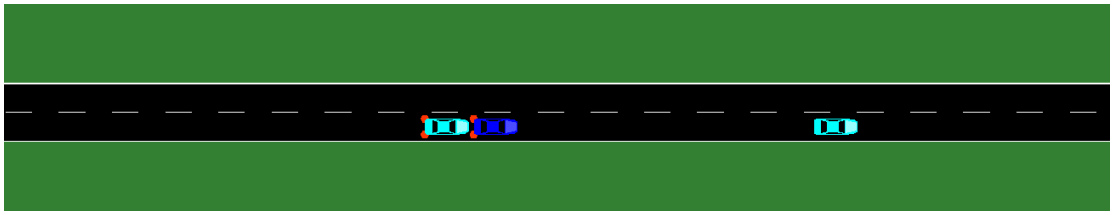

Figure 12. Diagram. Example of aggressive merge.
(AHDV – deep blue vehicles, AV – light blue vehicles)

Merging Process in SUMO-controlled Merge

In order to assign the cooperative characteristic in AVs and HDVs, SUMO's *'lcCooperativeSpeed'* parameter is set to 1. Setting this parameter to 1 allows the neighboring vehicles to slow down cooperatively for merging vehicles. When the algorithm requests that SUMO control the AHDV merging process, the neighboring vehicle (an HDV, as an aggressive merge would be undertaken for an AV) starts slowing down cooperatively to create a sufficient gap for AHDVs to merge. However, when TraCI is utilized to implement an aggressive merge, the AVs do not exhibit a cooperative

behavior, as they are unaware the AHDV will merge until it begins to encroach into the AV lane. Only upon this encroachment will the AV begin to slow.

Thus, a SUMO-controlled merge requires a sufficient gap before a lane change is performed, whereas the aggressive merges (using the *moveTo* command) are not affected by the gap availability. This results in the SUMO-controlled merge often requiring a longer time period for the merge, possible requiring slowing of the merging vehicle to find a suitable gap to complete. An example of the spacing between the lagging vehicle and the merging vehicle in a SUMO-controlled merge, which requires longer gaps to merge, is shown in figure 13.

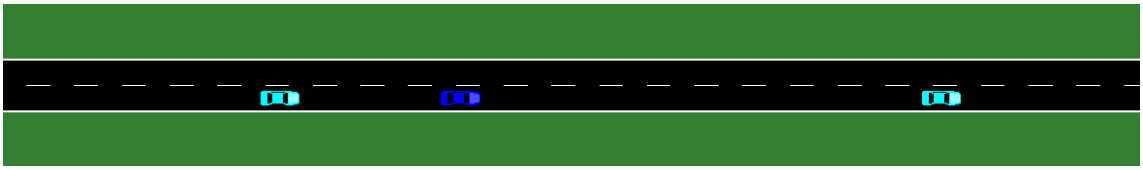

Figure 13. Diagram. Example of SUMO-controlled merge.
(AHDV – deep blue vehicles, AV – light blue vehicles)

EXPERIMENTS

Four experiments were conducted to study the developed aggressive merging models. The first experiment simulates a platoon of 10 AHDVs performing the aggressive merges, for two levels of congestion on the deceleration lane. The second and third experiments simulate AHDVs spread out in the mixed traffic flow performing the aggressive merges, for two levels of traffic demands. The distinction between the second and third experiments is the level of congestion in the deceleration lane, resulting from changing the signal timing at the ramp end intersection. The fourth experiment evaluates

the impact of aggressive merging on capacity. For all four experiments, a base case was also created without any aggressive vehicle behaviors.

Experiment 1: Aggressive Merging with Platooned Arrivals

Objectives

The objectives of the initial scenario are to: (1) demonstrate the aggressive merging behavior models under two different traffic conditions—uncongested deceleration lane and congested deceleration lane; and (2) visualize the difference in the impacts on the deceleration lane traffic between aggressive merging and SUMO-controlled merging.

Experiment 1 Design

A platoon of 10 AHDVs is introduced into the traffic stream on lane A_0, the left-most freeway lane. The platoon vehicles change their lane to the lane adjacent to the deceleration lane as soon as they enter the merging zone. The AHDVs then seek to merge into the deceleration lane, utilizing the targeting and lane-changing behavior as discussed previously. An entry volume of 1,350 vehicles/hour was used on lane A_0 with a 50 percent AV ratio. All vehicles on lane A_0 were exit vehicles. The uncongested deceleration-lane experiment was conducted before the queue started forming on the deceleration lane. The congested deceleration-lane experiment was conducted after a queue formed on the ramp and extended to the deceleration lane. For comparison, the base case introduces an equivalent platoon of 10 AHDVs, although functioning as HDVs, seeking to exit with the merge behavior controlled by SUMO.

Results

Figure 14 – figure 19 show the time–space diagrams (TSDs) for the merge zone, with the AHDV platoon trajectories indicated in red, and the AV and HDV trajectories in blue. AV and HDV travel occur on the deceleration lane, while AHDV travel may occur on the deceleration lane or adjacent mainline lane. Each graph starts at the beginning of the merge zone, at approximately x=5200 ft The ramp gore is at 5900 ft, and the intersection with the cross street is approximately at 7500 ft.

Discussion

The impacts of the AHDVs' aggressive merging behaviors can be observed in two ways: (1) the AHDVs' reduced travel times, and (2) the speed changes in the traffic on the target (i.e., deceleration) lane. The AHDVs' reduced travel times are shown by the time steps in which each red line ends. In each congestion scenario the AHDV platoon enters the merge zone at approximately the same time, i.e., at approximately t = 100 seconds for the uncongested scenarios—i.e., base (figure 14), aggressive merge with maximum advancement (figure 15**)**, and aggressive merge with zipper (figure 16)—and t = 960 for the congested scenarios—i.e., base (figure 17**)**, aggressive merge with maximum advancement (figure 18), and aggressive merge with zipper (figure 19). However, in each aggressive merge scenario, the platoon of AHDVs departs from the intersection at the end of the ramp (top of the TSD) earlier than in the base case with the non-aggressive HDV platoon. This is accomplished by the AHDVs queue-jumping (as seen by the crossing of the red and blue trajectories) by driving further downstream on the mainline, then performing aggressive merges near the ramp gore. The impact on the speed of the vehicles behind the merged AHDVs is witnessed by a flattening of the slopes on the

vehicle trajectories. In the vicinity of the merge activity (highlighted in yellow) the speeds of the following vehicles are reduced by approximately 17 mph in the uncongested scenario, and in the congested scenario following vehicles are forced by the AHDVs to briefly come to a complete stop to avoid colliding with the merging vehicles.

The travel time and speed impacts are more clearly seen in the congested deceleration-lane scenario compared to the uncongested scenario. This is due to the spacing between vehicles. Since vehicles were more spread out in the uncongested scenario, the impacts of aggressive merges were muted by the larger headways between the vehicles; in the congested scenario, the impacts of aggressive merges were directly passed along to the following vehicles.

The next two experiments investigate the impacts of the aggressive merging behaviors with AHDVs spread throughout the traffic flow.

Low Congestion

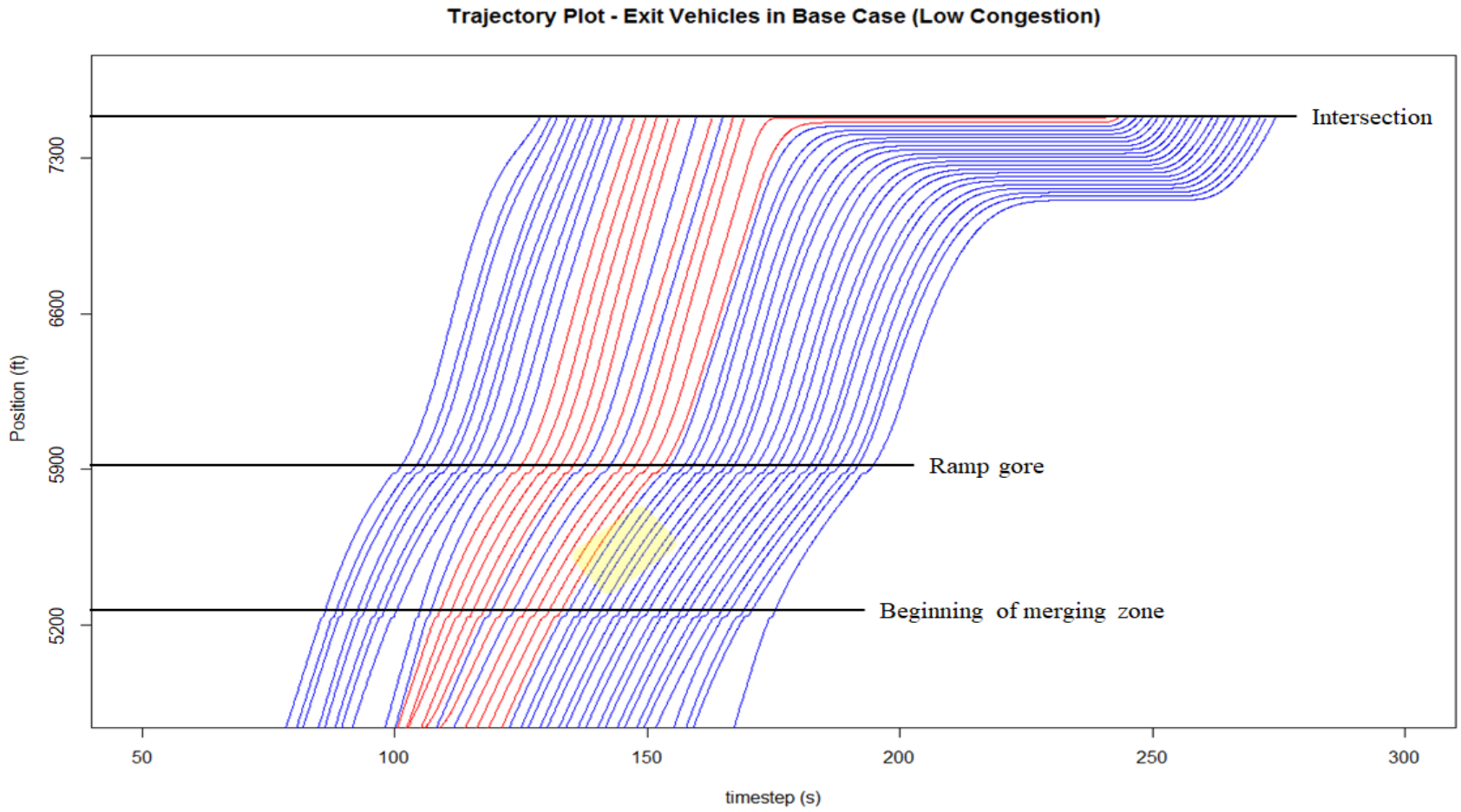

Figure 14. Plot. Base case time–space diagram in uncongested deceleration-lane scenario.

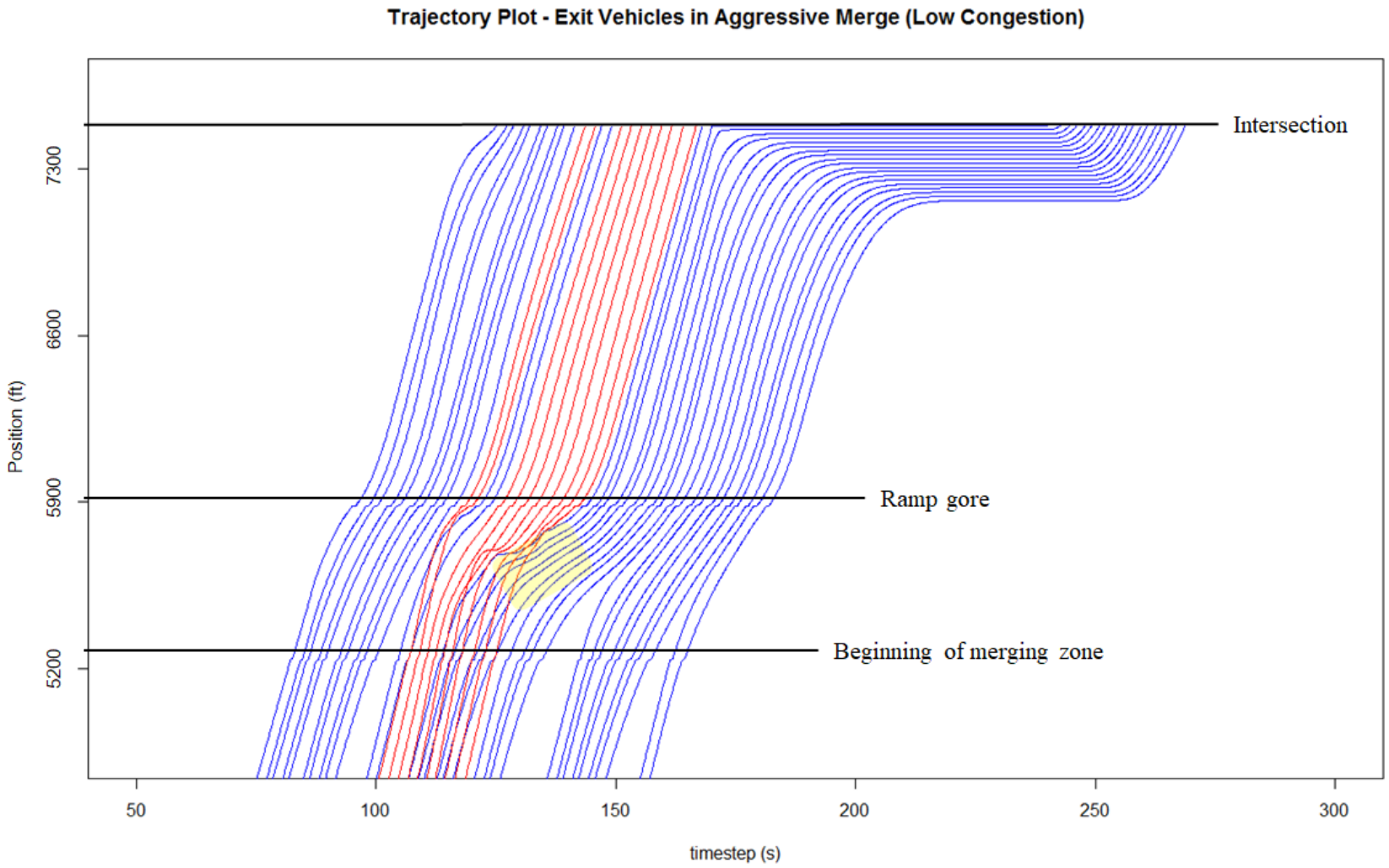

Figure 15. Plot. Aggressive merge with maximum advancement time–space diagram in uncongested deceleration-lane scenario.

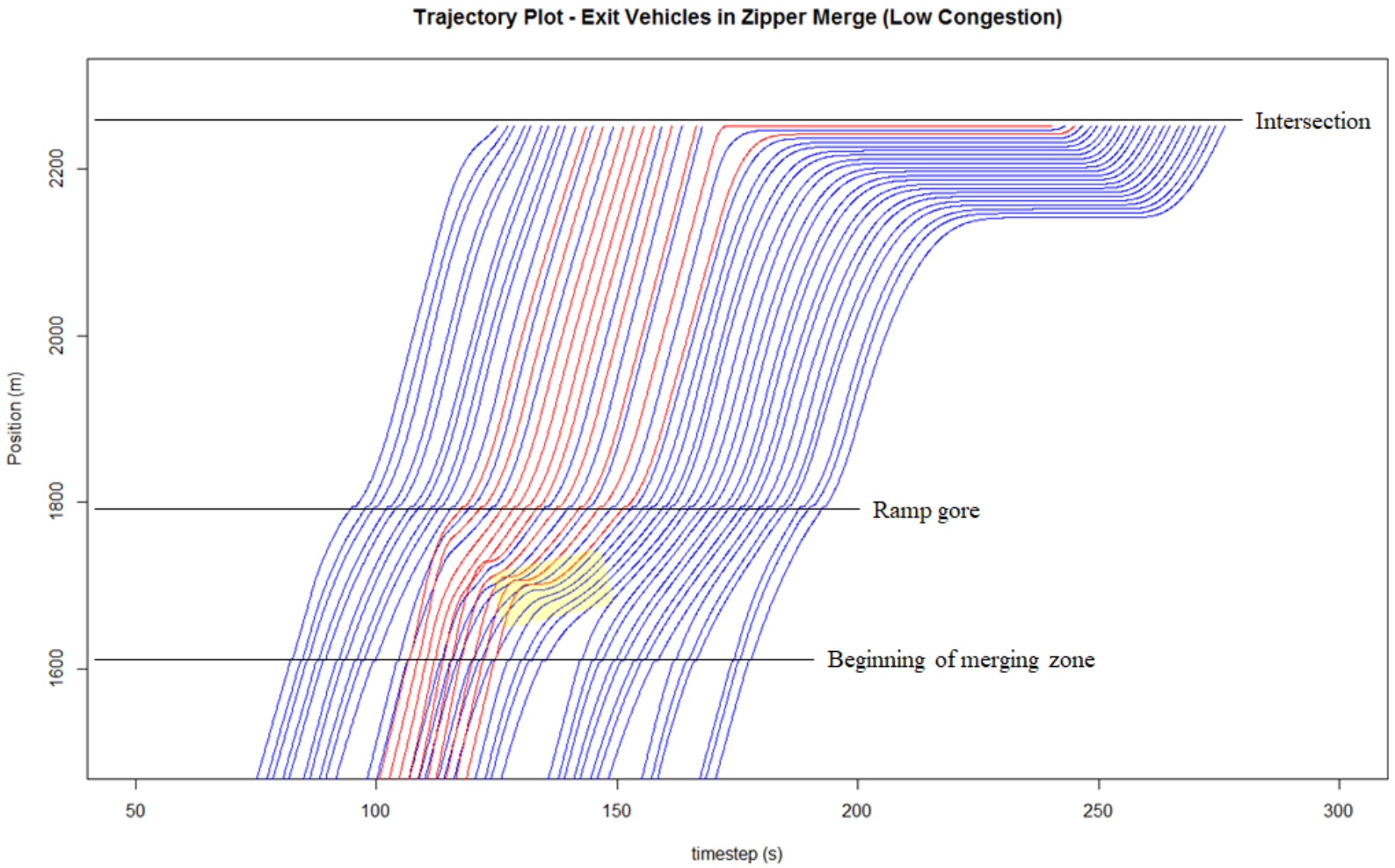

Figure 16. Plot. Aggressive merge with zipper time–space diagram in uncongested deceleration-lane scenario.

High Congestion

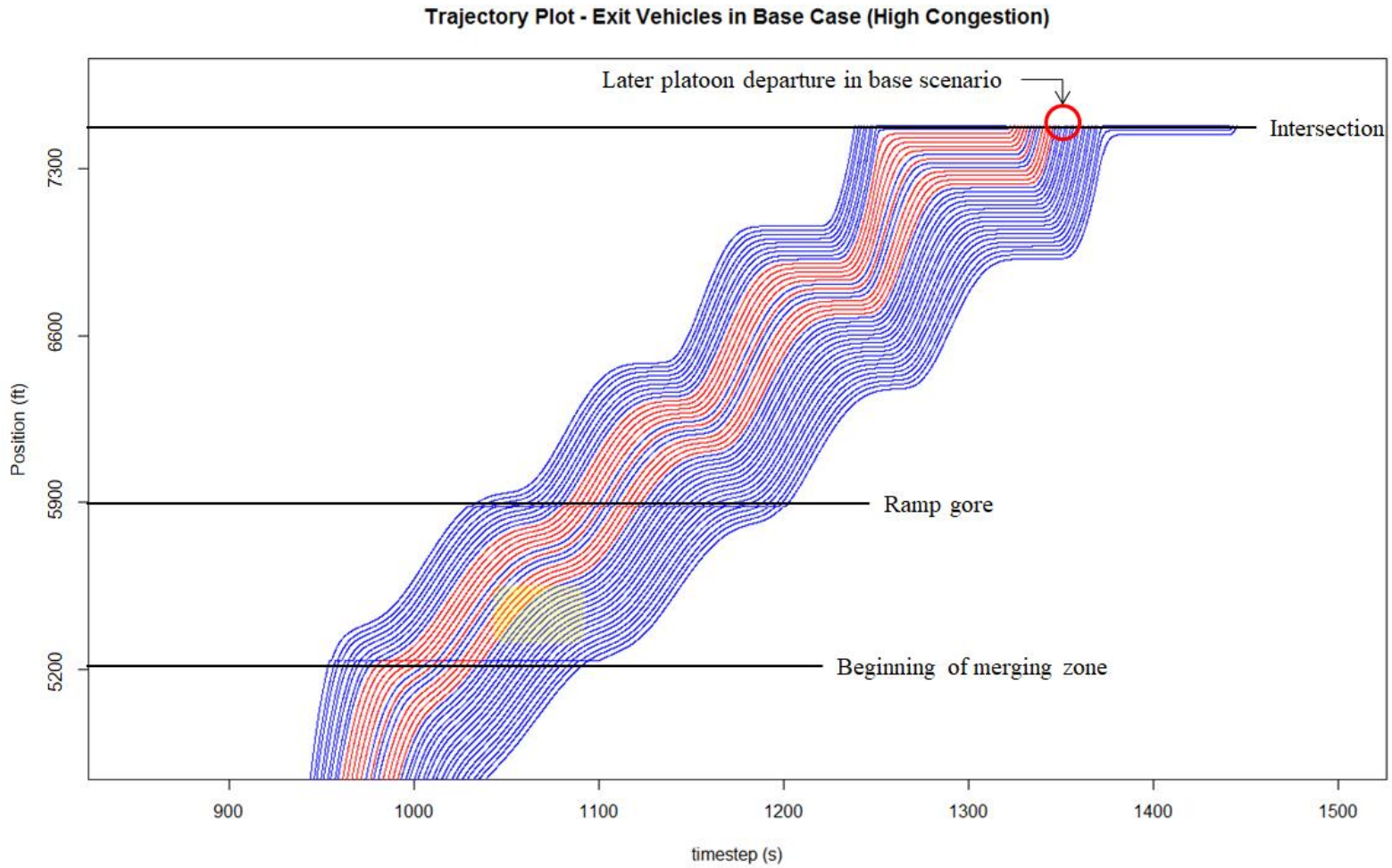

Figure 17. Plot. Base case time–space diagram in congested deceleration-lane scenario.

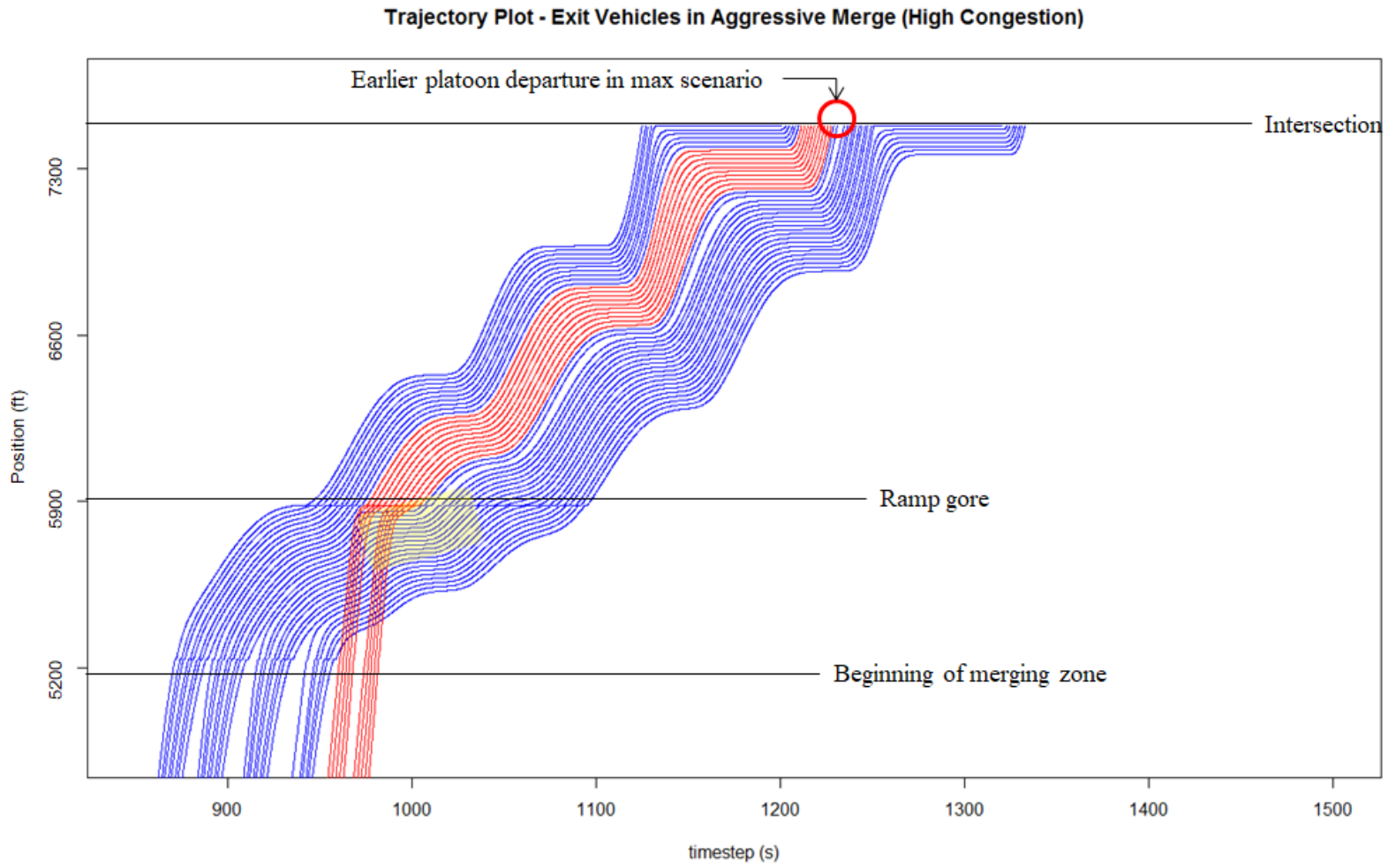

Figure 18. Plot. Aggressive merge with maximum advancement time–space diagram in congested deceleration-lane scenario.

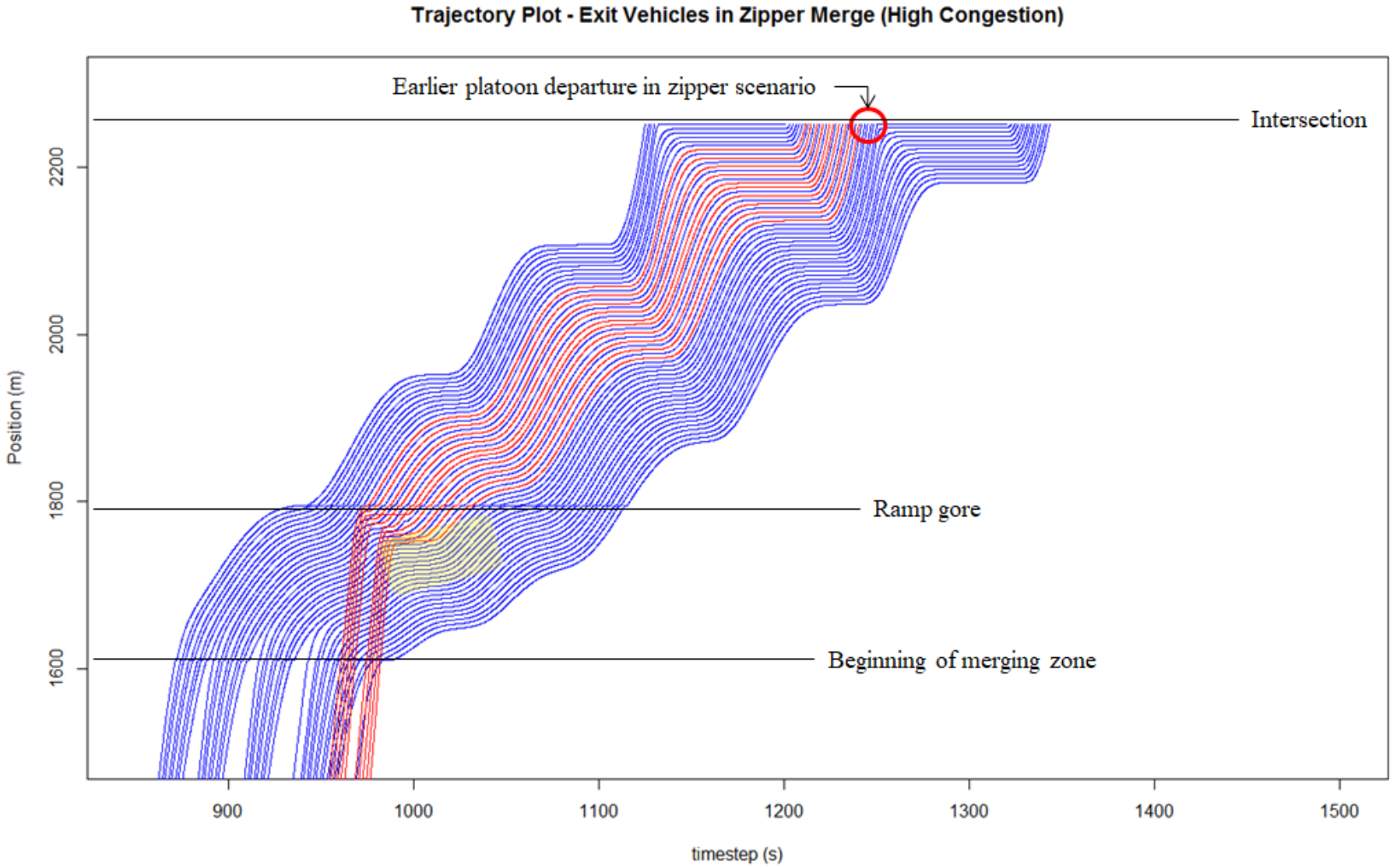

Figure 19. Plot. Aggressive merge with zipper time–space diagram in congested deceleration-lane scenario.

Experiment 2: Aggressive Merging with Random Arrivals

Objective

While the initial experiment investigated the impact of AHDVs in a platoon, the objective of this experiment is to investigate the impact of aggressive merging behavior under conditions where the AHDVs are distributed throughout the traffic stream.

Experiment Design

The roadway layout for this experiment is the same as the previous experiment. Traffic volume is balanced in the mainline lanes entering the merge zone. All exiting vehicles enter the merge zone already positioned in lane A_1 (see figure 2). Thus, all vehicles in the left-most lane A_0 are through vehicles only, while vehicles on lane A_1 consist of both through and exit vehicles. In this experiment, 35 percent of the traffic is assumed to exit; thus, 70 percent of the lane A_1 vehicles were assigned as exit vehicles, consisting of AVs, HDVs, and AHDVs (percentages described subsequently). All exit vehicles except for the AHDVs shift over to the deceleration lane B_2 when they reach the merging zone, at the start of the deceleration lane. The AHDVs continue to travel on lane B_1 and make a lane change to B_2 by either aggressive merge or SUMO-controlled merge, as defined previously.

Two levels of traffic demand were considered in this experiment—high traffic demand (1,200 vehicles/hour/lane) and low traffic demand (600 vehicles/hour/lane). For each traffic-demand level, five different AV ratios (percentage of the total traffic that is AV) and five different AHDV/HDV ratios (including the base case with no AHDVs) of exiting traffic not assigned as AV were considered, as shown in table 5.

The distinction between experiment 2 and experiment 3 (presented in the next section) is in the signal timing at the ramp end intersection. In this experiment, 50 seconds of green time and 70 seconds of red time are used for both the lower traffic-demand and higher traffic-demand conditions. This results in no queue spillback to the deceleration lane in the low traffic-demand case, but there was queueing on the deceleration lane in the high traffic-demand case. The base case consists of only AV and HDV. Each scenario has 10 replicate runs.

Figure **20 –** figure 23 show the average travel time of exit vehicles by vehicle type in each scenario. Note that the y-axis scales are different in the two sets of figures to accommodate the wider range of travel times in high traffic-demand conditions.

Table 6 and table 7 show the paired t-test results on the travel times of AHDVs compared to the travel times of AVs and HDVs. The ‘Difference’ column shows whether the difference is statistically significant (marked as TRUE if significantly different and FALSE otherwise).

Table 5. Vehicle assignment for experiments 2 and 3.

	AV Ratio	Start Lane	Lane A_0		Lane A_1				
		Direction	Through		Through		Exit		
		AHDV Ratio	HDV	AV	HDV	AV	HDV	AV	AHDV
Lower Traffic Demand	10%	0% (Base)	540	60	162	18	378	42	0
		25%	540	60	162	18	284	42	95
		50%	540	60	162	18	189	42	189
		75%	540	60	162	18	95	42	284
		100%	540	60	162	18	0	42	378
	20%	0% (Base)	480	120	144	36	336	84	0
		25%	480	120	144	36	252	84	84
		50%	480	120	144	36	168	84	168
		75%	480	120	144	36	84	84	252
		100%	480	120	144	36	0	84	336
	30%	0% (Base)	420	180	126	54	294	126	0
		25%	420	180	126	54	221	126	74
		50%	420	180	126	54	147	126	147
		75%	420	180	126	54	74	126	221
		100%	420	180	126	54	0	126	294
	40%	0% (Base)	360	240	108	72	252	168	0
		25%	360	240	108	72	189	168	63
		50%	360	240	108	72	126	168	126
		75%	360	240	108	72	63	168	189
		100%	360	240	108	72	0	168	252
	50%	0% (Base)	300	300	90	90	210	210	0
		25%	300	300	90	90	158	210	53
		50%	300	300	90	90	105	210	105
		75%	300	300	90	90	53	210	158
		100%	300	300	90	90	0	210	210
Higher Traffic Demand	10%	0% (Base)	1080	120	324	36	756	84	0
		25%	1080	120	324	36	567	84	189
		50%	1080	120	324	36	378	84	378
		75%	1080	120	324	36	189	84	567
		100%	1080	120	324	36	0	84	756
	20%	0% (Base)	960	240	288	72	672	168	0
		25%	960	240	288	72	504	168	168
		50%	960	240	288	72	336	168	336
		75%	960	240	288	72	168	168	504
		100%	960	240	288	72	0	168	672
	30%	0% (Base)	840	360	252	108	588	252	0
		25%	840	360	252	108	441	252	147
		50%	840	360	252	108	294	252	294
		75%	840	360	252	108	147	252	441
		100%	840	360	252	108	0	252	588
	40%	0% (Base)	720	480	216	144	504	336	0
		25%	720	480	216	144	378	336	126
		50%	720	480	216	144	252	336	252
		75%	720	480	216	144	126	336	378
		100%	720	480	216	144	0	336	504
	50%	0% (Base)	600	600	180	180	420	420	0
		25%	600	600	180	180	315	420	105
		50%	600	600	180	180	210	420	210
		75%	600	600	180	180	105	420	315
		100%	600	600	180	180	0	420	420

Results

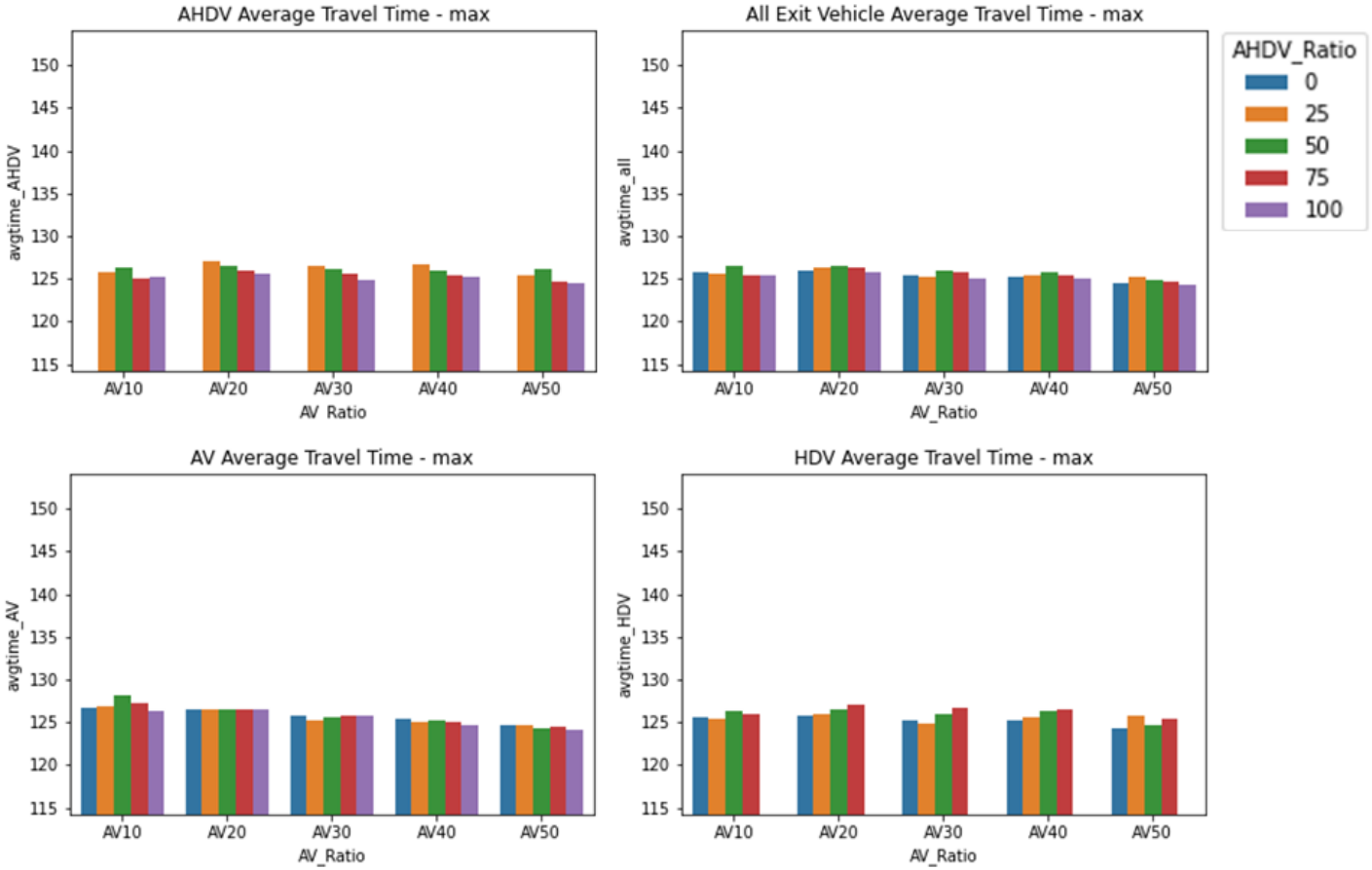

Figure 20**. Bar plots. Experiment 2: Average travel time in aggressive merge with maximum advancement scenarios by vehicle type in low traffic-demand condition.**

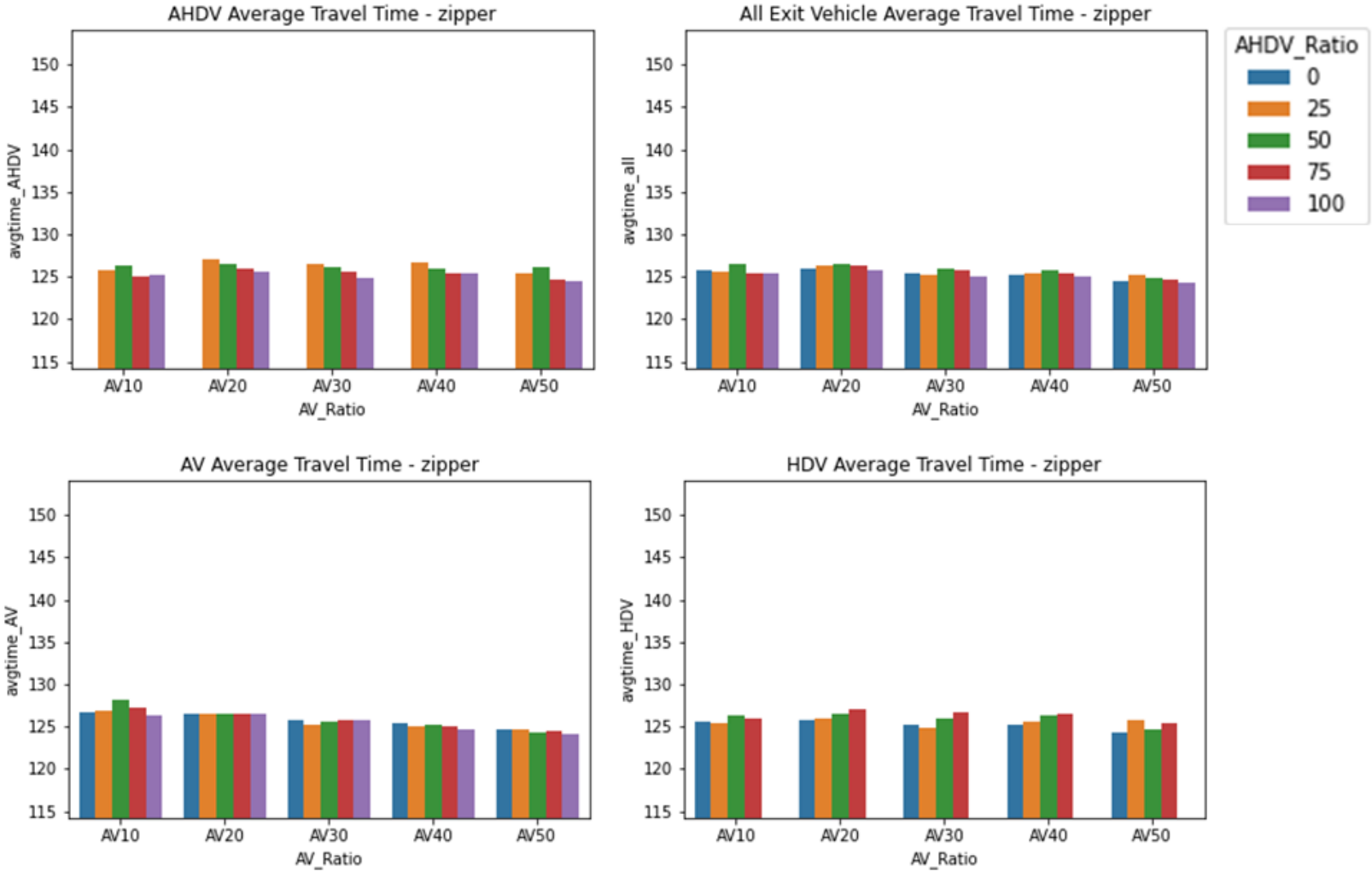

Figure 21. Bar plots. Experiment 2: Average travel time in aggressive merge with zipper scenarios by vehicle type in low traffic-demand condition.

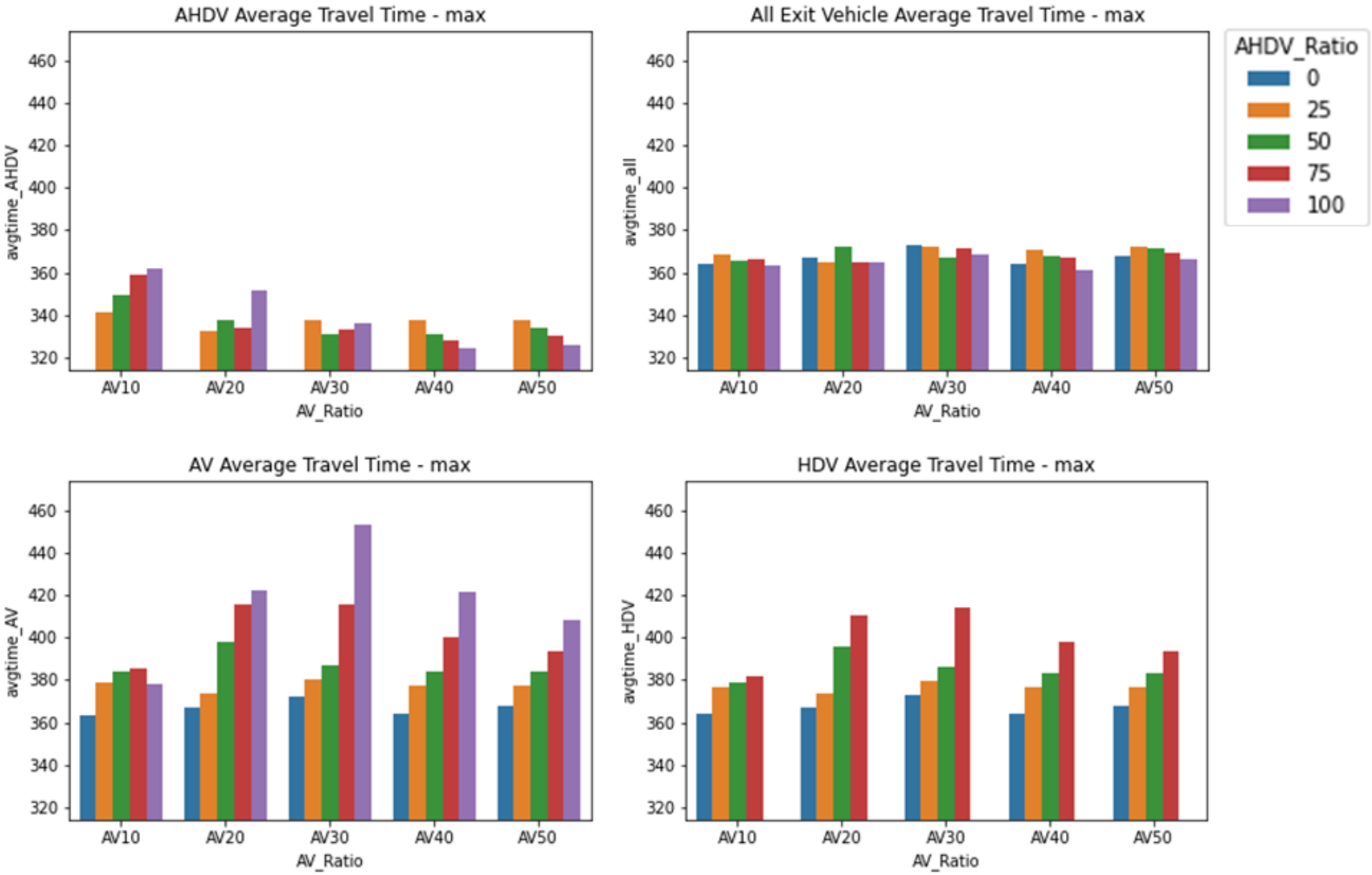

Figure 22. Bar plots. Experiment 2: Average travel time in aggressive merge with maximum advancement scenarios by vehicle type in high traffic-demand condition.

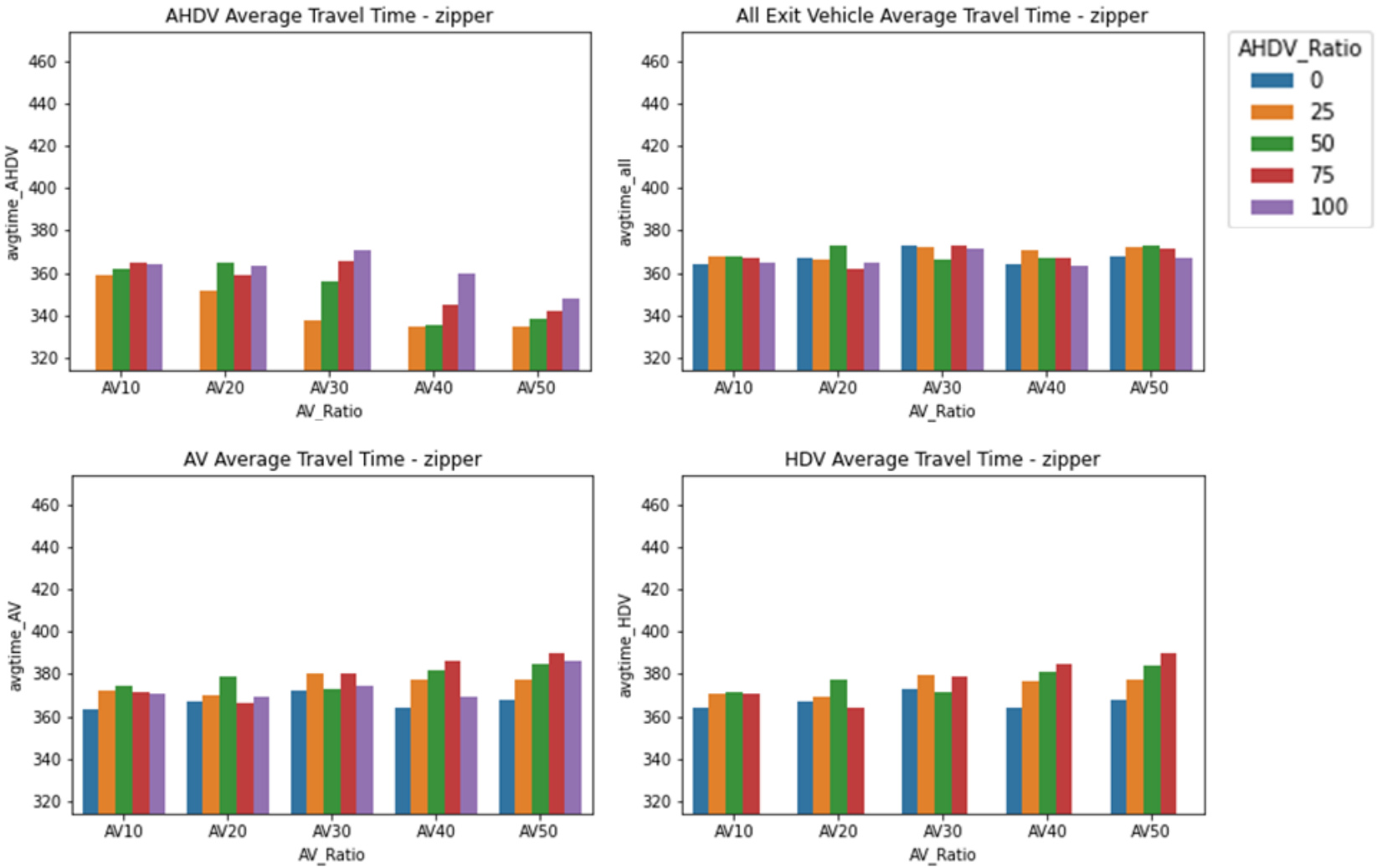

Figure 23. Bar plots. Experiment 2: Average travel time in aggressive merge with zipper by vehicle type in high traffic-demand condition.

Table 6. Experiment 2: Paired t-test on travel time in aggressive merge with maximum advancement scenarios.

	Volume = 600 veh/hr/ln, AV10				Volume = 600 veh/hr/ln, AV20			
AHDV Ratio	AHDV vs. AV		AHDV vs. HDV		AHDV vs. AV		AHDV vs. HDV	
	P-Value	Difference	P-Value	Difference	P-Value	Difference	P-Value	Difference
25	0.304	FALSE	0.429	FALSE	0.480	FALSE	0.065	FALSE
50	0.078	FALSE	0.958	FALSE	0.846	FALSE	0.749	FALSE
75	0.059	FALSE	0.060	FALSE	0.348	FALSE	0.044	TRUE
100	0.159	FALSE	-		0.238	FALSE	-	
	Volume = 600 veh/hr/ln, AV30				Volume = 600 veh/hr/ln, AV40			
AHDV Ratio	AHDV vs. AV		AHDV vs. HDV		AHDV vs. AV		AHDV vs. HDV	
	P-Value	Difference	P-Value	Difference	P-Value	Difference	P-Value	Difference
25	0.016	TRUE	0.007	TRUE	0.043	TRUE	0.069	FALSE
50	0.105	FALSE	0.410	FALSE	0.282	FALSE	0.461	FALSE
75	0.808	FALSE	0.071	FALSE	0.457	FALSE	0.132	FALSE
100	0.080	FALSE	-		0.157	FALSE	-	
	Volume = 600 veh/hr/ln, AV50				Volume = 1200 veh/hr/ln, AV10			
AHDV Ratio	AHDV vs. AV		AHDV vs. HDV		AHDV vs. AV		AHDV vs. HDV	
	P-Value	Difference	P-Value	Difference	P-Value	Difference	P-Value	Difference
25	0.476	FALSE	0.409	FALSE	3.20E-09	TRUE	5.45E-10	TRUE
50	0.003	TRUE	0.010	TRUE	1.43E-11	TRUE	6.33E-12	TRUE
75	0.764	FALSE	0.387	FALSE	1.65E-08	TRUE	2.56E-09	TRUE
100	0.624	FALSE	-		1.37E-08	TRUE	-	
	Volume = 1200 veh/hr/ln, AV20				Volume = 1200 veh/hr/ln, AV30			
AHDV Ratio	AHDV vs. AV		AHDV vs. HDV		AHDV vs. AV		AHDV vs. HDV	
	P-Value	Difference	P-Value	Difference	P-Value	Difference	P-Value	Difference
25	1.15E-11	TRUE	5.30E-12	TRUE	9.46E-13	TRUE	4.56E-13	TRUE
50	4.91E-12	TRUE	1.56E-12	TRUE	6.38E-12	TRUE	2.02E-12	TRUE
75	5.53E-09	TRUE	8.54E-09	TRUE	1.41E-11	TRUE	2.19E-11	TRUE
100	1.51E-10	TRUE	-		2.90E-11	TRUE	-	
	Volume = 1200 veh/hr/ln, AV40				Volume = 1200 veh/hr/ln, AV50			
AHDV Ratio	AHDV vs. AV		AHDV vs. HDV		AHDV vs. AV		AHDV vs. HDV	
	P-Value	Difference	P-Value	Difference	P-Value	Difference	P-Value	Difference
25	4.54E-14	TRUE	2.87E-13	TRUE	2.35E-12	TRUE	3.47E-12	TRUE
50	1.18E-11	TRUE	9.95E-12	TRUE	2.42E-11	TRUE	1.67E-11	TRUE
75	6.70E-11	TRUE	5.94E-11	TRUE	1.44E-11	TRUE	3.10E-11	TRUE
100	1.09E-10	TRUE	-		1.31E-09	TRUE	-	

Table 7. Experiment 2: Paired t-test on travel time in aggressive merge with zipper scenarios.

	Volume = 600 veh/hr/ln, AV10				Volume = 600 veh/hr/ln, AV20			
AHDV Ratio	AHDV vs. AV		AHDV vs. HDV		AHDV vs. AV		AHDV vs. HDV	
	P-Value	Difference	P-Value	Difference	P-Value	Difference	P-Value	Difference
25	0.304	FALSE	0.429	FALSE	0.480	FALSE	0.065	FALSE
50	0.078	FALSE	0.958	FALSE	0.846	FALSE	0.749	FALSE
75	0.05	FALSE	0.060	FALSE	0.350	FALSE	0.044	TRUE
100	0.15	FALSE			0.253	FALSE		
	Volume = 600 veh/hr/ln, AV30				Volume = 600 veh/hr/ln, AV40			
AHDV Ratio	AHDV vs. AV		AHDV vs. HDV		AHDV vs. AV		AHDV vs. HDV	
	P-Value	Difference	P-Value	Difference	P-Value	Difference	P-Value	Difference
25	0.016	TRUE	0.007	TRUE	0.043	TRUE	0.069	FALSE
50	0.105	FALSE	0.410	FALSE	0.282	FALSE	0.462	FALSE
75	0.811	FALSE	0.071	FALSE	0.458	FALSE	0.132	FALSE
100	0.081	FALSE			0.129	FALSE		
	Volume = 600 veh/hr/ln, AV50				Volume = 1200 veh/hr/ln, AV10			
AHDV Ratio	AHDV vs. AV		AHDV vs. HDV		AHDV vs. AV		AHDV vs. HDV	
	P-Value	Difference	P-Value	Difference	P-Value	Difference	P-Value	Difference
25	0.476	FALSE	0.409	FALSE	1.06E-07	TRUE	3.58E-08	TRUE
50	0.003	TRUE	0.010	TRUE	3.49E-07	TRUE	6.26E-08	TRUE
75	0.643	FALSE	0.417	FALSE	8.66E-08	TRUE	6.87E-08	TRUE
100	0.619	FALSE			1.08E-06	TRUE		
	Volume = 1200 veh/hr/ln, AV20				Volume = 1200 veh/hr/ln, AV30			
AHDV Ratio	AHDV vs. AV		AHDV vs. HDV		AHDV vs. AV		AHDV vs. HDV	
	P-Value	Difference	P-Value	Difference	P-Value	Difference	P-Value	Difference
25	8.65E-07	TRUE	7.89E-07	TRUE	8.07E-11	TRUE	1.34E-10	TRUE
50	2.12E-05	TRUE	3.16E-05	TRUE	0.001	TRUE	0.001	TRUE
75	9.28E-06	TRUE	7.57E-05	TRUE	1.51E-06	TRUE	2.02E-06	TRUE
100	3.80E-06	TRUE			1.50E-06	TRUE		
	Volume = 1200 veh/hr/ln, AV40				Volume = 1200 veh/hr/ln, AV50			
AHDV Ratio	AHDV vs. AV		AHDV vs. HDV		AHDV vs. AV		AHDV vs. HDV	
	P-Value	Difference	P-Value	Difference	P-Value	Difference	P-Value	Difference
25	9.95E-11	TRUE	1.96E-10	TRUE	5.05E-13	TRUE	1.29E-12	TRUE
50	1.99E-09	TRUE	1.19E-09	TRUE	1.11E-07	TRUE	6.41E-08	TRUE
75	7.77E-06	TRUE	1.31E-05	TRUE	1.97E-07	TRUE	3.99E-07	TRUE
100	1.15E-05	TRUE			2.58E-07	TRUE		

Discussion

The travel times of exit vehicles in low traffic-demand scenarios, as shown in figure **20** and figure 21, were not significantly impacted by the aggressive merges, with no clear

trends being apparent. The travel times between vehicle types or AV penetration rates never differ by more than a few seconds. No queue formed on the deceleration lane in low traffic demand, so most AHDVs performed lane changes to the deceleration lane immediately since the deceleration lane was empty. In a few cases where AHDVs performed aggressive merges, the impacts of the aggressive merges may have been muted because of the existence of large headways between the vehicles. As a result, the paired t-test in low traffic-demand conditions showed that AHDVs had no significant difference in travel time compared to AVs and HDVs in most scenarios. These results are in concurrence with the findings in experiment 1. In figure 15 and figure 16 (uncongested deceleration lane), the impact to the non-AHDV is clearly more muted than the impact seen in figure 18 and figure 19 (congested merge lane). The impacts of the aggressive merges were not passed down to the following vehicles in low traffic demand.

In high traffic-demand conditions, the AHDVs' travel times are significantly lower than the travel times of AVs and HDVs in all scenarios with the aggressive merges, as shown in table 6 and table 7. However, the overall average exit times remained relatively constant, implying that as the AHDVs were able to improve their travel time, the AVs and HDV suffered increased travel time. The HDVs' travel time did not increase to the same extent as the AVs'; however, they did see travel time increases, even though they were never "targeted" by the AHDV. The HDV increase results from HDVs in the deceleration lane following AVs that are targeted.

In aggressive merge with maximum advancement cases, it is also seen that the AHDV travel times show (figure 22) an increasing trend at the lower AV ratios (10 and 20 percent). However, the trend reverses when the AV ratios were high (30–50 percent).

The reason for this behavior is that when there is a smaller number of AVs to target, more AHDVs merged via SUMO-control (i.e., non-aggressive merge), which requires a longer time to complete. As the availability of target AVs increased with higher AV ratios, more AHDVs successfully completed aggressive merges by targeting AVs.

It was also observed during the simulation run that multiple AHDVs targeted the same AV on the deceleration lane, forcing the target AV, as well as the following traffic, to come to a complete stop, similar to the observations for the experiment 1 congested conditions.

However, the AHDV travel times in the aggressive merge with zipper cases in high congestion showed an increasing trend with higher AHDV ratios in all scenarios. It should be noted that there is no direct relationship between the AV ratios and AHDV ratios since the target selection is affected by both AV ratios and the position of the AHDVs. If an AHDV needs to target a following AV to the previous merge and the AHDV is closer to an HDV compared to the target AV, the AHDV will merge to the HDV via SUMO-controlled merge. Therefore, more AHDVs merged via SUMO-controlled merge as the AHDV ratios increased, which resulted in the increasing trend in travel time in all scenarios.

The bar charts suggested that the aggressive merge with maximum advancement had greater impact on the AV and HDV travel times than the aggressive merge with zipper in high flow rate conditions. In aggressive merge with maximum advancement cases, multiple AHDVs targeted the same AV on the deceleration lane, leading the target AV as well as the following traffic to come to a complete stop. Such behavior was also shown in the preliminary experiment. The blue slopes after the merge in figure 18 became flat,

indicating a complete stop due to the merge. However, in the aggressive merge with zipper cases, the target vehicle moved forward after a single AHDV's merge.

The net impacts of AHDVs' aggressive merging behaviors on all exit vehicles (AHDV, AV, and HDV) are shown in the 'All Exit Vehicle Travel Time' bar charts in figure **20–** figure 23. In low traffic-demand conditions, the net impact was insignificant since most AHDVs changed their lanes to the deceleration lane immediately after reaching the merging zone and the few cases of aggressive merges left little impacts on the target AVs and the following traffic. In high traffic-demand conditions, the net impact was insignificant due to the discussed trade-off effects. The AHDVs' travel-time decreases were achieved at the expense of the travel-time increases of the AVs and HDVs.

Experiment 3: Comparison of Impact of Demand versus Congestion on Travel Times

Objective

The objective of this experiment is to differentiate between the impact due to increased demand or congestion. Thus, in this experiment the ramp intersection signal times were adjusted such that the low-demand volume resulted in queuing on the deceleration lane and the high-demand volume had no queuing.

Results

Similar to experiment 2, figure 24 **–** figure 27 show the average travel time by exit vehicle type in each scenario. While the absolute travel times change due to the signal timing updates, trade-offs are again seen between the AHDVs and the AVs/HDVs. Except, the trade-off between the AHDVs and AVs/HDVs now occurs at the lower volume case, with no obvious trends in the high-volume case. Also similar to

experiment 2, the difference in the scenarios with queuing on the deceleration lane (i.e., the low-volume demand in this experiment) are predominately statistically significant, while the scenarios without queueing on the deceleration lane (i.e., high-volume scenarios) are not statistically significant, as shown in table 8 and table 9.

In aggressive merge with maximum advancement cases, the only significant difference in trends was seen in the AHDV delay across AV ratios, which was increasing throughout the low volume in experiment 3. Based on observations of the simulation, it was seen that the change in signal timing resulted in a slower-moving queue, increasing the time required for an AHDV to merge into the deceleration lane, even with aggressive merges. This resulted in more AHDV stacking in the adjacent lane, waiting to merge, and a higher sensitivity to the number of AHDVs.

In the aggressive merge with zipper cases, shown in figure 25, the AHDV travel times are similar in the higher AHDV ratio scenarios due to the same reason discussed above. Since each AHDV can merge in front of a single AV or a single HDV, the AHDV line becomes longer in lower AV ratios, regardless of the AHDV ratios. However, in higher AV ratio scenarios, more AHDVs can perform aggressive merges, which requires less gap compared to SUMO-controlled merges. As a result, the AHDV travel time becomes lower in the lower AHDV ratio with higher AV ratio scenarios.

From this experiment, in context with the previous experiments, it is seen that the presence of queuing (or near- or over-capacity conditions) is a critical factor in the impact of the AHDVs, as this presents significant opportunities for the aggressive behavior. The absolute volume has a lesser impact.

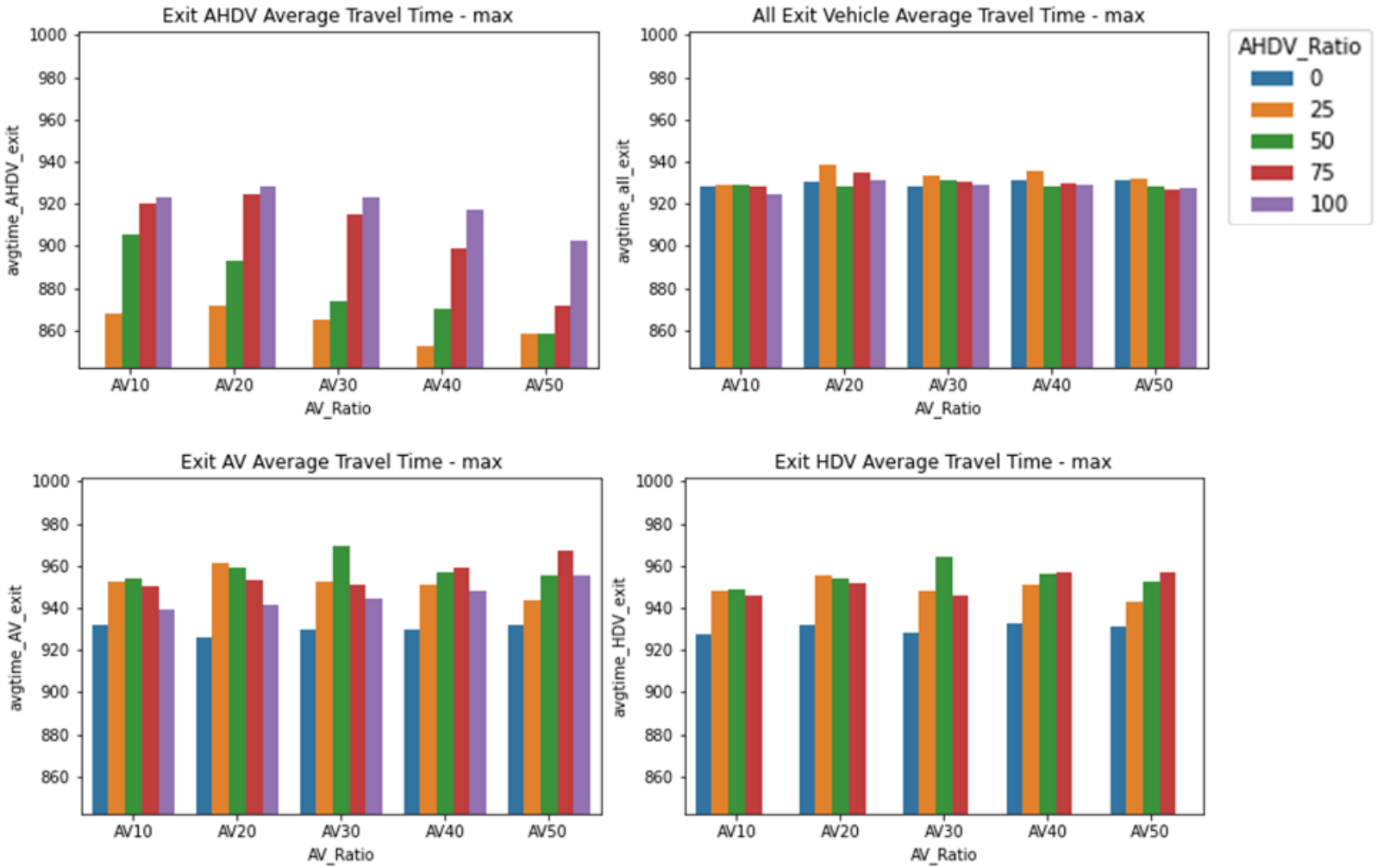

Figure 24. Bar plots. Experiment 3: Average travel time in aggressive merge with maximum advancement scenarios by vehicle type in low traffic-demand condition.

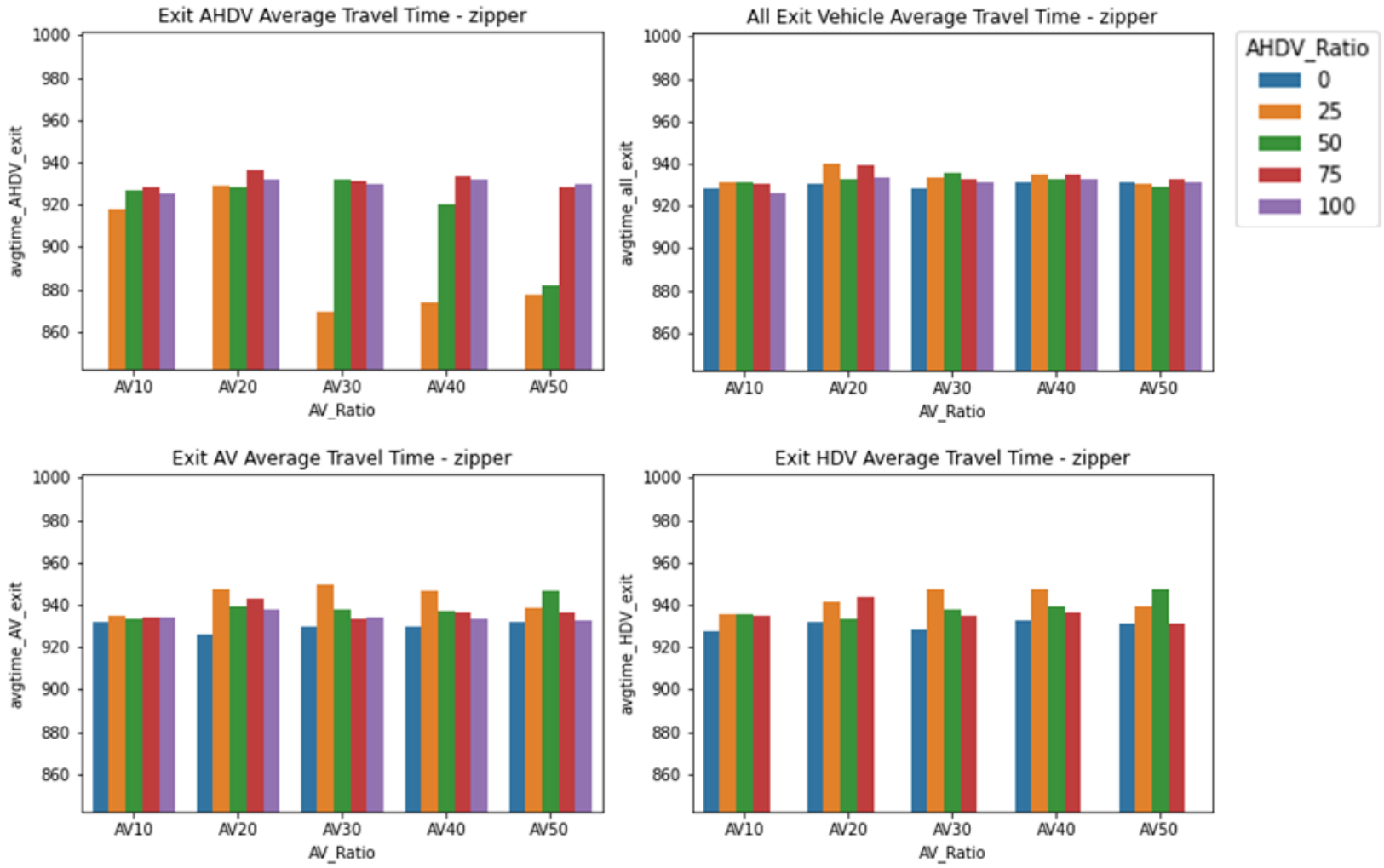

Figure 25. Bar plots. Experiment 3: Average travel time in aggressive merge with zipper scenarios by vehicle type in low traffic-demand condition.

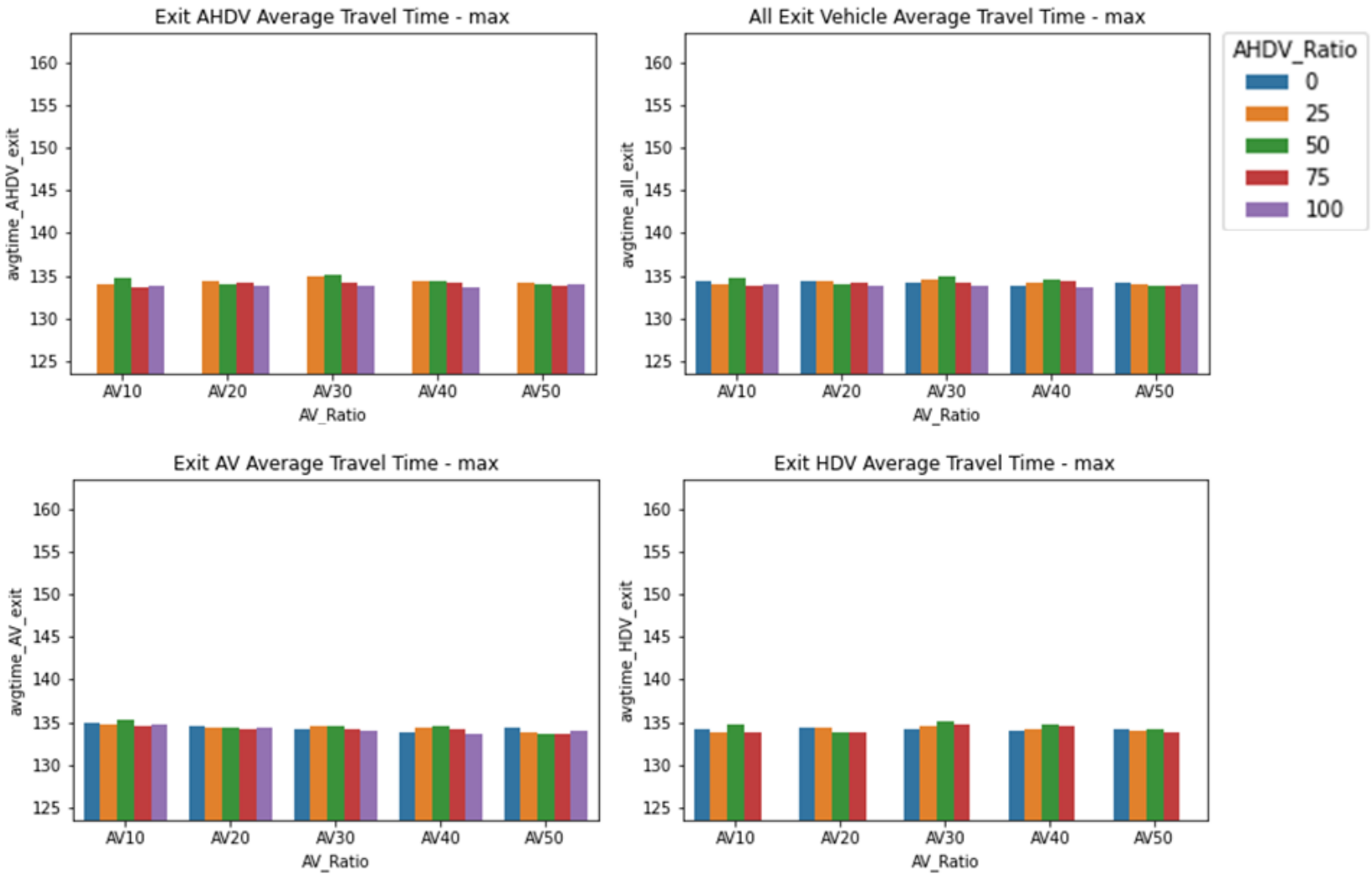

Figure 26. Bar plots. Experiment 3: Average travel time in aggressive merge with maximum advancement scenarios by vehicle type in high traffic-demand condition.

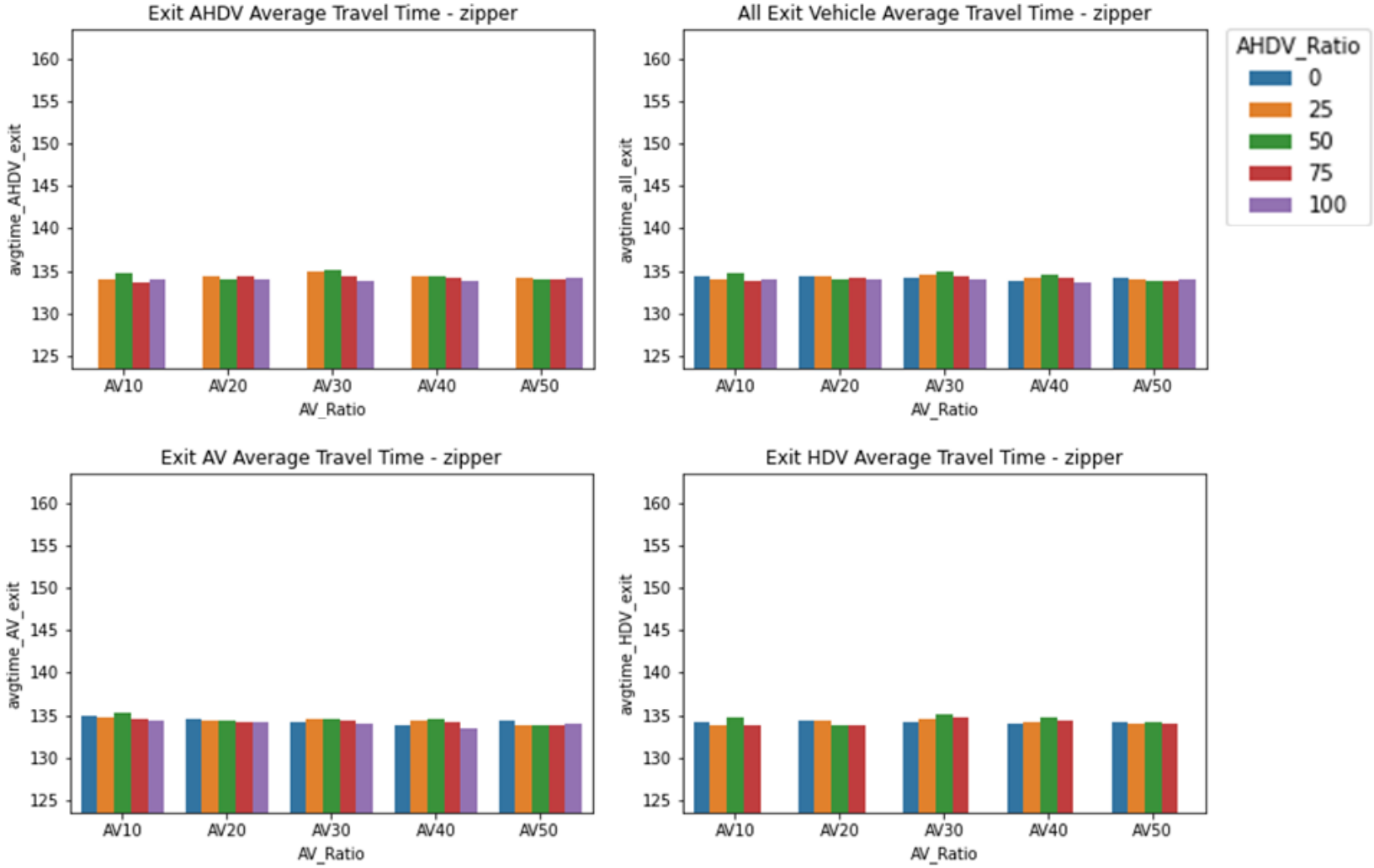

Figure 27. Bar plots. Experiment 3: Average travel time in aggressive merge with zipper scenarios by vehicle type in high traffic-demand condition.

Table 8. Experiment 3: Paired t-test on travel time in aggressive merge with maximum advancement scenarios.

	Volume = 600 veh/hr/ln, AV10				Volume = 600 veh/hr/ln, AV20			
AHDV Ratio	AHDV vs. AV		AHDV vs. HDV		AHDV vs. AV		AHDV vs. HDV	
	P-Value	Difference	P-Value	Difference	P-Value	Difference	P-Value	Difference
25	3.52E-13	TRUE	8.61E-13	TRUE	5.87E-12	TRUE	1.83E-10	TRUE
50	1.00E-07	TRUE	6.09E-07	TRUE	7.20E-07	TRUE	1.73E-06	TRUE
75	1.34E-07	TRUE	2.33E-06	TRUE	0.001	TRUE	0.004	TRUE
100	0.001	TRUE	-		0.080	FALSE	-	
	Volume = 600 veh/hr/ln, AV30				Volume = 600 veh/hr/ln, AV40			
AHDV Ratio	AHDV vs. AV		AHDV vs. HDV		AHDV vs. AV		AHDV vs. HDV	
	P-Value	Difference	P-Value	Difference	P-Value	Difference	P-Value	Difference
25	1.88E-11	TRUE	4.08E-11	TRUE	4.19E-09	TRUE	6.29E-10	TRUE
50	3.22E-10	TRUE	2.80E-10	TRUE	1.00E-05	TRUE	3.94E-06	TRUE
75	1.34E-06	TRUE	1.02E-05	TRUE	9.43E-07	TRUE	5.80E-07	TRUE
100	2.74E-05	TRUE	-		1.18E-05	TRUE	-	
	Volume = 600 veh/hr/ln, AV50				Volume = 1200 veh/hr/ln, AV10			
AHDV Ratio	AHDV vs. AV		AHDV vs. HDV		AHDV vs. AV		AHDV vs. HDV	
	P-Value	Difference	P-Value	Difference	P-Value	Difference	P-Value	Difference
25	2.71E-11	TRUE	3.24E-11	TRUE	0.154	FALSE	0.446	FALSE
50	2.69E-11	TRUE	8.97E-11	TRUE	0.247	FALSE	0.555	FALSE
75	4.77E-09	TRUE	4.39E-08	TRUE	0.040	TRUE	0.858	FALSE
100	1.24E-06	TRUE	-		0.079	FALSE	-	
	Volume = 1200 veh/hr/ln, AV20				Volume = 1200 veh/hr/ln, AV30			
AHDV Ratio	AHDV vs. AV		AHDV vs. HDV		AHDV vs. AV		AHDV vs. HDV	
	P-Value	Difference	P-Value	Difference	P-Value	Difference	P-Value	Difference
25	0.876	FALSE	0.314	FALSE	0.416	FALSE	0.273	FALSE
50	0.116	FALSE	0.250	FALSE	0.065	FALSE	0.869	FALSE
75	0.967	FALSE	0.220	FALSE	0.685	FALSE	0.111	FALSE
100	0.036	TRUE	-		0.109	FALSE	-	
	Volume = 1200 veh/hr/ln, AV40				Volume = 1200 veh/hr/ln, AV50			
AHDV Ratio	AHDV vs. AV		AHDV vs. HDV		AHDV vs. AV		AHDV vs. HDV	
	P-Value	Difference	P-Value	Difference	P-Value	Difference	P-Value	Difference
25	0.850	FALSE	0.610	FALSE	0.318	FALSE	0.603	FALSE
50	0.480	FALSE	0.292	FALSE	0.415	FALSE	0.437	FALSE
75	0.776	FALSE	0.109	FALSE	0.177	FALSE	0.931	FALSE
100	0.568	FALSE	-		0.960	FALSE	-	

Table 9. Experiment 3: Paired t-test on travel time in aggressive merge with zipper scenarios.

	Volume = 600 veh/hr/ln, AV10				Volume = 600 veh/hr/ln, AV20			
AHDV Ratio	AHDV vs. AV		AHDV vs. HDV		AHDV vs. AV		AHDV vs. HDV	
	P-Value	Difference	P-Value	Difference	P-Value	Difference	P-Value	Difference
25	4.92E-05	TRUE	4.50E-07	TRUE	0.001	TRUE	0.005	TRUE
50	0.075	FALSE	0.001	TRUE	0.006	TRUE	0.020	TRUE
75	0.043	TRUE	0.001	TRUE	0.005	TRUE	0.029	TRUE
100	0.007	TRUE			0.009	TRUE		
	Volume = 600 veh/hr/ln, AV30				Volume = 600 veh/hr/ln, AV40			
AHDV Ratio	AHDV vs. AV		AHDV vs. HDV		AHDV vs. AV		AHDV vs. HDV	
	P-Value	Difference	P-Value	Difference	P-Value	Difference	P-Value	Difference
25	3.91E-09	TRUE	2.62E-08	TRUE	5.33E-08	TRUE	4.52E-09	TRUE
50	0.027	TRUE	0.001	TRUE	0.001	TRUE	0.001	TRUE
75	0.049	TRUE	0.025	TRUE	0.224	FALSE	0.321	FALSE
100	0.050	FALSE			0.283	FALSE		
	Volume = 600 veh/hr/ln, AV50				Volume = 1200 veh/hr/ln, AV10			
AHDV Ratio	AHDV vs. AV		AHDV vs. HDV		AHDV vs. AV		AHDV vs. HDV	
	P-Value	Difference	P-Value	Difference	P-Value	Difference	P-Value	Difference
25	1.37E-07	TRUE	8.04E-08	TRUE	0.154	FALSE	0.446	FALSE
50	1.91E-07	TRUE	4.81E-08	TRUE	0.283	FALSE	0.634	FALSE
75	0.007	TRUE	0.354	FALSE	0.047	TRUE	0.790	FALSE
100	0.221	FALSE			0.251	FALSE		
	Volume = 1200 veh/hr/ln, AV20				Volume = 1200 veh/hr/ln, AV30			
AHDV Ratio	AHDV vs. AV		AHDV vs. HDV		AHDV vs. AV		AHDV vs. HDV	
	P-Value	Difference	P-Value	Difference	P-Value	Difference	P-Value	Difference
25	0.876	FALSE	0.314	FALSE	0.416	FALSE	0.273	FALSE
50	0.208	FALSE	0.1174	FALSE	0.064	FALSE	0.838	FALSE
75	0.878	FALSE	0.166	FALSE	0.705	FALSE	0.159	FALSE
100	0.164	FALSE			0.558	FALSE		
	Volume = 1200 veh/hr/ln, AV40				Volume = 1200 veh/hr/ln, AV50			
AHDV Ratio	AHDV vs. AV		AHDV vs. HDV		AHDV vs. AV		AHDV vs. HDV	
	P-Value	Difference	P-Value	Difference	P-Value	Difference	P-Value	Difference
25	0.855	FALSE	0.611	FALSE	0.360	FALSE	0.651	FALSE
50	0.522	FALSE	0.305	FALSE	0.381	FALSE	0.577	FALSE
75	0.981	FALSE	0.183	FALSE	0.114	FALSE	0.941	FALSE
100	0.097	FALSE			0.559	FALSE		

Experiment 4: Evaluation of Impact of Aggressive Merging on Capacity

Experiment Design

Experiment 4 examines the impacts of aggressive characteristics in vehicles near a freeway exit on the capacity of the exit lane. Vehicles with two levels of cooperative characteristics were used. The two levels were implemented with the lowest value and the highest value of the SUMO built-in parameter, *lcCooperativeSpeed*. Varying levels of cooperative behavior were emulated by changing the ratio of noncooperative (*lcCooperativeSpeed* = 0) and cooperative (*lcCooperativeSpeed* = 1) vehicles from 0 to 1. When a vehicle with cooperative behavior is available in the traffic, SUMO tries to perform the lane-changing for a vehicle in front of the farthest downstream cooperative vehicle that is reachable. This operation is very similar to the aggressive merging logic developed for AHDV in the previous experiments, albeit with a slightly less degree of control available to the modeler on which vehicles behave as aggressive vehicles than that achieved in experiments 1 to 3 with the explicit modeling of AHDVs.

The experiment is conducted in a two-lane freeway stretched out for 2 miles. A 2,000-ft deceleration lane is added at the end of the 2-mile freeway segment, which is then followed by an exit ramp, as shown in figure 1. All vehicles are seeking to exit the freeway using the ramp. As shown in figure 2, the left-lane (A_0) traffic travels with higher speed than the right-lane (A_1) traffic, creating the opportunity for the left-lane traffic to queue-jump. Both A_1 and A_0 traffic had a mix of vehicles with *lcCooperativeSpeed* of 1 and 0, indicating the highest level of cooperative characteristic and the lowest level of cooperative characteristic, respectively. The A_1 traffic volume was maintained the same throughout the simulation, whereas the A_0 traffic volumes

were increased every 900 seconds. Details on the vehicle assignment are provided in the following section.

The A_0 traffic's route was changed from traveling on the freeway mainline to taking the exit ramp when they arrive at the merging zone indicated in figure 1. Once the route change assignment is complete, the A_0 vehicles begin their lane-changing process. The lane-changing is controlled by SUMO. Some vehicles immediately change their lanes to lane B_1, while others continue to travel on lane B_0 depending on the availability of gaps on lane B_1. For the right lane, all A_1 traffic shifts uninterrupted to lane B_2.

It should be noted that this study assumes the same headways for all vehicle types—regardless of the level of cooperative characteristics. This eventually becomes a critical factor in explaining how the flow rate was not affected by the aggressive characteristics—but rather, there was a trade-off between the vehicle types that exited on the ramp.

Vehicle Classification

Two types of vehicles were considered in the experiments: human-driven vehicles with a SUMO *lcCooperativeSpeed* value of 0 (referred to as HV0 hereafter), and human-driven vehicles with *lcCooperativeSpeed* value of 1 (referred to as HV1 hereafter).

The value of 1 in the *lcCooperativeSpeed* parameter for a particular vehicle allows the vehicle's speed to be adjusted during the merge process. This is especially relevant for receiving-lane vehicles. The vehicle in the receiving lane adjusts it speed and cooperates with the merging vehicle, enabling the merging vehicle to perform the lane change. On the other hand, the value of 0 in the parameter results in no speed adjustment, and

consequently no cooperation, to make the merge or to allow the merge. The merge in this case is completely dependent on a pre-existing sufficient gap in front of the vehicle in the receiving lane.

Vehicle Assignment

The traffic on lane A_1 had a flow rate of 1,400 vehicles/hour throughout the simulation. Two scenarios were tested with different types of base vehicles in lane A_1. The lane A_1 traffic comprised all HV0 in the first scenario (experiment 4a), while that lane had all HV1 in the second scenario (experiment 4b). The traffic in lane A_0 was a mixture of HV0 and HV1. The ratios of HV0 and HV1 were varied across runs and the volumes were increased every15 minutes (900 seconds) within each run. The vehicle assignment matrix is shown in table 10. Each of the two experiments had five different sub-scenarios with five levels of the HV0/HV1 ratios, generating 10 runs (single trial per scenario).

Table 10. Vehicle assignment on lane A_0 for experiment 4a and experiment 4b.

Time Step (Seconds)	**Total Volume on A_0 (vehicle / 15-minute)**	**0% (vehicle / 15-minute)**		**25% (vehicle / 15-minute)**		**50% (vehicle / 15-minute)**		**75% (vehicle / 15-minute)**		**100% (vehicle / 15-minute)**	
		HV0	HV1	HV0	HV1	HV0	HV1	HV0	HV1	HV0	HV1
0	0	0	0	0	0	0	0	0	0	0	0
900	100	100	0	75	25	50	50	25	75	0	100
1800	150	150	0	113	38	75	75	38	113	0	150
2700	200	200	0	150	50	100	100	50	150	0	200
3600	250	250	0	188	63	125	125	63	188	0	250
4500	300	300	0	225	75	150	150	75	225	0	300
5400	350	350	0	263	88	175	175	88	263	0	350
6300	400	400	0	300	100	200	200	100	300	0	400
7200	450	450	0	338	113	225	225	113	338	0	450
8100	500	500	0	375	125	250	250	125	375	0	500

Results Visualization

The impacts of aggressive merging were investigated by studying the flow and speed metrics. Speed vs. flow plots, time vs. average speed plots, and time vs. flow plots were used to visualize the changes in response to the increase in demand over time (in 15-minute increments). The data for three locations—500 ft before the start of the deceleration lane on lane A_1, the start of the deceleration lane (on lane B_2), and the start of the ramp—were plotted. Time vs. average speed plots and time vs. flow plots were combined into dual-axis plots (see appendix B).

The 15-minute vehicle counts (table 11 – table 14) were measured at the start of the simulation where the vehicles entered the simulation and at the start of the ramp. The vehicle counts are also divided into the vehicle types by lane (A_0 HV0, A_0 HV1, A_1 HV0, and A_1 HV1) to measure the trade-off effects on each vehicle type.

Discussion

In experiment 4a, figure 62 – figure 67 in appendix B show the speed vs. flow plots at various locations across all HV1 to HV0 ratio cases. The 1-minute aggregate count observations were multiplied by 60 to generate the corresponding estimated hourly flow rates. As shown on the plots, the change in HV1 to HV0 ratios on lane A_0 did not lead to significant changes in capacity when all A_1 traffic consisted of HV0 (the condition of experiment 4a). The same headways were specified for cooperative vehicles (HV1) and noncooperative vehicles (HV0) in the simulation. The headways also remained the same before and after performing the merge. Even though the flow on lane B_2 (and thus lane A_1) was interrupted by the merge activity, the overall capacity of the exit lane was not

affected significantly since the merging vehicles had the same headways and the headway distribution on the exit lane remained the same.

While the average capacity was not affected, the change in HV1 to HV0 ratios did affect the variability and level of fluctuation in the flow, as can be seen by comparing the plots across the five different levels in figure 29 and figure 31. In the 0 percent HV1 case, since A_0 traffic only consisted of HV0, most A_0 vehicles were not able to change their lane to the deceleration lane but started building a queue at the end of lane B_1 (shown in figure 28). Lane changes occurred only when there were gaps between the platoons on lane B_2 caused by stochastic variation in the vehicle insertion.

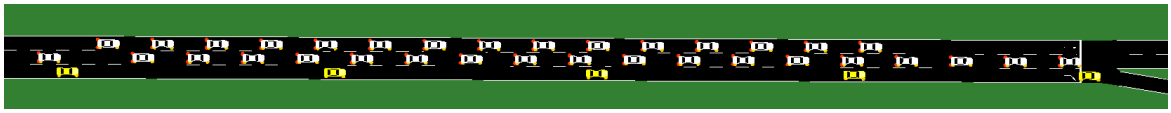

Figure 28. Diagram. Queue building at the end of lane B_1.

In 25–100 percent cases, a greater instability in flow was observed (see figure 29 and figure 30). These instabilities occur when an HV1 on lane B_1 (typically near the back of the queue) changed to lane B_2, using a gap caused by stochastic variation in the traffic. Once in lane B_2, the merged HV1 vehicle would allow vehicles waiting in the queue on lane B_1 to merge in front of it due to its cooperative characteristics, essentially clearing a portion of the B_1 queue. However, these instabilities did not last long nor occur frequently since they only occurred when there was a sufficient gap between the vehicle platoons on lane B_2 to allow the initial HV1 to merge. The total ramp volumes were unaffected by the HV1 ratios, as can be seen in figure 31 and table 12.

Unlike experiment 4a, experiment 4b (i.e., all vehicles in lane A-1 are HV1) did experience a change in capacity (figure 65 – figure 66 in appendix B). At the lower HV1 percentages from lane A_0, a lower ramp capacity (i.e., the number of vehicles that were able to successfully merge and exit) was observed. At the lower HV1 penetration rates the plots in figure 32 – figure 33 show that the flow on lane A_1 and B_2 was more frequently interrupted compared to experiment 4a (figure 29 and figure 30) since all A_1 traffic was HV1 and merges occurred freely and without building a long queue on lanes B-1 or B_0. The ability of traffic originating from A_1 to successfully exit the freeway was reduced over time, as seen in table 13, due to the merging vehicle originating from lane A_0 consuming a larger portion of the available capacity, and the merge maneuvers resulting in longer headways. This is reflective of the results in experiments 1, 2, and 3 where the AVs were seen to yield to the more aggressive vehicles. Interestingly, as the percentage of HV1s increased, the ramp capacity increased, reaching a level equivalent to experiment 4a. That is, when most vehicles are either fully cooperative or noncooperative, similar capacities are obtained; however, where a higher percentage of cooperative vehicles are positioned to be targeted by more aggressive vehicles, this aggressive-to-non-aggressive interaction can significantly reduce capacity.

Additionally, the served vehicles in the aggressive-to-non-aggressive interaction tend to be the aggressive vehicle. This is seen through the increasing queue length on lane A_1 as the percentage of noncooperative merging vehicles increased. These findings are congruent with the findings of experiments 2 and 3 where AHDVs benefited in reduced travel time by targeting AVs, while the AVs and the following traffic's travel time

increased. The AHDVs' gains were achieved at the expense of AVs and the other following traffic.

Such trade-off trends in aggressive vehicles taking advantage of cooperative vehicles are a potential significant issue in freeway control. For instance, heavy trucks are often viewed as a merge target in congested condition. In a scenario where an AV heavy truck on an exit lane is targeted by multiple aggressive drivers, the exit lane flow is likely to be interrupted as seen in experiment 4b. On the other hand, in a scenario where an AV heavy truck is unable to merge into the exit lane due to the uncooperative behaviors by the exit-lane vehicles, the adjacent lane flow will be disrupted as demonstrated in experiment 4a. The aggressiveness experienced by AVs will potentially not be limited to AV trucks but may be experienced by any AV. Even where the overall capacity may not be significantly changed, the increased fluctuations in the flow will potentially negatively impact the operations as well as the safety conditions in the upstream traffic.

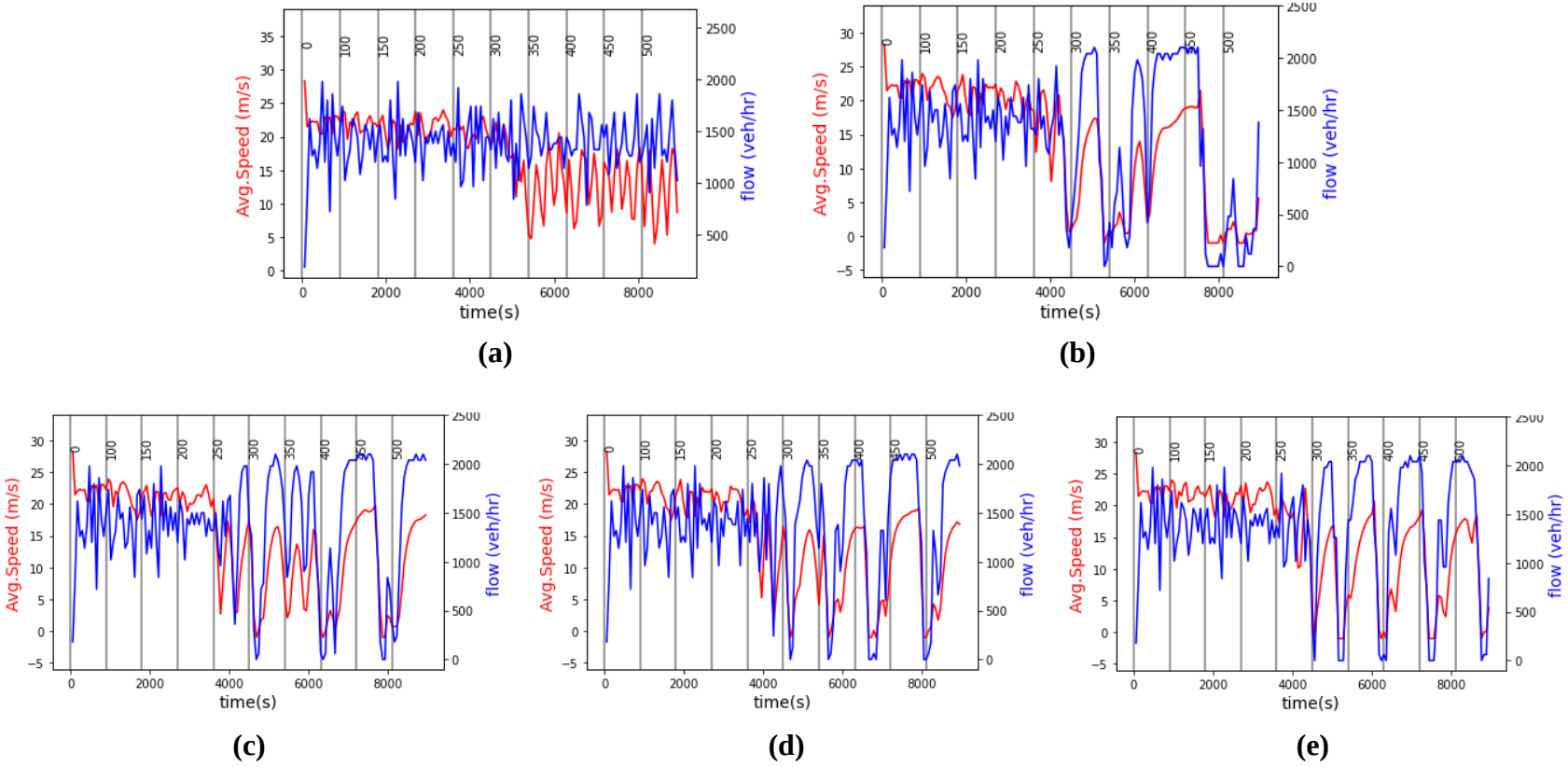

Figure 29. Plot. Time vs. average speed & flow plots at *500 ft before the start of the deceleration lane* in experiment 4a: (a) 0%, (b) 25%, (c) 50%, (d) 75%, and (e) 100%.

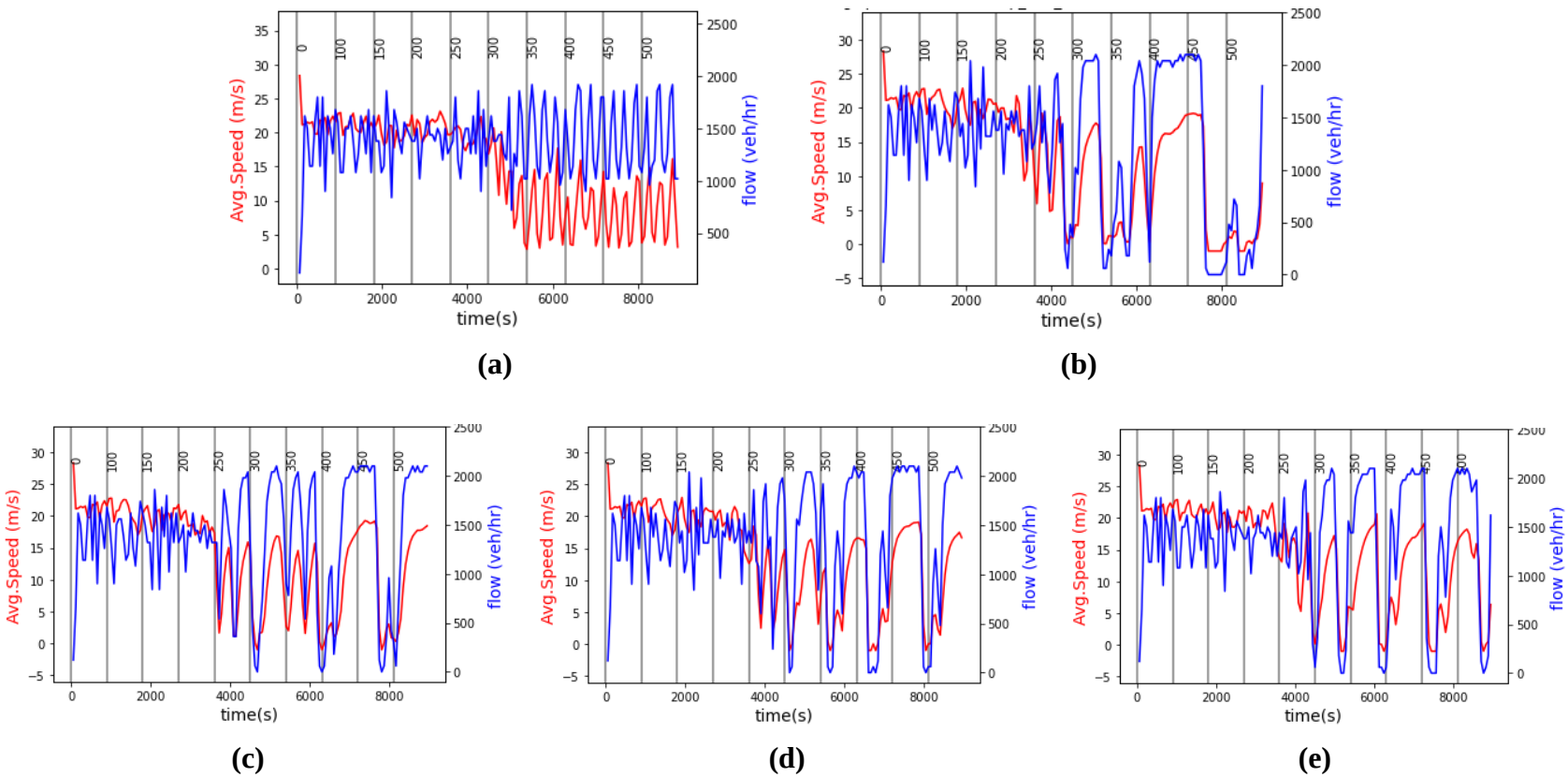

Figure 30. Plot. Time vs. average speed & flow plots *at the start of the deceleration lane* in experiment 4a: (a) 0%, (b) 25%, (c) 50%, (d) 75%, and (e) 100%.

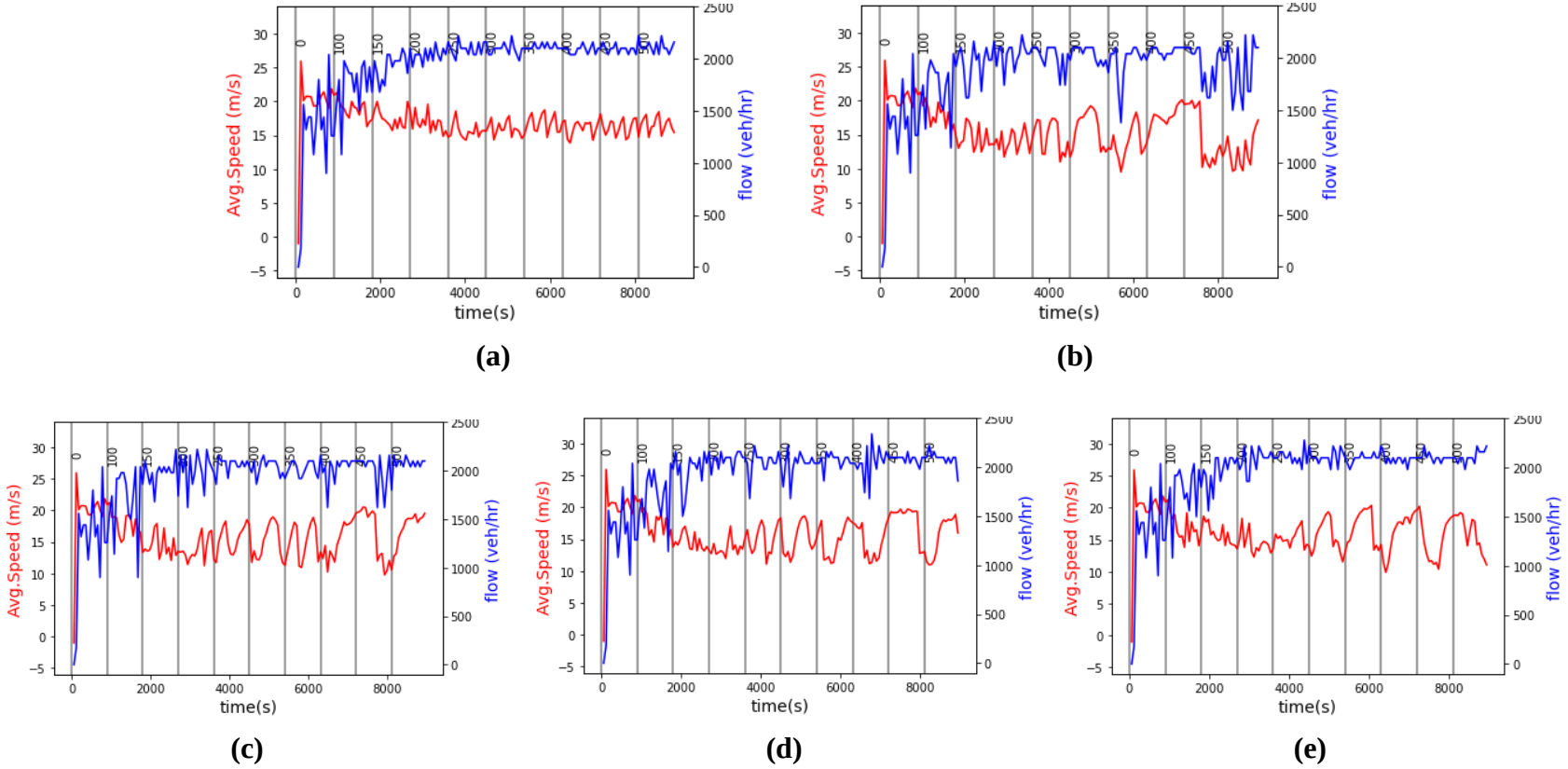

Figure 31. Plot. Time vs. average speed & flow plots *at the start of the ramp* in experiment 4a: (a) 0%, (b) 25%, (c) 50%, (d) 75%, and (e) 100%.

Table 11**. Vehicle count by vehicle type at entry point in experiment 4a (vehicles / 15 minutes).**

Time Step											
		0	**900**	**1800**	**2700**	**3600**	**4500**	**5400**	**6300**	**7200**	**8100**
0%											
Entry Point	**A_0 HV0**	0	100	150	200	250	300	350	326	166	180
	A_0 HV1	0	0	0	0	0	0	0	0	0	0
	A_0 Total	0	100	150	200	250	300	350	326	166	180
	A_1 HV0	350	350	351	349	350	351	350	350	350	350
	A_1 HV1	0	0	0	0	0	0	0	0	0	0
	A_1 Total	350	350	351	349	350	351	350	350	350	350
25%											
Entry Point	**A_0 HV0**	0	75	113	150	188	225	263	300	26	184
	A_0 HV1	0	100	151	50	63	75	88	100	9	61
	A_0 Total	0	175	264	200	251	300	351	400	35	245
	A_1 HV0	350	350	351	351	351	350	351	351	351	305
	A_1 HV1	0	0	0	0	0	0	0	0	0	0
	A_1 Total	350	350	351	351	351	350	351	351	351	305
50%											
Entry Point	**A_0 HV0**	0	50	75	100	125	150	175	126	113	81
	A_0 HV1	0	100	150	100	125	150	175	127	112	82
	A_0 Total	0	150	225	200	250	300	350	253	225	163
	A_1 HV0	350	350	351	349	350	351	350	350	350	350
	A_1 HV1	0	0	0	0	0	0	0	0	0	0
	A_1 Total	350	350	351	349	350	351	350	350	350	350
75%											
Entry Point	**A_0 HV0**	0	25	38	50	63	75	88	75	60	17
	A_0 HV1	0	100	151	150	188	225	263	225	178	48
	A_0 Total	0	125	189	200	251	300	351	300	238	65
	A_1 HV0	350	350	351	351	351	350	351	351	350	350
	A_1 HV1	0	0	0	0	0	0	0	0	0	0
	A_1 Total	350	350	351	351	351	350	351	351	350	350
100%											
Entry Point	**A_0 HV0**	0	0	0	0	0	0	0	0	0	0
	A_0 HV1	0	100	150	200	250	300	350	321	158	223
	A_0 Total	0	100	150	200	250	300	350	321	158	223
	A_1 HV0	350	350	351	349	350	351	350	350	350	350
	A_1 HV1	0	0	0	0	0	0	0	0	0	0
	A_1 Total	350	350	351	349	350	351	350	350	350	350

Table 12. Vehicle count by vehicle type at ramp in experiment 4a (vehicles / 15 minutes).

		Time Step									
		0	**900**	**1800**	**2700**	**3600**	**4500**	**5400**	**6300**	**7200**	**8100**
0%											
Ramp	**A_0 HV0**	0	82	130	166	179	183	190	157	159	209
	A_0 HV1	0	0	0	0	0	0	0	0	0	0
	A_0 Total	0	82	130	166	179	183	190	157	159	209
	A_1 HV0	286	350	349	343	345	341	339	366	365	321
	A_1 HV1	0	0	0	0	0	0	0	0	0	0
	A_1 Total	286	350	349	343	345	341	339	366	365	321
25%											
Ramp	**A_0 HV0**	0	59	110	136	164	107	237	0	179	282
	A_0 HV1	0	79	143	67	45	41	56	0	64	109
	A_0 Total	0	138	253	203	209	148	293	0	243	391
	A_1 HV0	286	341	341	326	294	361	197	516	243	83
	A_1 HV1	0	0	0	0	0	0	0	0	0	0
	A_1 Total	286	341	341	326	294	361	197	516	243	83
50%											
Ramp	**A_0 HV0**	0	39	72	80	83	128	50	105	107	33
	A_0 HV1	0	78	144	87	88	102	52	126	81	59
	A_0 Total	0	117	216	167	171	230	102	231	188	92
	A_1 HV0	286	341	351	349	344	279	403	277	316	424
	A_1 HV1	0	0	0	0	0	0	0	0	0	0
	A_1 Total	286	341	351	349	344	279	403	277	316	424
75%											
Ramp	**A_0 HV0**	0	20	37	47	41	44	48	64	18	50
	A_0 HV1	0	79	146	146	114	130	143	188	46	150
	A_0 Total	0	99	183	193	155	174	191	252	64	200
	A_1 HV0	286	341	345	333	358	333	327	259	458	323
	A_1 HV1	0	0	0	0	0	0	0	0	0	0
	A_1 Total	286	341	345	333	358	333	327	259	458	323
100%											
Ramp	**A_0 HV0**	0	0	0	0	0	0	0	0	0	0
	A_0 HV1	0	80	141	197	192	257	115	132	254	195
	A_0 Total	0	80	141	197	192	257	115	132	254	195
	A_1 HV0	286	350	347	323	335	271	408	389	272	334
	A_1 HV1	0	0	0	0	0	0	0	0	0	0
	A_1 Total	286	350	347	323	335	271	408	389	272	334

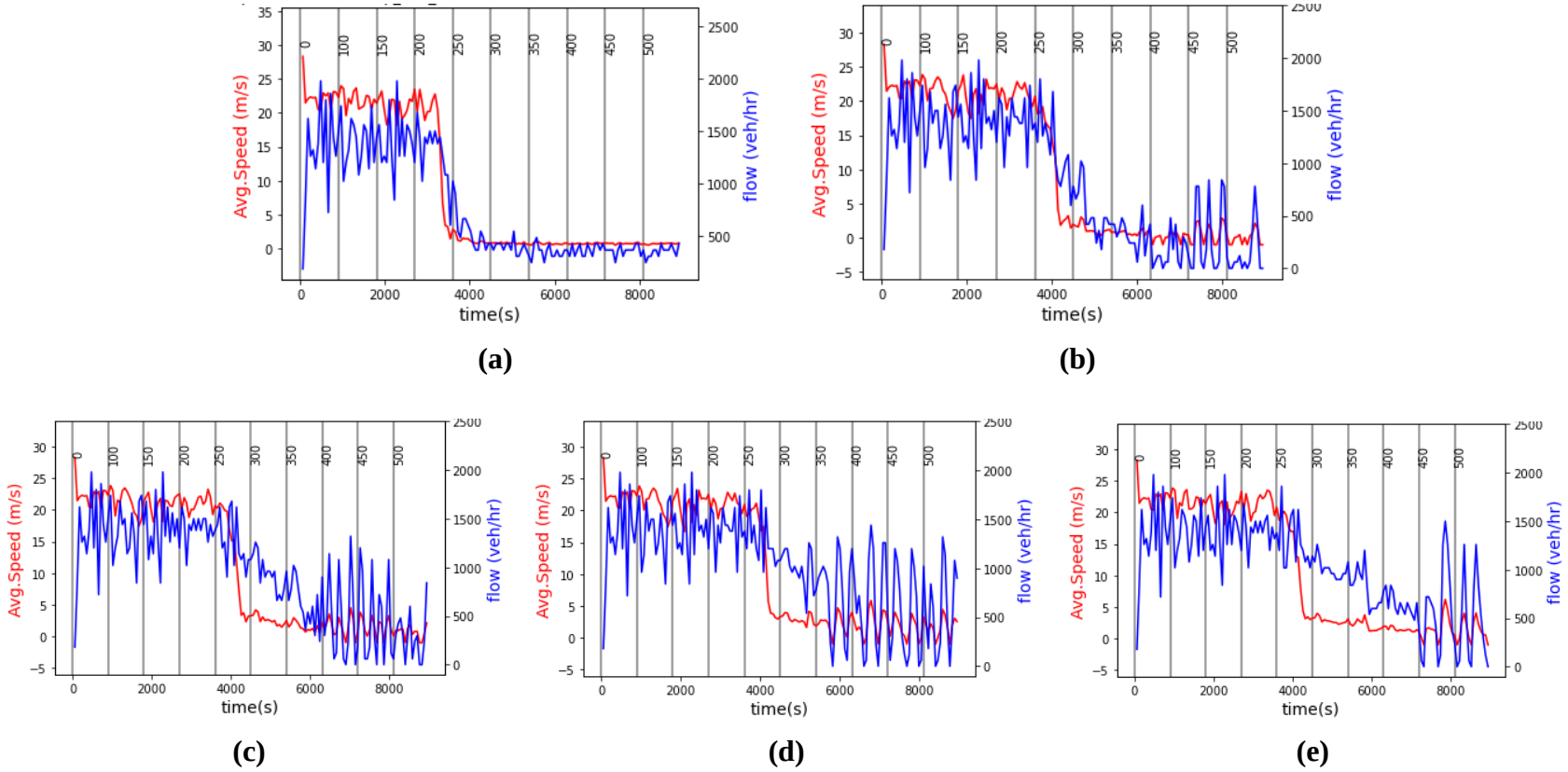

Figure 32. Plot. Time vs. average speed vs. flow plots at 500 ft before the start of the deceleration lane in experiment 4b: (a) 0%, (b) 25%, (c) 50%, (d) 75%, and (e) 100%.

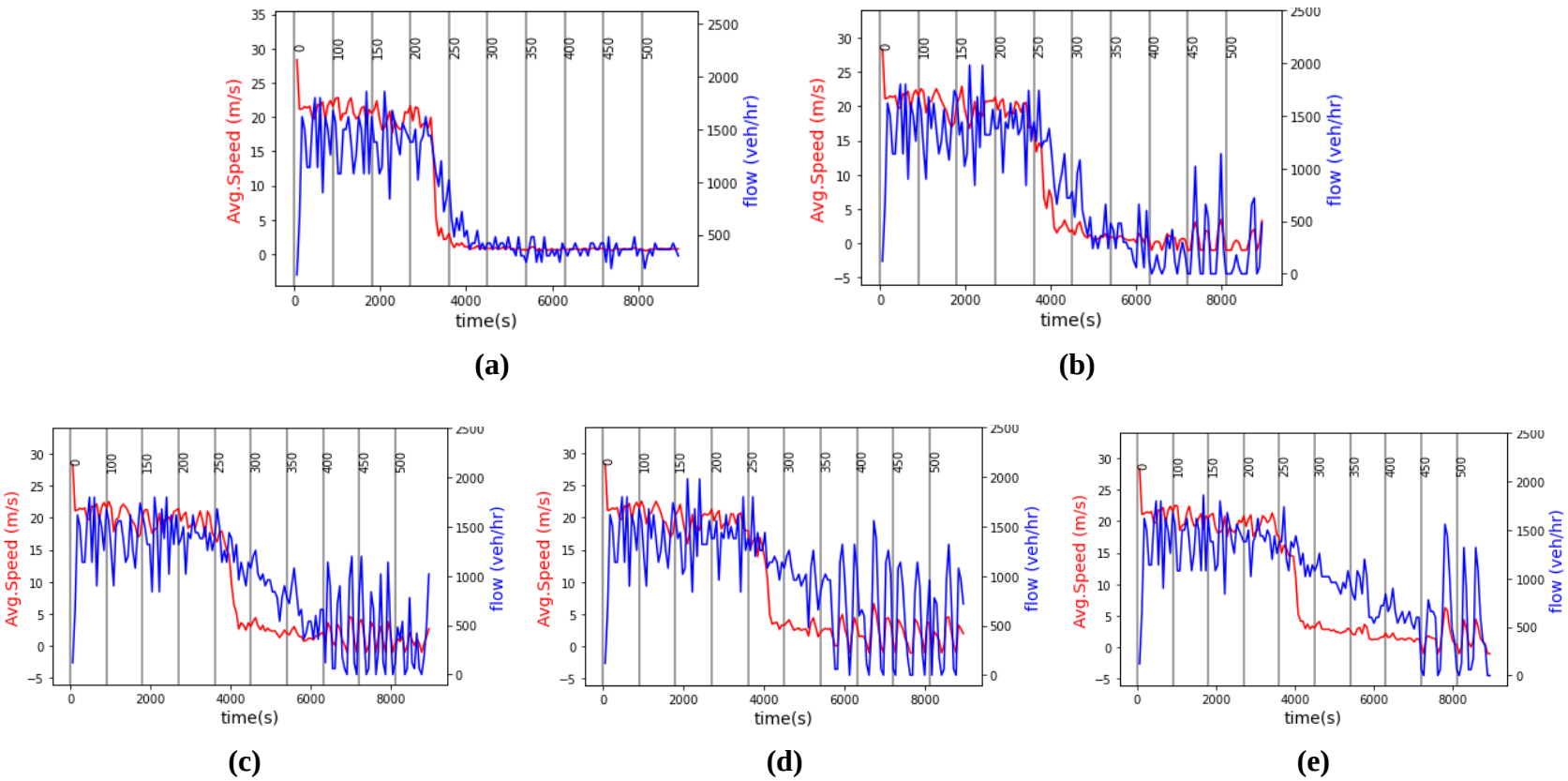

Figure 33. Plot. Time vs. average speed vs. flow plots at the start of the deceleration lane in experiment 4b: (a) 0%, (b) 25%, (c) 50%, (d) 75%, (e) 100%.

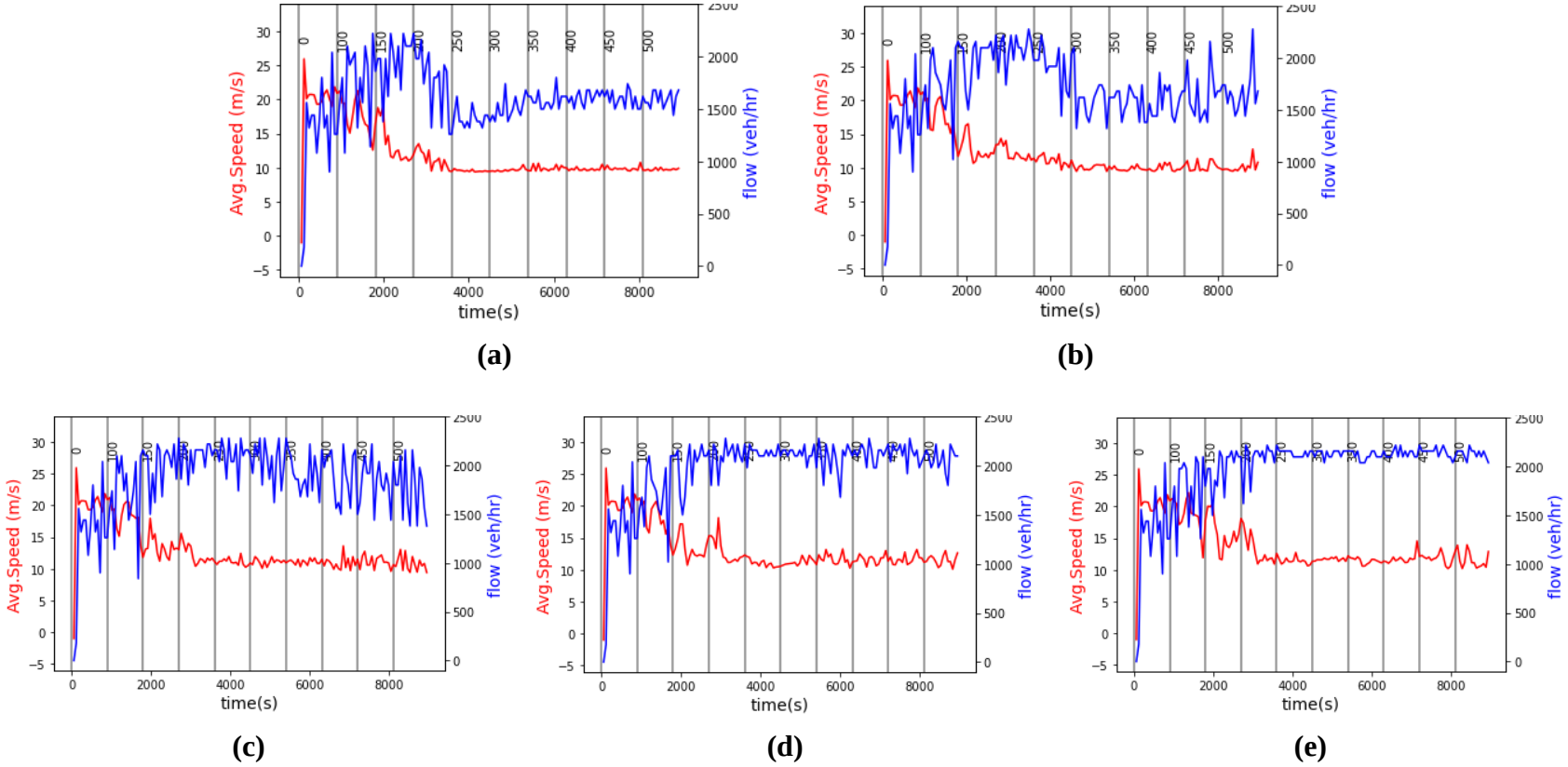

Figure 34. Plot. Time vs. average speed vs. flow plots at the start of ramp in experiment 4b: (a) 0%, (b) 25%, (c) 50%, (d) 75%, and (e) 100%.

Table 13**. Vehicle count by vehicle type at entry point in experiment 4b (vehicles / 15 minutes).**

Time Step											
		0	**900**	**1800**	**2700**	**3600**	**4500**	**5400**	**6300**	**7200**	**8100**
0%											
Entry Point	**A_0 HV0**	0	100	150	200	250	300	350	401	450	394
	A_0 HV1	0	0	0	0	0	0	0	0	0	0
	A_0 Total	0	100	150	200	250	300	350	401	450	394
	A_1 HV0	0	0	0	0	0	0	0	0	0	0
	A_1 HV1	350	350	351	349	350	242	95	87	93	87
	A_1 Total	350	350	351	349	350	242	95	87	93	87
25%											
Entry Point	**A_0 HV0**	0	75	113	150	188	225	263	300	338	322
	A_0 HV1	0	100	151	50	63	75	88	100	113	108
	A_0 Total	0	175	264	200	251	300	351	400	451	430
	A_1 HV0	0	0	0	0	0	0	0	0	0	0
	A_1 HV1	350	350	351	351	351	350	201	71	39	76
	A_1 Total	350	350	351	351	351	350	201	71	39	76
50%											
Entry Point	**A_0 HV0**	0	50	75	100	125	150	175	200	225	219
	A_0 HV1	0	100	150	100	125	150	175	200	225	219
	A_0 Total	0	150	225	200	250	300	350	400	450	438
	A_1 HV0	0	0	0	0	0	0	0	0	0	0
	A_1 HV1	350	350	351	349	350	351	349	150	131	97
	A_1 Total	350	350	351	349	350	351	349	150	131	97
75%											
Entry Point	**A_0 HV0**	0	25	38	50	63	75	88	100	113	125
	A_0 HV1	0	100	151	150	188	225	263	300	338	374
	A_0 Total	0	125	189	200	251	300	351	400	451	499
	A_1 HV0	0	0	0	0	0	0	0	0	0	0
	A_1 HV1	350	350	351	351	351	350	351	205	155	138
	A_1 Total	350	350	351	351	351	350	351	205	155	138
100%											
Entry Point	**A_0 HV0**	0	0	0	0	0	0	0	0	0	0
	A_0 HV1	0	100	150	200	250	300	350	401	450	499
	A_0 Total	0	100	150	200	250	300	350	401	450	499
	A_1 HV0	0	0	0	0	0	0	0	0	0	0
	A_1 HV1	350	350	351	349	350	351	350	226	137	146
	A_1 Total	350	350	351	349	350	351	350	226	137	146

Table 14. Vehicle count by vehicle type at ramp in experiment 4b (vehicles / 15 minutes).

Time Step											
		0	**900**	**1800**	**2700**	**3600**	**4500**	**5400**	**6300**	**7200**	**8100**
0%											
Ramp	**A_0 HV0**	0	86	143	189	232	281	309	312	312	309
	A_0 HV1	0	0	0	0	0	0	0	0	0	0
	A_0 Total	0	86	143	189	232	281	309	312	312	309
	A_1 HV0	0	0	0	0	0	0	0	0	0	0
	A_1 HV1	286	345	343	264	119	95	86	92	86	90
	A_1 Total	286	345	343	264	119	95	86	92	86	90
25%											
Ramp	**A_0 HV0**	0	65	106	146	180	216	242	262	248	270
	A_0 HV1	0	86	142	67	59	70	72	73	95	87
	A_0 Total	0	151	248	213	239	286	314	335	343	357
	A_1 HV0	0	0	0	0	0	0	0	0	0	0
	A_1 HV1	286	336	357	328	240	122	84	55	69	61
	A_1 Total	286	336	357	328	240	122	84	55	69	61
50%											
Ramp	**A_0 HV0**	0	43	71	95	122	145	164	171	184	194
	A_0 HV1	0	86	141	109	119	144	160	169	165	171
	A_0 Total	0	129	212	204	241	289	324	340	349	365
	A_1 HV0	0	0	0	0	0	0	0	0	0	0
	A_1 HV1	286	335	358	333	287	220	157	139	107	77
	A_1 Total	286	335	358	333	287	220	157	139	107	77
75%											
Ramp	**A_0 HV0**	0	22	35	49	60	73	84	90	100	98
	A_0 HV1	0	86	142	149	181	222	246	265	292	296
	A_0 Total	0	108	177	198	241	295	330	355	392	394
	A_1 HV0	0	0	0	0	0	0	0	0	0	0
	A_1 HV1	286	336	359	333	293	238	187	177	142	125
	A_1 Total	286	336	359	333	293	238	187	177	142	125
100%											
Ramp	**A_0 HV0**	0	0	0	0	0	0	0	0	0	0
	A_0 HV1	0	85	144	191	240	287	335	366	407	410
	A_0 Total	0	85	144	191	240	287	335	366	407	410
	A_1 HV0	0	0	0	0	0	0	0	0	0	0
	A_1 HV1	286	346	349	329	296	247	194	168	130	123
	A_1 Total	286	346	349	329	296	247	194	168	130	123

Summary

This chapter models aggressive merging behaviors in human drivers toward AVs in a mixed traffic environment. The existing literature review suggests that the general outlook on autonomous vehicles is optimistic in that most studies anticipate enhanced

roadway performance and safety in a mixed traffic environment. However, these studies had a common assumption—autonomous vehicles and human roadway users will have cooperative interactions. This study asks the question of 'what happens if the interactions are not always cooperative between autonomous vehicles and human drivers?'.

Experiments 1 through 3 showed that the presence of human drivers' aggressive merging behaviors had adverse effects on AVs and HDVs. The adverse effects had more significance in high congestion, when there is a queue in the deceleration lane. The impacts of AHDVs' aggressive merges were muted by the larger headways between vehicles in low congestion when there is no queue in the deceleration lane. Based on the experiment 2 and experiment 3 results, AHDVs had a higher travel-time gain with higher level of aggressive behaviors, which in return had greater adverse effects on the AVs' and the HDVs' travel times. However, AHDVs had a greater travel-time reduction with higher AV ratios when the traffic on the deceleration lane was moving relatively quicker. When the traffic on the deceleration lane was not moving quickly, AHDVs ended up blocking the other AHDVs from performing the aggressive merges regardless of the AV ratios.

Experiment 4 took a closer look at the impact of cooperative behavior–induced aggressive merges on capacity. It was seen that when most vehicles are either fully cooperative or noncooperative similar capacities are obtained; however, where a higher percentage of cooperative vehicles are positioned to be targeted by more aggressive vehicles, this aggressive-to-non-aggressive interaction can significantly reduce travel time. In addition, it was seen, similar to experiments 1 through 3, that AHDV gains were achieved at the expense of AVs. Finally, even in those scenarios where the overall

capacity was not significantly changed in response to the variation of the percentage of cooperative vehicles in the traffic, increased fluctuations in the flow may potentially negatively impact operations as well as the safety conditions in the upstream traffic.

The findings of this study suggest that despite the general beliefs in the benefits of autonomous vehicles, there may be adverse impacts on the non-aggressive vehicle travel times in the presence of human drivers' aggressive merging behaviors in a mixed traffic environment, especially in congested conditions. Thus, when the potential benefits of the AV are most needed, i.e., at or near capacity, it is possible that human interaction may negate many of the potential savings.

While there are certainly limitations to the study, one of the most noteworthy limitations may be a lack of validation. As the interaction between AVs and human-driven vehicles is rare—and some may argue non-existent or at least still "novel"—it is impossible to validate the behavioral assumptions made. However, this same limitation exists for all mixed-fleet studies. It is the goal of this effort to provide a meaningful data point to the range of potential behavioral, and subsequently operational, outcomes.

CHAPTER 5. DATA COLLECTION FOR DRIVER BEHAVIOR

DATA COLLECTION PLAN

The initial objective of the data collection task was to obtain trajectory data for drivers performing aggressive merges and use these data to finetune the aggressive merge model. However, several physical site-specific limitations prevented the collection of these data. The Georgia Department of Transportation's (GDOT) permanent cameras on roadside poles did not provide a view that could be used for trajectory data extraction. These views suffered from excessive occlusion of the vehicles in the lanes away from the camera. Drone data collection was contemplated as an alternative. However, such efforts were thwarted by the restrictions on the airspace due to nearby airports and helipads and also the lack of cooperation from nearby business owners.

The data collection therefore was focused on supplementing the effort on studying the impact of headways (which are affected by the aggressive behavior as well as other automated vehicle behavior, such as platooning) on capacity, which will be presented in chapter 6. The data collection effort measured the saturation headways at two typical intersections in Georgia during the PM peak period on weekdays.

DATA COLLECTION METHOD

Site Selection for Drone Video Data Collection

For collecting data, two sites were chosen on mainline Peachtree Industrial Boulevard (PIB). The sites were chosen in a way that the drone can be docked within the GDOT right of way and away from any no-fly zones (figure 35). At the two intersections shown

in figure 35, the objective was to obtain trajectories of the vehicles departing from a standing queue when the signal indication changed to green. To ensure sufficient demand to achieve these conditions, the data collection was performed during the PM-peak hours between 3 PM and 6 PM on weekdays.

The data were collected at an elevation of approximately 350–400 ft above the ground. Hence, no interactions with the overhead wires were expected. However, special considerations had to be made to maneuver around the wires while taking off and landing the equipment. In the event of a breeze, the equipment would get offset from the data collection spot to balance the effect of the wind and hence the equipment had to be readjusted accordingly from time to time in reaction to the automatic mid-air adjustments. The equipment was not operated on a day with any heavy rain or thunderstorm forecast.

Drone Video Data Processing Using the DataFromSky Viewer

The field-collected drone video data were processed to extract vehicle trajectories using the services of an external vendor, DataFromSky (DataFromSky 2021a) via their online service portal. The platform uses artificial intelligence (AI) and computer vision to detect vehicle movements and produce annotated vehicle trajectories. The processed data are returned from the platform in the form of a data package called a "tracking log" with a file extension, ".tlgx". To extract vehicle trajectories and measure other traffic-flow characteristics, tracking logs are further processed in the DataFromSky Viewer software (DataFromSky 2021b). Figure 36 shows a sample of the annotated vehicle trajectories for one of the intersections, loaded from a tracking log in DataFromSky Viewer.

(a)

(b)

Figure 35. Maps. Sites chosen for data collection: (a) at the intersection of PIB@ North Berkeley Lake Road, (b) at the intersection of PIB@ Medlock Bridge Road. (red lines = GDOT right-of-way boundaries, X = docking station for drone) Source: Google® Maps

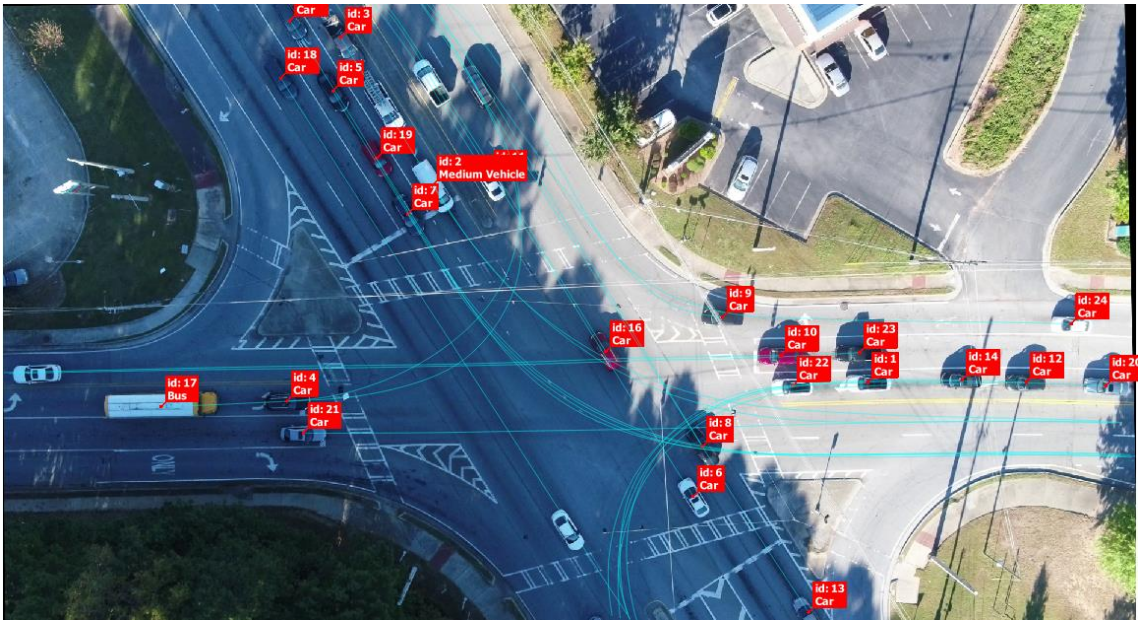

Figure 36. Map. Annotated vehicle trajectories in DataFromSky Viewer. Source: Google Maps

After loading a tracking log in DataFromSky Viewer, the post-processing of the data is performed using the following three steps:

1. Manual georeferencing.
2. Manual annotation configuration.
3. Exporting analysis data.

Manual Georeferencing

Georeferencing ensures that the video footage is properly mapped, oriented, and scaled to allow accurate calculation of trajectory data, including position, speed, and acceleration. A minimum of three points in the footage scene are assigned coordinates extracted from Google® Maps. If acceptable positioning accuracy is achieved, the points are shown in green with precision indication in the DataFromSky Viewer, as illustrated in figure 37; otherwise, the points are flagged in red.

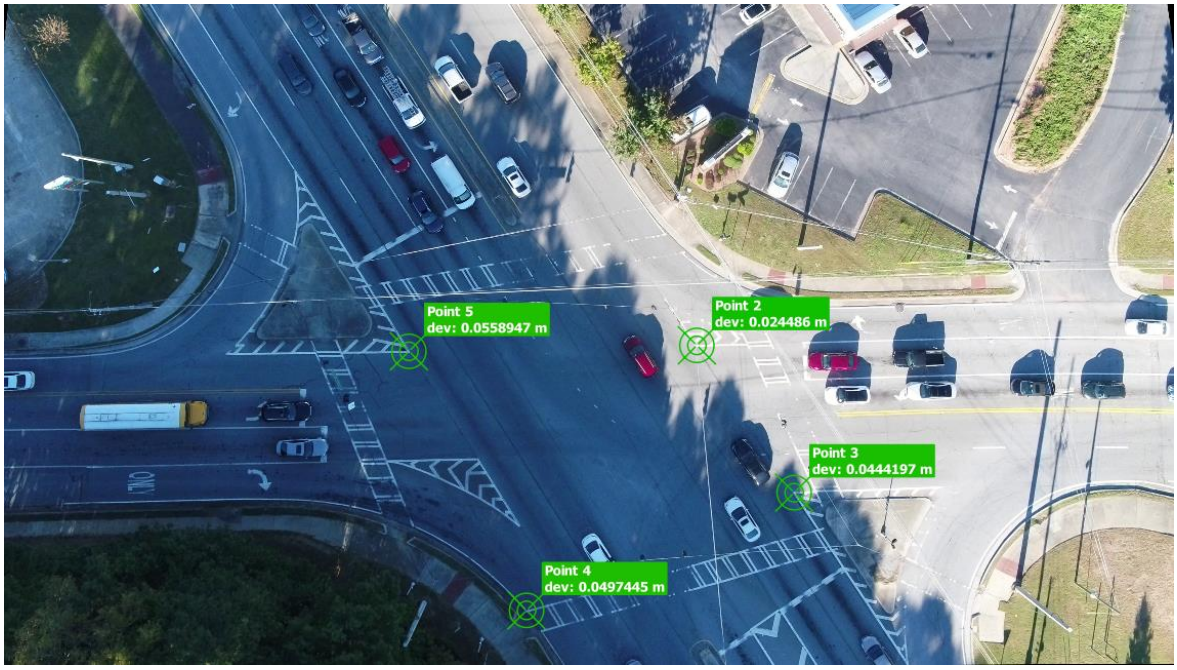

Figure 37. Map. Manual georeferencing in DataFromSky Viewer.
Source: Google Maps

Manual Annotation Configuration

This step involves inserting data collection points. For this study, data collection points were gates positioned at stop lines for headway measurements. Figure 38 shows two gates labeled as EB_Ln1 and EB_Ln2 for the two through-movement lanes. When a vehicle crosses a gate, data are collected, including the vehicle type, time of exit, and speed.

Figure 38. Map. Inserting gates at stop line.Source: Google Maps

Exporting Analysis Data

The last step involves exporting the analysis data to a comma-separated values (CSV) file for further analysis using other methods/tools as needed by the research study. As shown in figure 39, the options include exporting entire trajectories and exporting gate-crossing events.

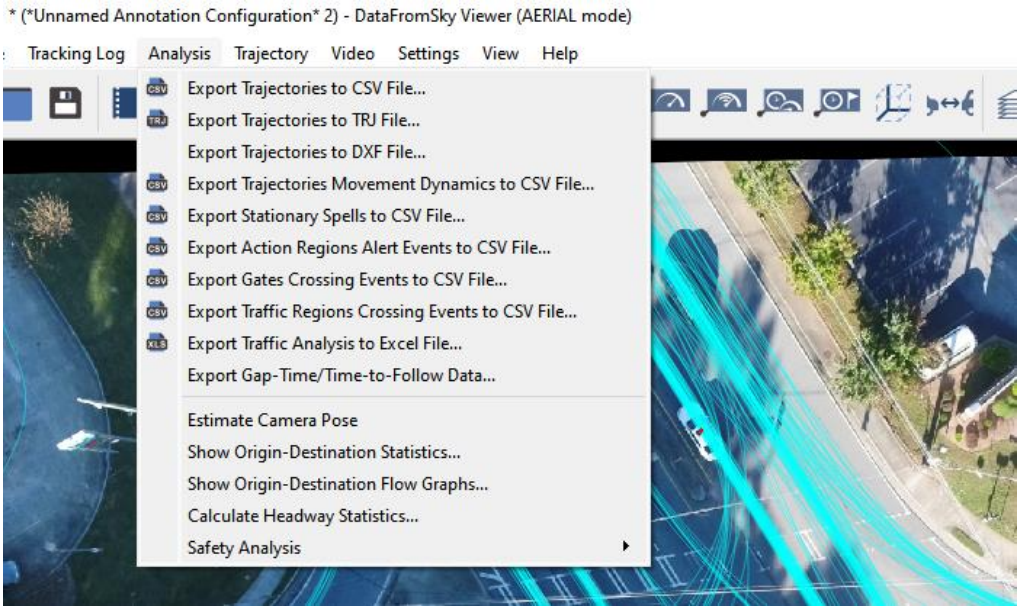

Figure 39. Screenshot. Exporting analysis data from DataFromSky Viewer.

OBSERVATIONS/RESULTS

The output of the post-processing analysis of the trajectories was the individual vehicle headways. A deconvolution analysis was performed in Python using the GaussianMixture function in the scikit-learn module (INRIA 2021) to separate out the headways of vehicles that relate to the saturation flow from the other headways. The average saturation headways for the through movements were found to be in the range of 1.84 to 2.28 in the different lanes at the different intersection approaches. The average saturation headways for the protected left turns were in the range of 1.89 to 2.33. The detailed lane-by-lane results are presented in appendix A.

CHAPTER 6. SIMPLIFIED CAPACITY ANALYSIS TOOL

INTRODUCTION

This chapter presents a Simplified Capacity Analysis Tool for exploring the potential impact of various levels of CAV market penetration on signalized intersection capacity. SCAT is an Excel-based tool that provides through and left-turn movement capacity estimates for user-selected phase timings. While numerous CAV development efforts are underway, with varying degrees of success, there is no accepted representative CAV technology nor is there a generally accepted (or governmentally required) set of CAV behavioral characteristics for vehicles that may ultimately be deployed on the public roadways. As such, it is not possible to develop a single, authoritative estimate of the impact of CAVs on capacity. Thus, SCAT draws on findings from the literature, as well as a project-based simulation, presenting 10 different potential CAV impact scenarios. The analyst may utilize SCAT to explore a range of potential futures and understand the sensitivity of current intersection, as well as future designs, to potential CAV operating characteristics.

CAV SATURATION FLOW OVERVIEW

The following section discusses the CAV saturation flow estimates included in SCAT. While the saturation flow modeling approaches in the literature differ widely, there are several overarching vehicle behavioral components covered by each. The key components of most models (generally microscopic) are their approach to car following, platooning, and lane changing.

Car following refers to the behavior of a following vehicle behind a lead vehicle, within a lane. The output of a car-following model is the following vehicle's acceleration, that is, should the following vehicle accelerate, decelerate, or maintain its current speed. There are enumerable approaches to developing car-following models, but commonly they consist of some function of a desired or minimum time gap, the spacing between vehicles, speed, and desired or maximum accelerations and decelerations. However, other parameters or traffic-condition characteristics may also be part of a car-following algorithm.

Platooning is arguably a special case of car following. However, platooning vehicles tend to travel in lock-step, that is, the reaction time between vehicles is practically (if not actually) reduced to zero. In addition, headways may be significantly lower than the minimum found in most car-following models. To implement platooning, it is assumed that the following vehicle is either connected (i.e., in communication) with the lead vehicle or has sufficient sensors to allow for a reaction time nearing 0 seconds. Many CAV models will impose limits on the length of platoons. This may be either due to assumed technology limits or as a safety constraint where breaks in platoons are deemed necessary to allow for interaction with human-driven vehicles in a mixed-fleet environment.

Lane changing, while influenced by car following and platooning, is the process by which a vehicle decides whether and if to implement a lane change. Commonly, lane changing is considered as discretionary (e.g., a vehicle changes lanes to advance its position in the traffic stream) or mandatory (e.g., a lane change is required to enter a freeway from an on-ramp). Lane change models may also incorporate behavioral

changes, such as cooperative breaking, by the vehicle in the destination lane. Lane-changing models are critical in multilane facilities and often a determining factor in the capacity of bottlenecks, weaving areas, merges, diverges, etc.

Within the literature, freeway-based CAV models are significantly more common than arterial models. Given the current lack of arterial models, the majority of the models included in SCAT are developed and calibrated for freeway scenarios. However, SCAT is focused on the capacity of vehicles departing from an approach, ignoring the effects of lane changing. Thus, the freeway models utilized were for developed basic freeway segment saturation flows rather than weaving areas, limiting the influence of the model's CAV lane-changing behaviors. The model impacts are focused on the changes in car-following and platooning related to the market penetration of CAVs. While arterial-specific models would be preferred, the referenced models should give a sense of the variation in capacity that may be witnessed for departing vehicles at a signalized intersection.

However, a direct application of any one of these models to a specific intersection would likely provide findings with minimum reliability given the significant uncertainty in the characteristics and deployment timeline of CAV technology. Rather, a more productive use of SCAT (or direct reference of the literature) is to explore the sensitivity of projected traffic demands and designs across the range of future predictions. These models provide a sense of the various assumed CAV headways, platooning, and other characteristics. Designers and policy makers can also consider the impacts of various timelines for increasing market penetration rates. Ultimately, testing a design against multiple potential

CAV futures aids in understanding its robustness in the face of significant uncertainty and the potential and cost to "future-proof" designs.

SCAT SATURATION FLOW MODELS

Prior to describing the use of SCAT, the models included are briefly discussed. While the term CAV is utilized as a broad descriptor in this chapter, it will be seen that the selection of models includes a range of vehicle types: connected vehicle (CV), AV, CAV, and cooperative adaptive cruise control (CACC). It will also be seen that adaptive cruise control (ACC) or CACC models are often utilized for the car-following behavior in a CAV model. The discussion provided for each model will utilize the term from the given reference.

Capacity Adjustment Factors for Connected and Automated Vehicles in the Highway Capacity Manual, Draft Phase 1 Report, Pooled Fund Study (Schroeder et al. 2021)

This project sought to develop CAV capacity adjustment factors for use in the *Highway Capacity Manual* (HCM). The effort utilized an agent-based simulation modeling approach implemented in VISSIM, developing capacity adjustment factors for freeway segments (i.e., basic, merge, diverge, and weaving), signalized intersections (i.e., through movements and protected and permitted left-turn movements), two-way stop-controlled intersections, and roundabouts (i.e., yield control entry). The CAVs modeled were assumed to be SAE[1] Level 4 or 5, that is, for the facilities being modeled the vehicle was

[1] Society of Automotive Engineers Levels of Driving Automation™ are defined in SAE J3016 from Level 0 (no driving automation) to Level 5 (full driving automation).

assumed to operate with no human intervention. Capacity adjustment factors were developed over CAV penetration rates from 0 to 100 percent.

As with all CAV modeling efforts, limited field data are available and CAV technology is in a continual state of flux. In Schroeder et al. (2021), it is highlighted that a key objective was the development of a minimum achievable gap. Developing such a gap required a number of assumptions regarding "CAV capability, Human-driven vehicle capability, Platooning behavior, Left-turn behavior, Inter-platoon gaps, Intra Platoon gaps, Maximum platoon size, System reliability, and Traffic Stream Composition." Assumptions were based on a review of the literature and best judgment. The number of required assumptions should not be taken as a criticism of this effort; it is simply a reflection of the current state of uncertainty in the ultimate characteristics of CAVs and a source of the differences seen in the capacity impact estimates throughout the literature.

A signalized intersection of a four-lane roadway (40-mph speed limit) with a two-lane roadway (30-mph speed limit), with all approaches having a left-turn bay, was utilized as the base model. A 100-second cycle was utilized with volume demands set to approximate a 0.7 volume-to-capacity ratio. The human-driven vehicles were modeled using Wiedemann 74 driving behavior, with parameters adjusted to match the base saturation flow provided by the HCM. The CAV car-following model is based on a Cooperative Adaptive Cruise Control algorithm developed by Milanes and Shladover (2014). The VISSIM application programming interface (API) is used to implement CAV-based platoon and lane-changing behavior. Ideal conditions are assumed, such as, "no interaction with non-motorized road users, no adverse weather impacts, and a facility without driveways or access points impacting saturation flow rates." This effort also

found no significant impact to startup and clearance lost times based on the CAV penetration rate. As one of the few studies to directly consider lost time, the assumption of no-impact is applied to all models included in SCAT.

Included within SCAT are the Schroeder et al. developed capacity adjustment factors for the through movement and protected and permitted left turns. The Schroeder et al. (2021) document also included development of saturation flow rate adjustments for permitted left turns. However, these are not included within SCAT as the adjustment factors are specific to the intersection signal timing and left-turn movement opposing volume, and thus not generally applicable. However, for a given volume set and signal timing, if desired, a SCAT user may update the saturation flows on the SCAT Saturation Flow Adjustment Worksheet, using the factors from Schroeder et al. and a base saturation flow (i.e., 0 percent AVs) calculated using the HCM for the given conditions.

"Modeling Impacts of Cooperative Adaptive Cruise Control on Mixed Traffic Flow in Multi-lane Freeway Facilities" (Liu et al. 2018b)

The effort by Liu et al. (2018b) models CACC vehicles on freeway facilities. This effort focuses on the "disengagement of CACC strings"; that is, the forming and releasing of platoons of CACC vehicles in a mixed (human-driven and CACC) vehicle environment. Liu et al. considers managed-lane scenarios as well as the implementation of vehicle awareness devices (VADs), which enable a manually driven vehicle to be a CACC platoon leader. The values utilized in SCAT are based on the homogenous freeway segment results found in Liu et al. as this provides the closest approximation for the departure from a signal (i.e., not incorporating significant lane changing or weaving).

However, while not incorporated into SCAT, Liu et al. (2018b) also include significant effort related to bottleneck behavior at ramp junctions.

Similar to Schroeder et al. (2021), the CACC car-following is based on Milanes and Shladover (2014). In addition, the "NGSIM oversaturated flow human driver model" of Yeo et al. (2008) is utilized. Liu et al. implement a logic allowing a CACC vehicle to join a platoon of existing CACC vehicles, utilizing a reduced headway and thus higher flow rates. Where a platoon is at the maximum-allowed platoon length, the next CACC vehicle will initiate a new platoon, becoming a platoon leader. As part of the effort, a managed lane limited to CACC is considered. Finally, several updates are proposed to the lane-changing rules. Lastly, the 0 percent CACC model is calibrated to field conditions while CACC behavior is based on the literature and best judgment.

"Autonomous and Connected Cars: HCM Estimates for Freeways with Various Market Penetration Rates" (Shi and Prevedouros 2016)

This effort considers the impact of driverless vehicles on level of service (LOS) as measured in the *Highway Capacity Manual*, with a concentration on freeway conditions. To determine the impact on LOS, Shi and Prevedouros (2016) focus on the driverless vehicle car-following headway and penetration rate. For the traffic stream, Shi and Prevedouros utilize a weighted average of the car-following headways for human-driven and driverless vehicles. A driverless vehicle headway of 0.5 second is assumed. Critically, platoon size is not limited, which is a constraint in many other efforts intended to aid the ability of human-driven vehicles to successfully operate in a facility with a high percentage of driverless vehicles. Thus, as the penetration rate approaches 100 percent, the saturation flow rate approaches 7,200 vehicles per hour per lane. The assumptions of

Shi and Prevedouros result in significantly higher capacities than any of the other literature included in this effort.

"Enhanced Intelligent Driver Model to Access the Impact of Driving Strategies on Traffic Capacity" (Kesting et al. 2010)

The intelligent driver model is a commonly implemented and enhanced model for ACC as well as the car-following component of CAV models. The enhanced IDM utilized in SCAT provides an advancement over the original IDM model by Kesting et al. (2010). The IDM seeks to provide "controllable stability properties" with "smooth transitions between acceleration and deceleration behavior" based on six parameters: desired speed, free acceleration, desired time gap, jam distance, maximum acceleration, and desired deceleration. The IDM provides a continuous function that combines free-road driving and a deceleration model to maintain a desired safety gap. The enhanced IDM improves upon the original model by addressing instability that could be introduced by certain lane-changing behavior. A constant acceleration heuristic is introduced to address overreaction in breaking that may occur in the original IDM. While a number of scenarios are considered within the enhanced IDM paper, SCAT integrates the results for a freeway segment outflow from a traffic jam, as this is most analogous to an intersection approach departure. A critical caveat to these results is that Kesting et al. provides capacities only for ACC penetration rates of 0 to 50 percent. Thus, the results in SCAT should not be applied for penetrations greater than 50 percent. Additionally, results in SCAT are given for a default set of traffic conditions (0 percent) trucks and driving behaviors (safety time gap, maximum acceleration, and comfortable acceleration). While not dramatically different, estimated capacities given differing driving behavior

assumptions were seen in Kesting et al. (2010) to vary by up to several hundred vehicles per hour as the penetration rate increased based on the selected parameter values.

"A Mixed Traffic Capacity Analysis and Lane Management Model for Connected and Automated Vehicles: A Markov Chain Method" (Ghiasi et al. 2017)

Ghiasia et al. (2017) provide an analytical approach for determining the capacity of a highway segment at various CAV market penetration levels. Utilizing a Markov chain approach (i.e., a stochastic modeling approach where the likelihood of the next event is dependent on the previous event), Ghiasia et al. model the spatial headway distributions of the traffic stream. A key element of the model is reflecting the various leader–follower pairings (i.e., CAV–CAV, CAV–Human Driven [HV], HV–CAV, and HV–HV) in their stochastic model. However, as with all other efforts reported, this effort relies on a set of assumed distributions for these leader–follower headway pairings, particularly with CAVs. This effort also includes platooning intensity, a measure of the likelihood of vehicles platooning. Platooning intensity allows the model to account for differing platooning strategies, for instance, CAVs seeking other CAVs to create platoons versus platooning opportunities based on a random ordering of vehicles in the traffic stream. (All other models discussed assume platooning opportunities based on random ordering of vehicles.) Ghiasi et al. (2017) is one of the limited number of efforts that demonstrates that increasing capacity with increasing CAV penetration is not guaranteed and that for a given set of "conservative CAV technology scenarios" capacity may decrease.

VISSIM Simulation

The final model included in the analysis is based on a VISSIM simulation completed as part of the current study. The model utilizes results from the CoEXist project (CoEXist

2021b). The CoEXist project was a European effort to “strengthen the capabilities of urban road authorities for the planning and integration of connected and automated vehicles on their networks.” (CoEXist 2021a). As part of the CoEXist project, PTV Group developed for VISSIM a series of new features and parameters set for the modeling of CAVs (Sukennik 2018, Sukennik and Kautzsch 2018).

PTV Group developed three AV models: AV Cautious, AV Normal, and AV Aggressive. For each of these models, a set of Wiedemann 99 CC0 through CC9 parameters were calibrated for CAVs. CC0 through CC9 are driving-behavior parameters of the Weidemann 99 car-following model; interested readers are directed to the final report of GDOT Research Project 18-33, *VISSIM 11 Simulation Guidance*, for a detailed discussion of each parameter and parameter calibration (Hunter 2021). In addition, parameters were developed for the Wiedemann 74 model, which is generally utilized for arterial operations; however, robust calibration was not undertaken for these parameters and they are not yet recommended for use. In addition, recommendations for the necessary and free lane-change CAV parameter sets were generated, including characteristics such as maximum and accepted deceleration, inclusion of advanced merging and cooperative lane change, and safety distance factor, minimum headway, and maximum cooperation for braking. Updates to driver behaviors at signals were also defined (i.e., behavior at amber, behavior at red, reaction time distribution, reduced safety distance factor, reduced safety start upstream of the stop line, and reduced safety end upstream of stop line.) PTV Group has introduced the ability for vehicle class–specific platooning, enabling the modeling of CAVs at close spacings. Importantly, maximum

platoon lengths may be set, with platoon splitting where the number of CAVs in a row exceeds the platoon limit.

For the VISSIM simulation-based saturation flows given in SCAT, a single-lane approach of an intersection was modeled. A 100-second cycle was utilized with a 30-second phase on the subject approach. Demand was set to ensure a constant standing queue. Saturation flow was calculated by measuring the departure headway of the fourth through twelfth vehicle on the approach, each cycle. For the saturation flows reported in SCAT, the Weidemann 99 AV normal settings were utilized with a maximum platoon length of seven vehicles. AV market penetration rates were modeled from 0 to 100 percent, in 10 percent increments. Ten replications were completed for each penetration rate. Finally, to better represent Georgia conditions, the base model (0 percent AVs) headways were calibrated utilizing the data collection at Peachtree Industrial Blvd and Medlock Bridge Rd, as discussed in the data collection chapter of the report. While not provided in SCAT, model runs were also completed using the AV Aggressive setting. However, the saturation values were only slightly higher than the AV Normal. This is likely due to the single-lane approach eliminating any impact of aggressive merging and utilizing the same platoon length.

INSTRUCTIONS FOR SIMPLIFIED CAPACITY ANALYSIS TOOL

The use of SCAT is intended to be straightforward. SCAT is set to provide the capacity of each phase at a signalized intersection based on 10 different CAV models, at penetration rates from 0 to 100 percent. A simple eight-phase dual-ring control scheme is assumed, with protected-only lefts. The analyst provides the phase length and number of

lanes per movement, and yellow, red clear, and lost time. Currently the model does not incorporate permitted lefts, shared through plus left-turn lanes, or right-turn-on-red. For each analysis all lanes are assigned the same per-lane saturation flow. To explore different saturation values, it is necessary to run the analysis for each CAV model assumption separately. Finally, multi-lane analysis assumes a linear increase in capacity, with no degradation in service due to lane changes, unbalanced lane flows, etc. That is, the capacity for two lanes is taken to be double that of one lane, the capacity for three lanes is triple one lane, etc.

The capacity calculation utilized is shown in equation 6:

$$c_i = n_i s_i \left(\frac{\emptyset i - lt}{C}\right)$$

Where:

c_i = Capacity of phase i

n_i = number of lanes for phase (or movement) i

s_i = saturation flow for phase (or movement) i

$\emptyset i$ = Length phase i

lt = Lost time

C = Cycle length

(6)

The saturation flow is based on the literature or simulation results, and the phase lengths, lost time, and number of lanes per movement are provided by the analyst.

SCAT has three analysis sections:

1. **Individual Scenario Analysis** allows an analyst to explore the impact on phase capacity of different AV, CAV, or CACC models.
2. **Scenario Comparative Analysis** allows the analyst to compare the capacities for two saturation flow models, for all phases.
3. **Phase Comparative Analysis** allows for the comparison of all capacity scenarios across a single phase.

In addition, SCAT allows for the adjustment of all models to the same base saturation flow, that is, the saturation flow with 0 percent CAVs is set to the same value for all models. When drawn from the literature, each saturation flow model has its own assumed base saturation flow, ranging from approximately 1,900 veh/hr/ln to 2,400 veh/hr/ln. To help explore the relative difference with increasing or decreasing CAV penetration rates, SCAT enables the normalization of base saturation flows. However, caution should be exercised in the interpretation of these values. The applied normalization is a simple linear adjustment to all saturation values for a given model. That is, if the reported base value in the source literature is 2,100 veh/hr/ln for a given model, and the analyst wishes to consider all models at a base saturation flow of 2,000 veh/hr/ln, then 100 veh/hr/ln will be subtracted from the saturation flow value at all penetration levels. This adjustment is intended to provide convenience for comparing models' relative rates of change. However, the models have not been executed with the new base saturation flow as in the original literature source. It some models it is likely that the linear adjustment assumption is an oversimplification of the impact of changing the base saturation flow. For instance, another reasonable assumption could be to reduce the base rate for the given model to the

same value (i.e., set the 0 percent penetration rate to 2,000 veh/hr/ln) and make proportionally smaller changes to the saturation flow as the penetration rate increases. At 100 percent CAV, the saturation flow would be unchanged from the original source literature, as the base saturation flow (i.e., all human drivers) has little influence on the 100 percent CAV market penetration saturation flow.

Individual Scenario Analysis

To complete the Individual Scenario Analysis, enter the following information in the Data Input Section (figure 40):

1. Enter the desired Phase Lengths (in seconds).
2. Enter values for Yellow, Red Clear, and Lost Time under Other Signal Data.
3. Enter values for the Number of Lanes for each Phase.
4. Select the saturation flow Analysis Option to be analyzed.
5. Select the checkbox under Base Saturation Flow if all models are to be set to the same base saturation flow.

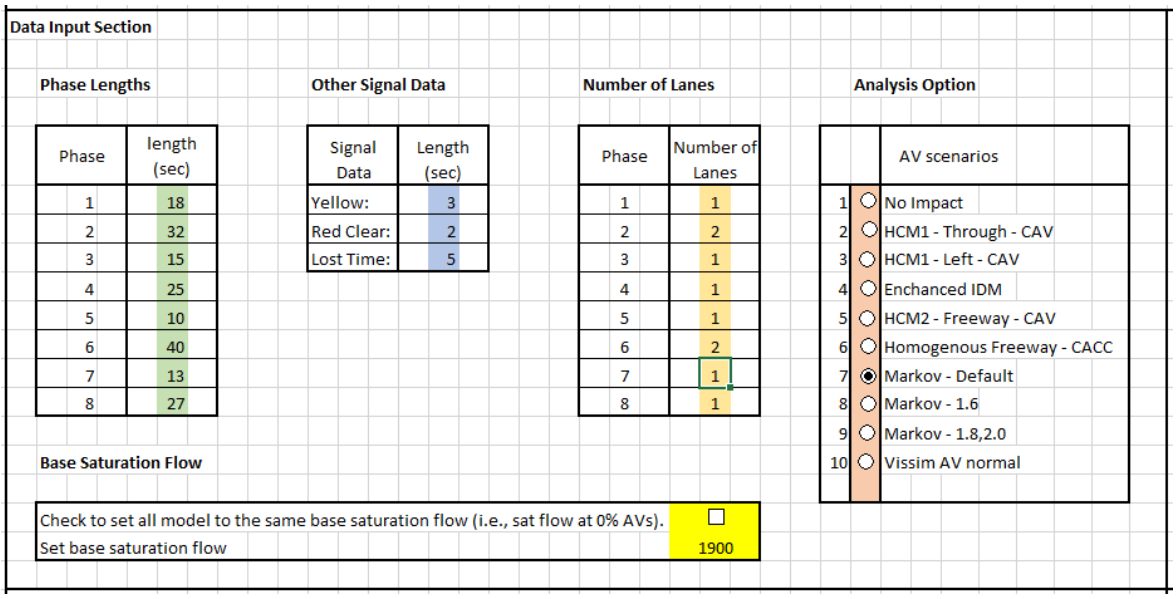

Figure 40. Screenshot. SCAT – Individual Scenario Analysis – example Data Input Section.

The analyst can confirm that the signal control has been correctly input by reviewing the Data Phase Layout section (figure 41). Separate checks are provided to confirm that the rings have the same cycle length and that the phase pairs on each side of the barrier have the same sum. The analyst should confirm each of these reads “OK”.

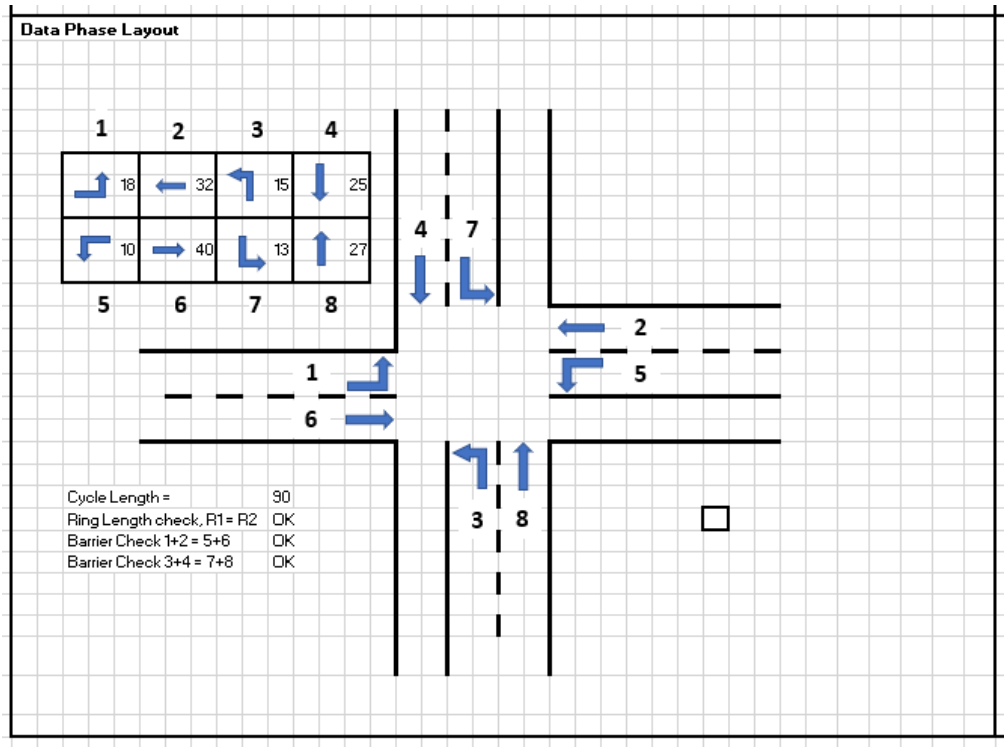

Figure 41. Screenshot. SCAT – Individual Scenario Analysis – example Data Phase Layout section.

The calculated capacity values for the selected analysis option will be shown in Analysis – Table Output (figure 42) and graphically in Analysis – Graphical Output (figure 43).

Analysis - Table Output

Capacity - veh per phase per penetration rate

	AV Penetration Rate										
Phase	0	10	20	30	40	50	60	70	80	90	100
1	482	499	515	532	553	579	612	654	706	770	848
2	1712	1773	1830	1892	1966	2058	2176	2325	2511	2739	3014
3	401	416	429	443	461	482	510	545	589	642	707
4	669	693	715	739	768	804	850	908	981	1070	1178
5	268	277	286	296	307	322	340	363	392	428	471
6	2140	2216	2288	2365	2457	2573	2720	2907	3139	3424	3768
7	348	360	372	384	399	418	442	472	510	556	612
8	722	748	772	798	829	868	918	981	1059	1156	1272

Equation Parameters	
Option	7
c4	-3E-06
c3	0.002
c2	-0.081
c1	9.139
b	2407.9

Figure 42. Screenshot. SCAT – Individual Scenario Analysis – example Analysis – Table Output section.

Analysis - Graphical Output

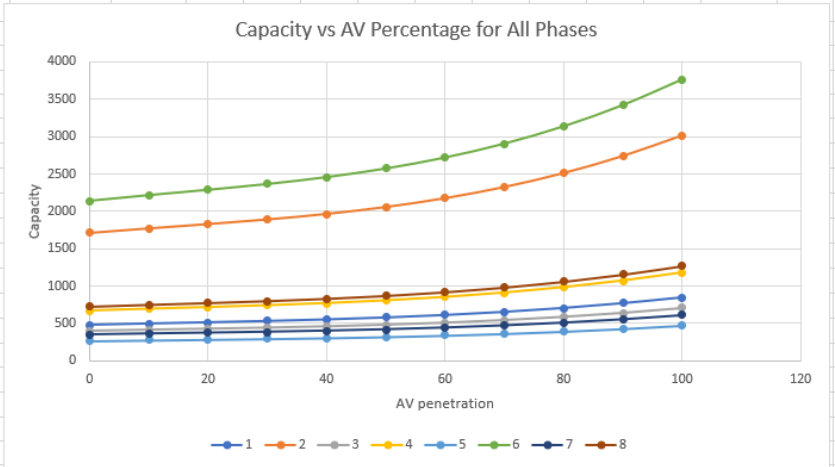

Figure 43. Screenshot. SCAT – Individual Scenario Analysis – example Analysis – Graphical Output section.

Scenario Comparative Analysis

To complete the Scenario Comparative Analysis, enter the following information in the Data Input section (figure 44):

1. Select the checkboxes for two scenarios for comparison under Scenario Selection and Select.
2. Enter the AV penetration rates as Range Low and Range High values under AV Penetration Range (default is 0 to 100).
3. Confirm there are no errors in the range selection, i.e., Error Checks read “OK”.

All other data are drawn from the Individual Scenario Analysis.

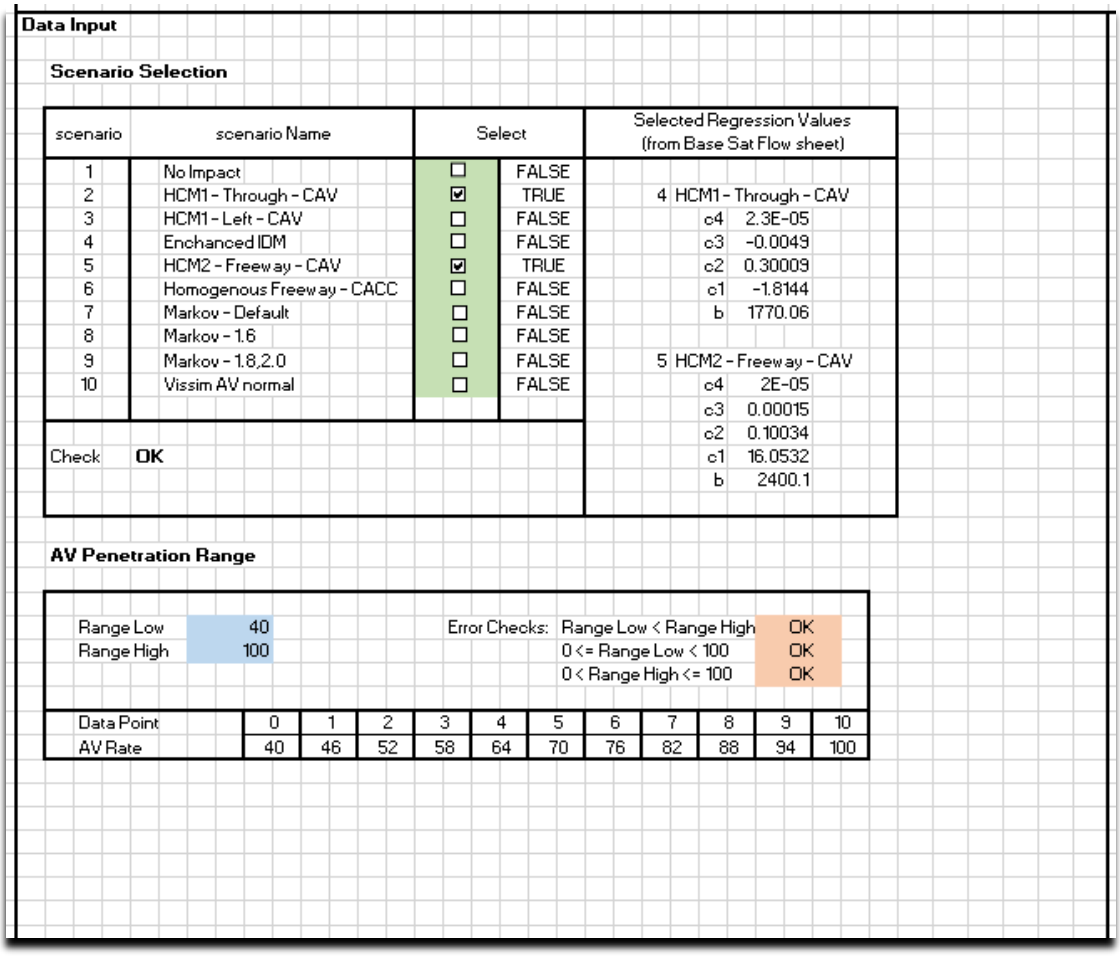

Data Input

Scenario Selection

scenario	scenario Name	Select	
1	No Impact	☐	FALSE
2	HCM1 - Through - CAV	☑	TRUE
3	HCM1 - Left - CAV	☐	FALSE
4	Enchanced IDM	☐	FALSE
5	HCM2 - Freeway - CAV	☑	TRUE
6	Homogenous Freeway - CACC	☐	FALSE
7	Markov - Default	☐	FALSE
8	Markov - 1.6	☐	FALSE
9	Markov - 1.8,2.0	☐	FALSE
10	Vissim AV normal	☐	FALSE

Check **OK**

Selected Regression Values (from Base Sat Flow sheet)

4	HCM1 - Through - CAV	
	c4	2.3E-05
	c3	-0.0049
	c2	0.30009
	c1	-1.8144
	b	1770.06
5	HCM2 - Freeway - CAV	
	c4	2E-05
	c3	0.00015
	c2	0.10034
	c1	16.0532
	b	2400.1

AV Penetration Range

Range Low	40	Error Checks:	Range Low < Range High: OK
Range High	100		0 <= Range Low < 100: OK
			0 < Range High <= 100: OK

Data Point	0	1	2	3	4	5	6	7	8	9	10
AV Rate	40	46	52	58	64	70	76	82	88	94	100

Figure 44. Screenshot. SCAT – Scenario Comparative Analysis – example Data Input section.

Next, the capacity values for each phase, for each or the two selected models will be provided in the Capacity Tables section (figure **45**) and the graphical results will be provided in the Capacity Graphs section (figure 46). It is critical to note that the Capacity Tables and Capacity Graphs will reflect the Base Saturation Flow adjustment selection in the Individual Scenario Analysis, Data Input Section.

Capacity Tables

HCM1 - Through - CAV

	AV Penetration Rate										
Phase	40	46	52	58	64	70	76	82	88	94	100
Phase1	385	390	393	396	397	397	396	395	394	394	396
Phase 2	1367	1385	1398	1407	1410	1410	1407	1403	1400	1400	1407
Phase 3	320	325	328	330	331	331	330	329	328	328	330
Phase 4	534	541	546	549	551	551	550	548	547	547	549
Phase 5	214	216	218	220	220	220	220	219	219	219	220
Phase 6	1709	1731	1748	1758	1763	1763	1759	1754	1750	1750	1758
Phase 7	278	281	284	286	287	286	286	285	284	284	286
Phase 8	577	584	590	593	595	595	594	592	590	591	593

CAUTION - Enchanced IDM Model Valid for AV Penetration 0 to 60.

HCM2 - Freeway - CAV

	AV Penetration Rate										
Phase	40	46	52	58	64	70	76	82	88	94	100
Phase1	653	691	735	786	844	911	989	1079	1183	1303	1440
Phase 2	2322	2458	2614	2794	3001	3241	3518	3838	4207	4632	5120
Phase 3	544	576	613	655	703	760	824	899	986	1086	1200
Phase 4	907	960	1021	1091	1172	1266	1374	1499	1643	1809	2000
Phase 5	363	384	409	437	469	506	550	600	657	724	800
Phase 6	2902	3073	3268	3493	3751	4051	4397	4797	5259	5790	6400
Phase 7	472	499	531	568	610	658	715	780	855	941	1040
Phase 8	979	1037	1103	1179	1266	1367	1484	1619	1775	1954	2160

HCM1 - Through - CAV - HCM2 - Freeway - CAV

AV Penetration Rate											
Phase	40	46	52	58	64	70	76	82	88	94	100
Phase1	-268	-302	-342	-390	-447	-515	-594	-685	-790	-909	-1044
Phase 2	-954	-1073	-1216	-1387	-1591	-1830	-2110	-2435	-2807	-3232	-3713
Phase 3	-224	-252	-285	-325	-373	-429	-495	-571	-658	-758	-870
Phase 4	-373	-419	-475	-542	-621	-715	-824	-951	-1097	-1263	-1451
Phase 5	-149	-168	-190	-217	-249	-286	-330	-380	-439	-505	-580
Phase 6	-1193	-1342	-1520	-1734	-1988	-2288	-2638	-3043	-3509	-4040	-4642
Phase 7	-194	-218	-247	-282	-323	-372	-429	-495	-570	-657	-754
Phase 8	-403	-453	-513	-585	-671	-772	-890	-1027	-1184	-1364	-1567

CAUTION - Enchanced IDM Model Valid for AV Penetration 0 to 60.

Figure 45**. Screenshot. SCAT – Scenario Comparative Analysis – example Capacity Tables section.**

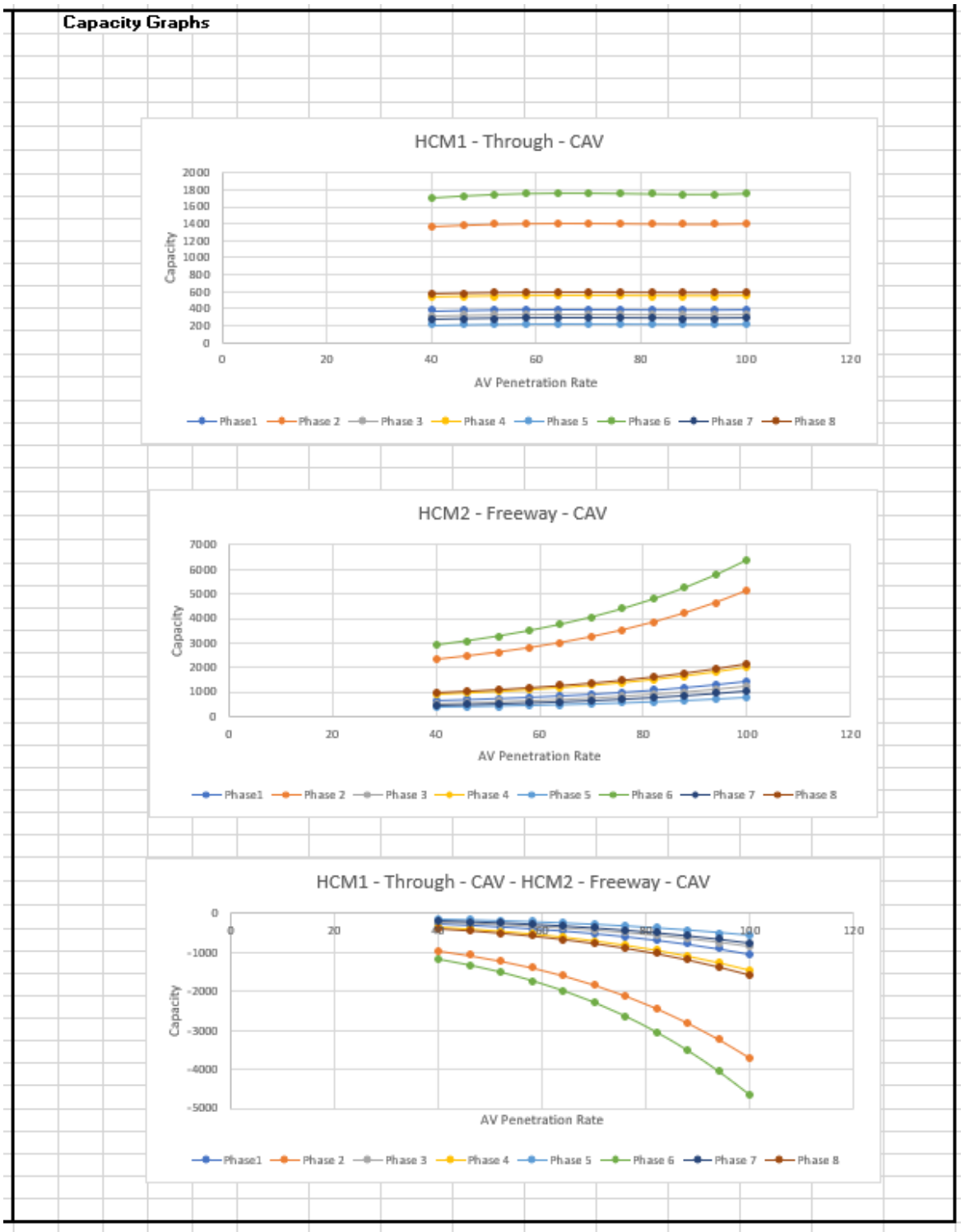

Figure 46. Screenshot. SCAT – Scenario Comparative Analysis – example Capacity Graphs section.

Phase Comparative Analysis

To complete the Phase Comparative Analysis, complete the following steps in the Data Input section (figure 47):

1. Enter the Phase to be compared across models under Selected Phase.
2. Enter the AV penetration rates as Range Low and Range High values under Desired AV Rates (default 0 to 100).
3. Confirm there are no errors in the range selection, i.e., Error Checks read "OK".

All other data are drawn from Individual Scenario Analysis.

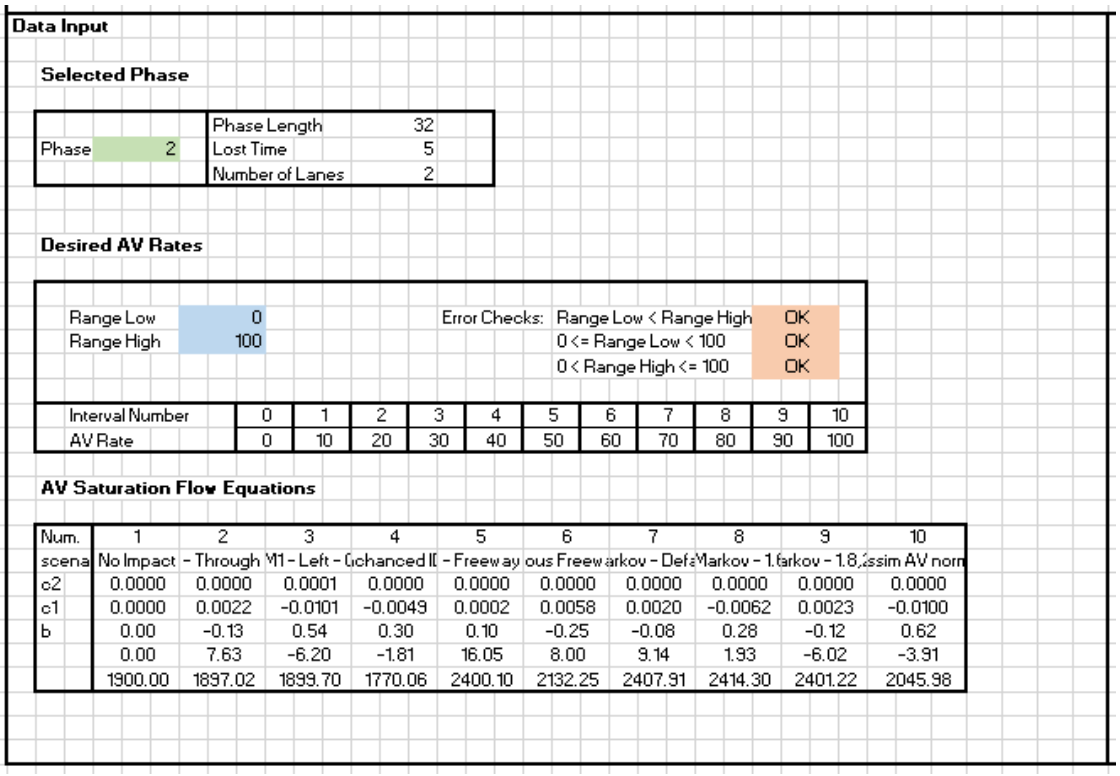

Data Input

Selected Phase

Phase	2	Phase Length	32
		Lost Time	5
		Number of Lanes	2

Desired AV Rates

Range Low	0	Error Checks:	Range Low < Range High	OK
Range High	100		0 <= Range Low < 100	OK
			0 < Range High <= 100	OK

Interval Number	0	1	2	3	4	5	6	7	8	9	10
AV Rate	0	10	20	30	40	50	60	70	80	90	100

AV Saturation Flow Equations

Num.	1	2	3	4	5	6	7	8	9	10
scena	No Impact	- Through	M1 - Left -	Enhanced I	- Freeway	ous Freew	arkov - Def	Markov - 1.	farkov - 1.8,	ssim AV norm
c2	0.0000	0.0000	0.0001	0.0000	0.0000	0.0000	0.0000	0.0000	0.0000	0.0000
c1	0.0000	0.0022	-0.0101	-0.0049	0.0002	0.0058	0.0020	-0.0062	0.0023	-0.0100
b	0.00	-0.13	0.54	0.30	0.10	-0.25	-0.08	0.28	-0.12	0.62
	0.00	7.63	-6.20	-1.81	16.05	8.00	9.14	1.93	-6.02	-3.91
	1900.00	1897.02	1899.70	1770.06	2400.10	2132.25	2407.91	2414.30	2401.22	2045.98

Figure 47. Screenshot. SCAT – Phase Comparative Analysis – example Data Input section

Next, the capacity values for the given phase, for each model will be provided in the Capacity Per AV Scenario table (figure 48) and the graphical results will be provided in

the Capacity Graph section (figure 49). As before, it is critical to note that the Capacity Tables and Capacity Graph will reflect the Base Saturation Flow adjustment selection in the Individual Scenario Analysis, Data Input Section.

Phase 2 Capacity per AV scenario

	AV Peneration Rate										
Sat Flow Model	0	10	20	30	40	50	60	70	80	90	100
No Impact	1140	1140	1140	1140	1140	1140	1140	1140	1140	1140	1140
HCM1 - Through - CAV	1138	1178	1209	1239	1272	1314	1368	1436	1521	1623	1742
HCM1 - Left - CAV	1140	1129	1152	1186	1218	1243	1267	1304	1378	1522	1779
Enchanced IDM	1062	1066	1091	1123	1154	1176	1188	1190	1185	1181	1187
HCM2 - Freeway - CAV	1440	1543	1659	1796	1959	2160	2413	2734	3144	3664	4320
Homogenous Freeway - CAC	1279	1316	1340	1369	1415	1487	1590	1728	1900	2101	2324
Markov - Default	1445	1496	1544	1597	1659	1737	1836	1962	2119	2311	2543
Markov - 1.6	1449	1473	1511	1546	1568	1570	1549	1507	1452	1395	1350
Markov - 1.8,2.0	1441	1399	1350	1300	1253	1211	1177	1149	1125	1102	1074
Vissim AV normal	1228	1236	1287	1355	1421	1473	1504	1517	1519	1525	1557

CAUTION - Enchanced IDM Model Valid for AV Penetration 0 to 60

Figure 48. Screenshot. SCAT – Phase Comparative Analysis – example Capacity Per AV Scenario section.

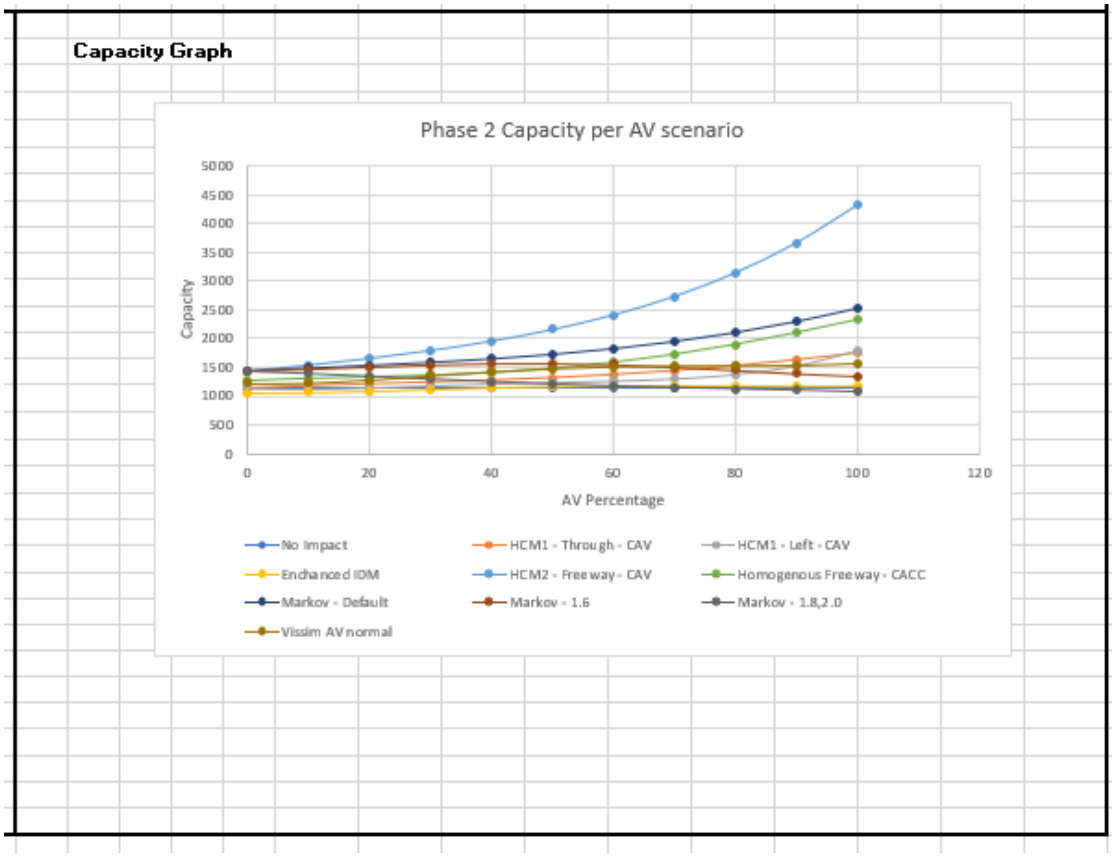

Figure 49. Screenshot. SCAT – Phase Comparative Analysis – example Capacity Graph section.

SUMMARY

This chapter presented a Simplified Capacity Analysis Tool for exploring the potential impact of various levels of CAV market penetration on signalized intersection capacity. As seen, SCAT is an Excel-based tool that provides capacity estimates for user-selected phase timings. To reflect the lack of a single accepted representative CAV technology model, SCAT—drawing on the literature and a simulation modeling effort—incorporates results from a selection of saturation flow models across CAV market penetration rates from 0 to 100 percent. The analyst may utilize SCAT to explore a range of potential futures and understand the sensitivity of current intersections, as well as future designs, to potential CAV operating characteristics.

To allow for a broader application, next steps in the development of SCAT should incorporate left-turn–permitted movements and shared lanes. Additionally, an ability for analysts to enter a given intersection volume set to be compared directly against model capacities should be added, automating the creation of volume-to-capacity ratios for the various models. Finally, as the development of CAV technology and traffic models is in constant flux, a frequent review and update of the selected models should be undertaken. As new models are developed based on additional field data, recent technology advances, changes in legislation related to required AV characteristics, etc., the addition of these to the SCAT saturation flow estimates will allow for an increasingly robust analysis.

CHAPTER 7. CONCLUSIONS AND RECOMMENDATIONS

Many studies support an optimistic outlook on the traffic-flow impacts of autonomous vehicles based on models that assume both AVs and human-driven vehicles express cooperative behaviors. However, these studies have not considered the impacts on traffic performance of potential aggressive interactions of HDVs with AVs in a mixed environment (i.e., AVs and HDVs). Concerns of such interactions occurring are not unwarranted as mobility service companies have observed aggressive human-driver behaviors directed at their AV test fleets, as well as the already existing aggressive behavior that may be observed at merge locations with heavy queuing.

To aid in understanding the potential impact of aggressive HDV with AV interactions, this effort has investigated a merging situation at an off-ramp. Three classes of vehicles are simulated: AVs, HDVs, and aggressive human-driven vehicles. AHDVs represent human-driven vehicles with aggressive merging-behavior characteristics. To perform this study, AHDV behavior at a merge section of a freeway exit ramp, in a mixed traffic environment, is simulated using the open-source traffic simulation package SUMO (Eclipse Foundation 2020). Two types of potential AHDV merging behavior when interacting with an AV are modeled: (1) aggressive merge with maximum advancement, and (2) aggressive merge with zipper. The aggressive merge with maximum advancement represents the highest level of aggressive behavior. The AHDVs with this behavior target the farthest reachable AV on the deceleration lane to act as the following vehicle in the receiving lane, i.e., the AHDV will lane change in front of the AV, essentially without regard for the available gap. In the second type, the aggressive merge with zipper, the

AHDVs continue to target downstream AVs in the exit lane, but avoid the scenario where the same AV is targeted by multiple AHDVs.

The impacts of the AHDVs' aggressive behaviors in a mixed-traffic environment (i.e., AVs, HDVs, and AHDVs) on different network traffic characteristics, such as travel time and capacity, is demonstrated. Four experiments are conducted to explore the impact of the AHDV behavior on traffic operations. The first experiment observes the change in speed of the target AV, as well as the following traffic, when a platoon of 10 AHDVs merges in front of the AV near a freeway exit. The second and third experiments observe the travel times of exiting AHDVs and other vehicles when AHDVs are randomly distributed throughout the traffic stream with varying percentages of AVs and AHDVs in the traffic composition. The fourth experiment considers the impact on capacity in a similar merging situation where vehicle behavior is set as cooperative or noncooperative utilizing SUMO driver-behavior parameters.

Experiments 1 through 3 showed that the presence of human drivers' aggressive merging behaviors had adverse effects on AVs and HDVs. The adverse effects were more significant in high congestion, when there is a queue on the deceleration lane. The impacts of AHDVs' aggressive merges were muted by the larger headways between vehicles in low congestion when there is no queue on the deceleration lane. Based on the experiment 2 and experiment 3 results, AHDVs had a higher travel time gain with higher level of aggressive behaviors, which in return had greater adverse effects on the AVs' and the HDVs' travel times. Throughout the experiments, the system-wide travel time tended to be relatively stable, indicating that the AHDV travel-time improvements came at the expense of AVs' and other vehicles' travel time.

Experiment 4 took a closer look at the impact of cooperative behavior–induced aggressive merges on capacity. It was seen that when most vehicles are either fully cooperative or noncooperative, similar capacities are obtained; however, where a higher percentage of cooperative vehicles are positioned to be targeted by more aggressive vehicles, this aggressive-to-non-aggressive interaction can significantly reduce capacity. In addition, it was seen that, similar to experiments 1 through 3, AHDV gains were achieved at the expense of AVs. Finally, even in those scenarios where the overall capacity was not significantly changed in response to the variation in the percentage of cooperative vehicles in the traffic, increased fluctuations in the flow may potentially negatively impact operations as well as the safety conditions in the upstream traffic.

As a final component of this research, an Excel-based Simplified Capacity Analysis Tool is developed. This tool draws predicted saturation flow rates, at various connected and autonomous vehicle market penetration rates, from the literature and a simulation experiment. These saturation flow rates are utilized to determine potential phase capacities at a signalized intersection. While the freeway SUMO experiments focused on the impact of lane changing, SCAT explores the impact of CAV car-following and platooning behaviors. It is seen that a wide variation in capacity predictions may be found throughout the literature, from slight reductions to significant increases in capacity as AV market penetration increases. Across the literature, when considering the car-following aspect of AV operations, it is clear that two key sets of assumptions are driving the predictions: the first is the headways selected by the AVs in a mixed traffic environment, and the second is the characteristic of AV platoons, i.e., platooned vehicle spacing and maximum platoon length.

The findings of this study suggest that despite the general beliefs in the benefits of autonomous vehicles, there may be adverse impacts on the non-aggressive vehicle travel times in the presence of human drivers' aggressive merging behaviors in a mixed-traffic environment, especially in congested conditions. Thus, when the potential benefits of the AV are most needed, i.e., at or near capacity, it is possible that human interaction may negate many of the potential savings.

RECOMMENDATIONS

Given the high state of uncertainty in AV driving-behavior characteristics and a similar level of uncertainty in the behavior of human-driven vehicles when interacting with AVs, it is extremely difficult to incorporate AVs into current planning and design processes with any sense of assuredness. In the near-term this uncertainty will likely only increase with the development of more AV models, countless future predictions, trial AV deployment successes and failures, etc. However, based on this project, GDOT can likely achieve an early sense of the ultimate operational impacts of AVs by tracking three primary leading indicators:

1. As AV tests continues, or low market penetration occurs, is a rise in aggressive interactions witnessed?
2. What are the headways being adopted by AV manufactures, and what are the potential regulatory requirements?
3. Are platoons implemented in AVs, and if so, what are the spacing requirements and maximum length restrictions, which are again potentially manufacturer and/or regulatory agency driven?

As the direction of each of these indicators becomes clearer, GDOT will be able to select the more likely futures from the many potential predicted futures, allowing AV penetration to begin to influence design and policy decisions in a more informed manner.

For example, if it is seen that human-driven vehicles begin to express aggressive interaction with AVs, then GDOT may need to revisit signal control at ramp junctions, where eliminating queueing on the freeway is a priority to minimize targeting opportunities. Additionally, design changes such as increasing use of delineator posts immediately upstream of the gore area may be required. Similarly, as platooning parameters clarify, signal control may be revisited, optimizing detection and control strategies to incorporate processing of maximum platoon lengths, that is, optimal control will minimize splitting platoons.

Lastly, this study did not address potential safety impacts that could arise from aggressive human-driven vehicle – AV interaction. Future efforts need to investigate potential safety impacts and begin to develop recommendations for design, operations, or policy mitigations.

APPENDIX A: OBSERVED HEADWAYS

PIB AT BERKELEY LAKE (33.985340, −84.171123)

Through Movement Headways

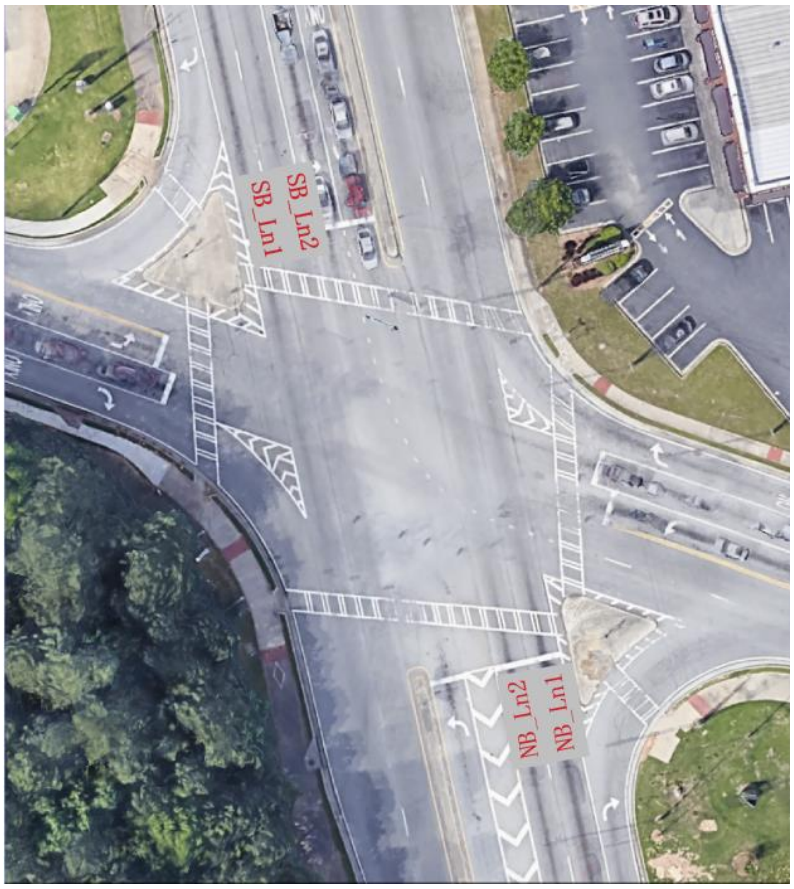

Figure 50. Map. Through movements – PIB at Berkeley Lake.
Source: Google Maps

Table 15. Through movement headway distribution – PIB at Berkeley Lake.

Movement	Lane	Gaussian Dist 1			Gaussian Dist 2		
		mu1	SD1	Weighting 1	mu2	SD2	Weighting 2
NB	Lane 1	1.976	0.576	0.811	3.469	1.525	0.189
	Lane 2	1.839	0.522	0.719	3.117	1.186	0.281
SB	Lane 1	2.088	0.675	0.832	4.781	1.858	0.168
	Lane 2	2.107	0.710	0.814	5.369	2.152	0.186

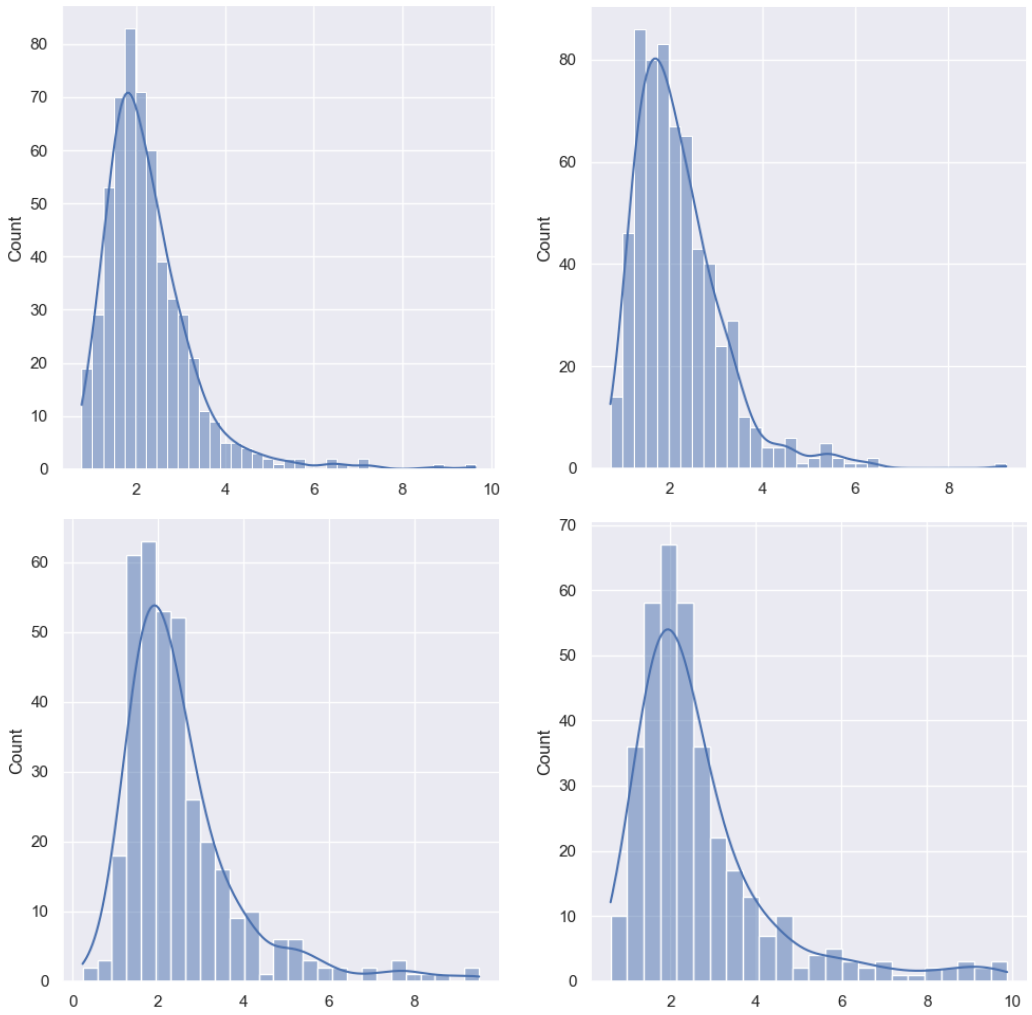

Figure 51. Plot. PIB at Berkeley Lake through movement headway data visualization (top left – NB Lane 1, top right – NB Lane 2, bottom left – SB Lane 1, bottom right – SB Lane 2).

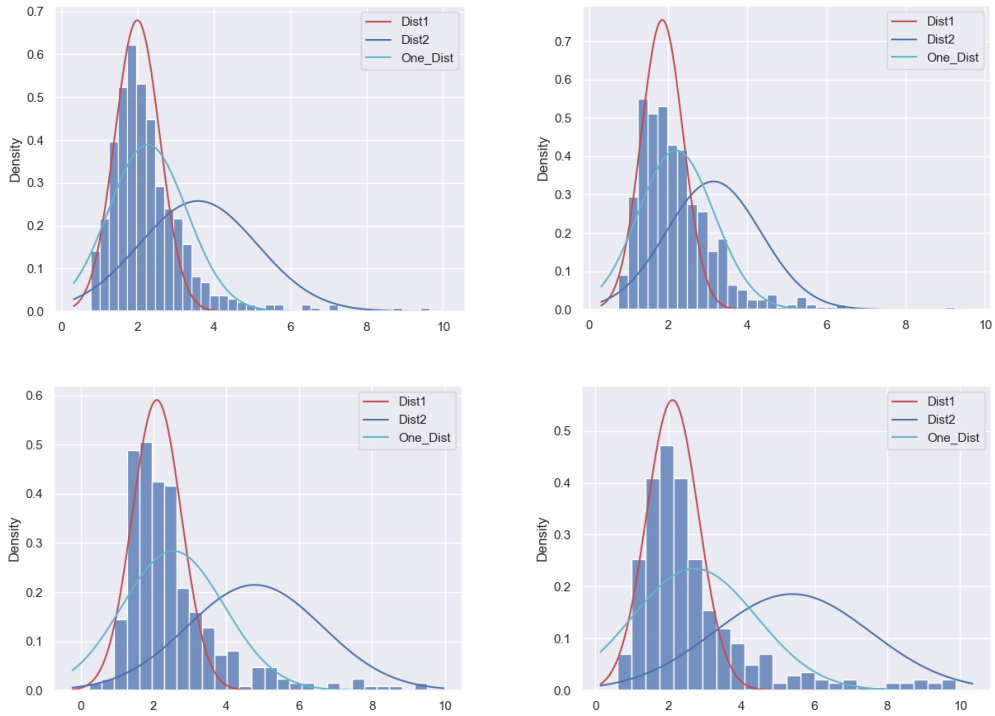

Figure 52**. Plot. PIB at Berkeley Lake through movement headway distribution (top left – NB Lane 1, top right – NB Lane 2, bottom left – SB Lane 1, bottom right – SB Lane 2).**

Left-turn Movement Headways

Figure 53**. Map. Left-turn movements – PIB at Berkeley Lake.**
Source: Google Maps

Table 16. Left-turn movement headway distribution – PIB at Berkeley Lake.

Movement	Lane	Gaussian Dist 1			Gaussian Dist 2		
		mu1	SD1	Weighting 1	mu2	SD2	Weighting 2
EBL	Lane 1	2.326	0.628	0.786	4.764	1.893	0.214
WBL	Lane 1	2.248	0.490	0.757	4.746	1.920	0.243
SBL	Lane 1	1.889	0.296	0.613	3.175	0.673	0.387
	Lane 2	1.907	0.394	0.607	2.838	0.554	0.393

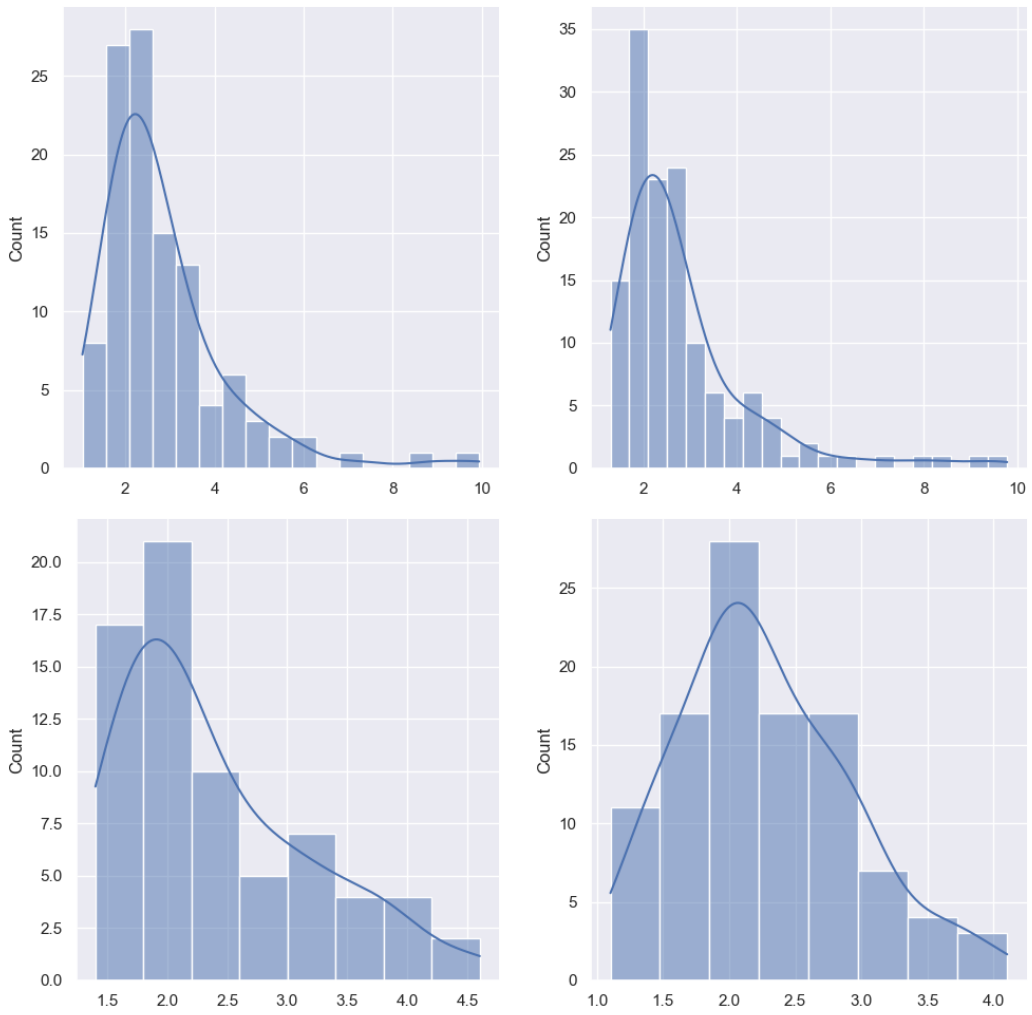

Figure 54**. Plot. PIB at Berkeley Lake left-turn movement headway visualization (top left – Eastbound Lane, top right – Westbound Lane, bottom left – SB Lane 1, bottom right – SB Lane 2).**

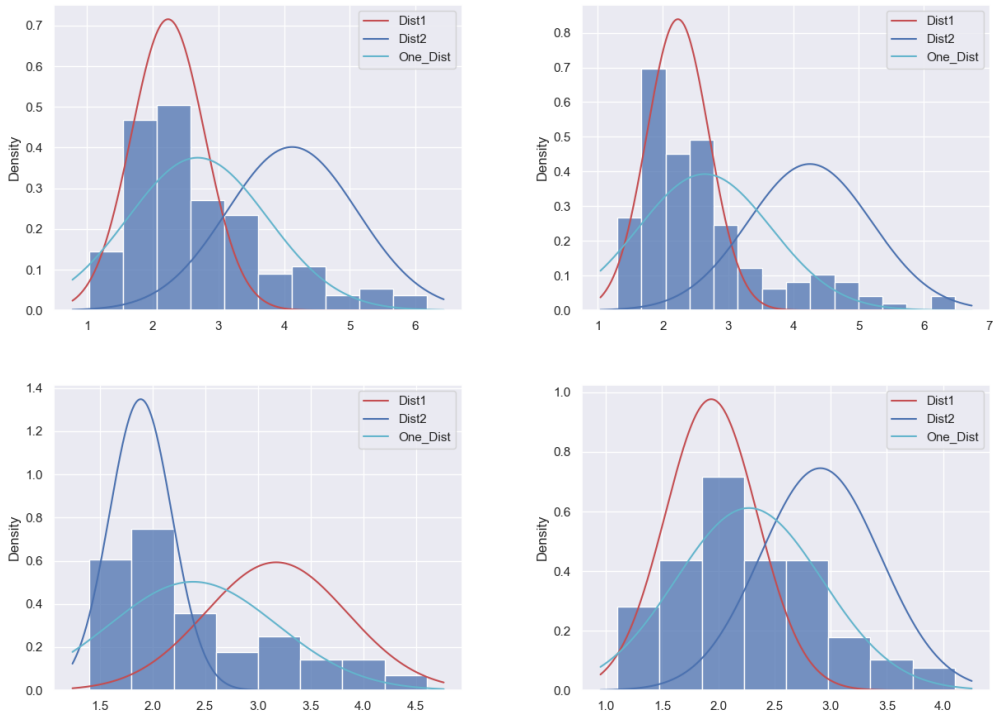

Figure 55**. Plot. PIB at Berkeley Lake left-turn movement headway distribution (top left – Eastbound Lane, top right – Westbound Lane, bottom left – SB Lane 1, bottom right – SB Lane 2).**

PIB AT MEDLOCK BRIDGE ROAD (33.961047, −84.208518)

Through Movement Headways

Figure 56**. Map. Through movement – PIB at Medlock Bridge Road.**
Source: Google MapTable 17. Through movement headway distribution – PIB at Medlock Bridge Road.

Movement	Lane	Gaussian Dist 1			Gaussian Dist 2		
		mu1	SD1	Weighting 1	mu2	SD2	Weighting 2
WB	Lane 1	2.281	0.758	0.712	5.087	1.873	0.288
	Lane 2	2.207	0.729	0.799	5.157	1.764	0.201
EB	Lane 1	2.205	0.672	0.754	4.746	1.811	0.246
	Lane 2	1.939	0.613	0.774	4.011	1.652	0.226

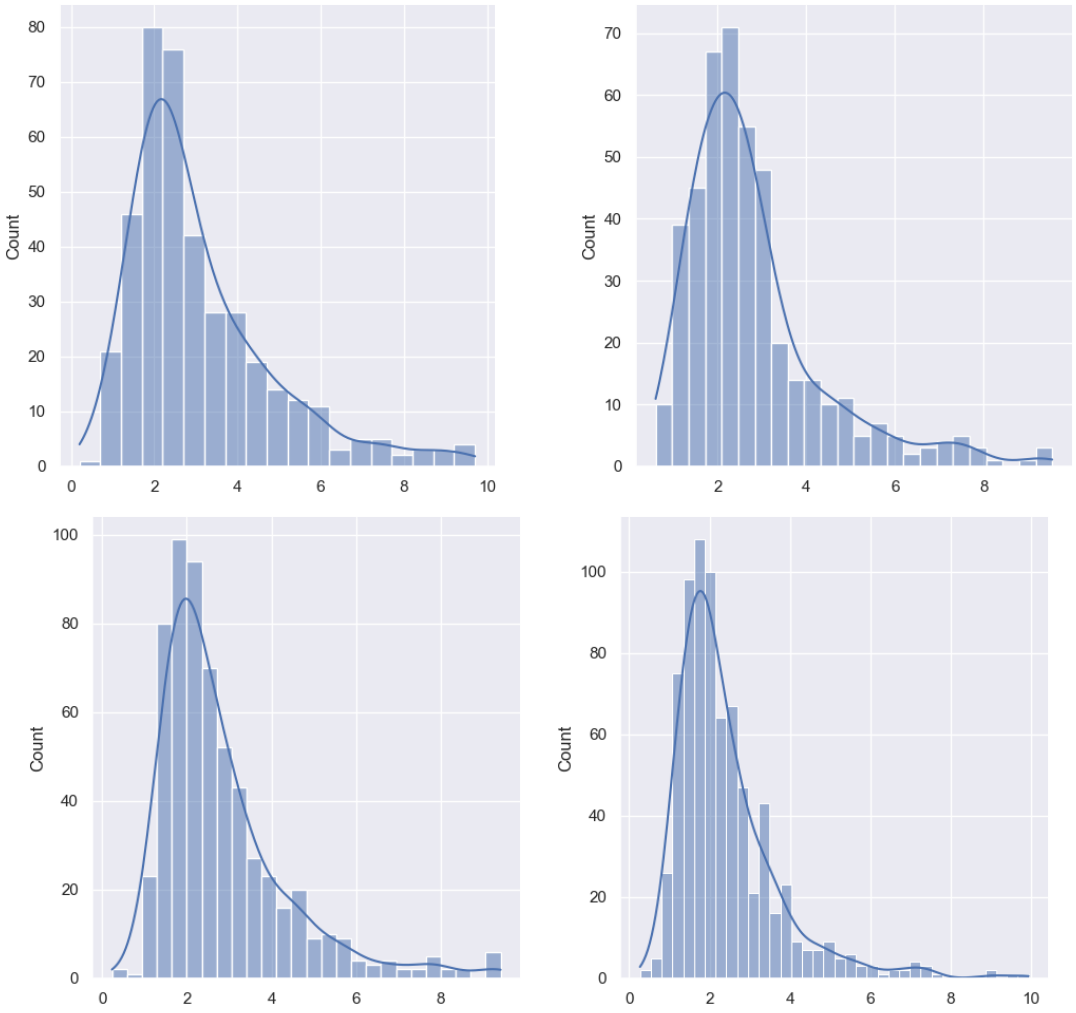

Figure 57**. Plot. PIB at Medlock Bridge Road through movement headway data visualization (top left – WB Lane 1, top right – WB Lane 2, bottom left – EB Lane 1, bottom right – EB Lane 2).**

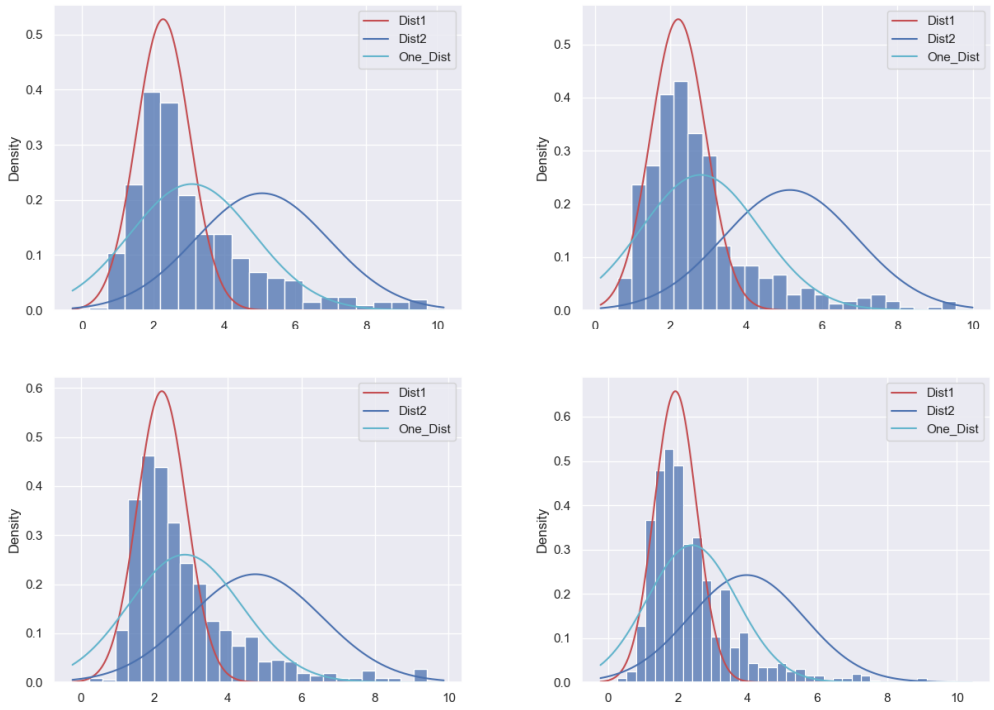

Figure 58**. Plot. PIB at Medlock Bridge Road through movement headway distribution (top left – WB Lane 1, top right – WB Lane 2, Bottom Left – EB Lane 1, bottom right – EB Lane 2).**

Left-turn Movement Headways

Figure 59. Map. Left-turn movement – PIB at Medlock Bridge Road.
Source: Google Maps

Table 18. Left-turn movement headway distribution – PIB at Medlock Bridge Road.

Movement	Lane	Gaussian Dist 1			Gaussian Dist 2		
		mu1	SD1	Weighting 1	mu2	SD2	Weighting 2
EBL	Lane 1	2.120	0.426	0.647	3.251	0.755	0.353
WBL	Lane 1	2.250	0.491	0.759	4.759	1.919	0.241

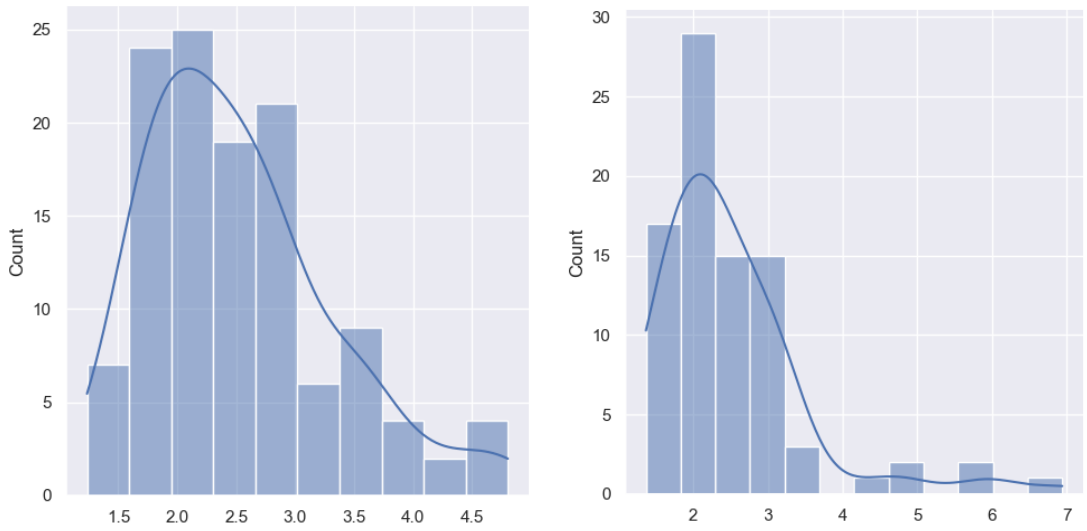

Figure 60. Plot. PIB at Medlock Bridge Road left-turn movement headway data visualization.

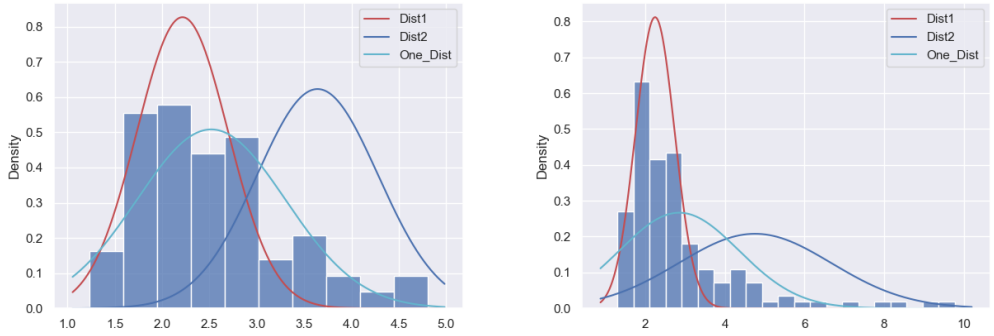

Figure 61**. Plot. PIB at Medlock Bridge Road left-turn movement headway distribution (left – EB lane, right – WB lane).**

APPENDIX B: SPEED – FLOW PLOTS FOR EXPERIMENT 4A AND 4B

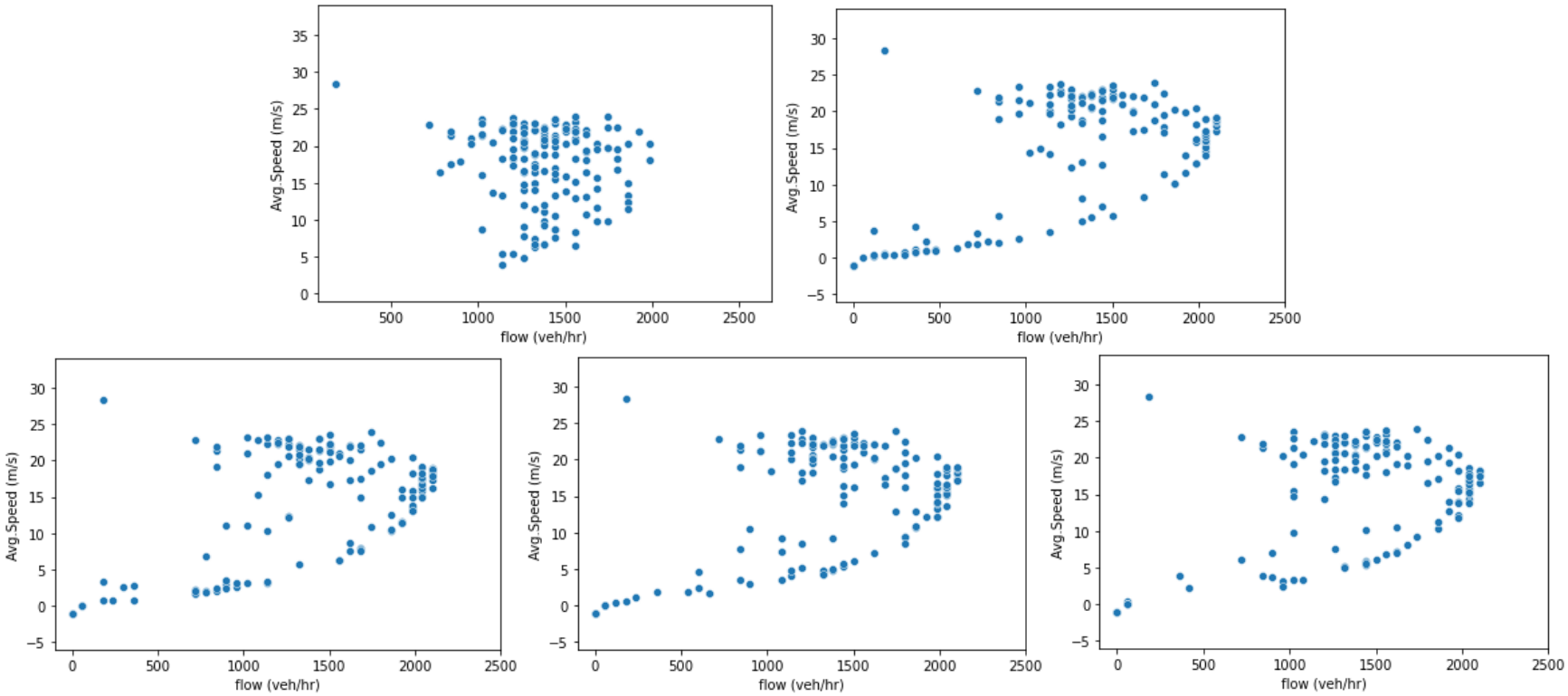

Figure 62. Plot. Speed vs. flow plots at 500 ft before the start of the deceleration lane in experiment 4a (top left – 0%, top right – 25%, bottom left – 50%, bottom middle – 75%, bottom right – 100%).

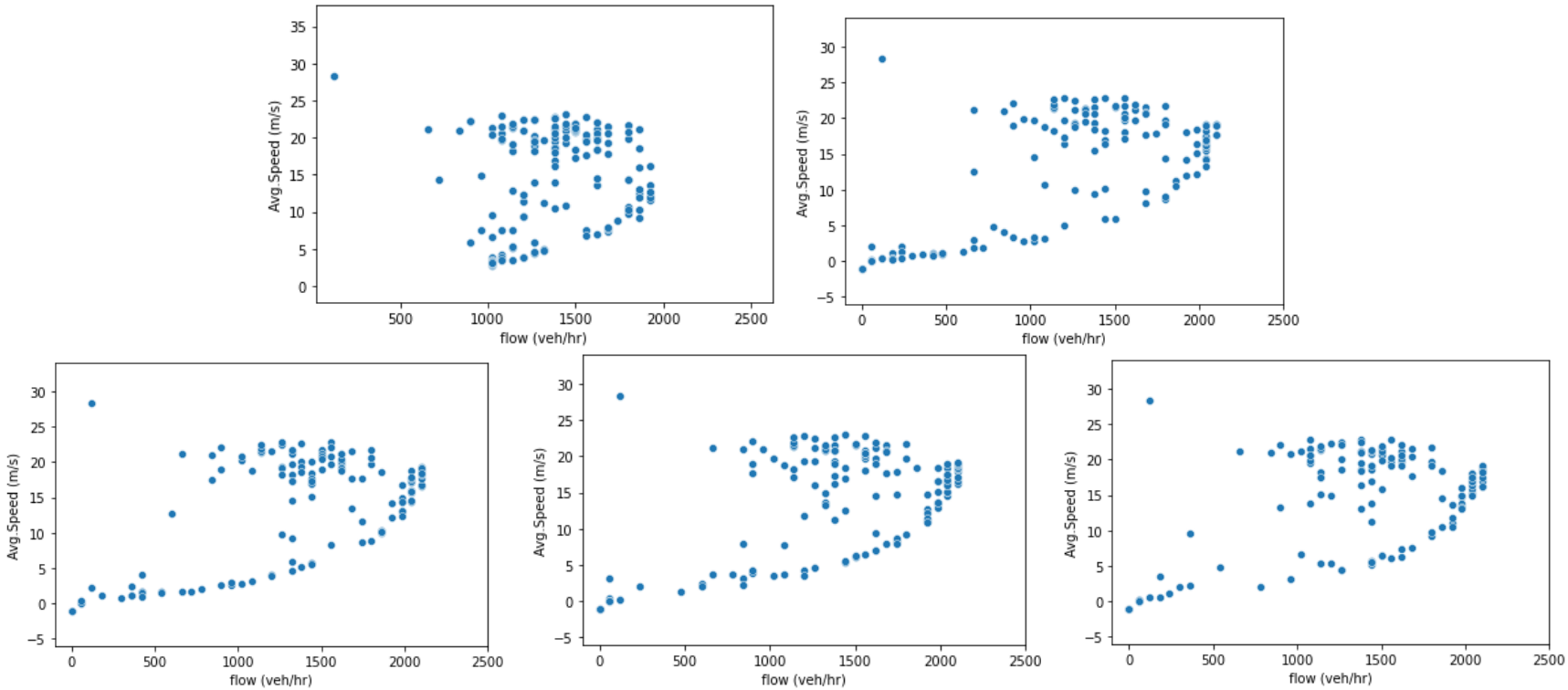

Figure 63. Plot. Speed vs. flow plots at the start of the deceleration lane in experiment 4a (top left – 0%, top right – 25%, bottom left – 50%, bottom middle – 75%, bottom right – 100%).

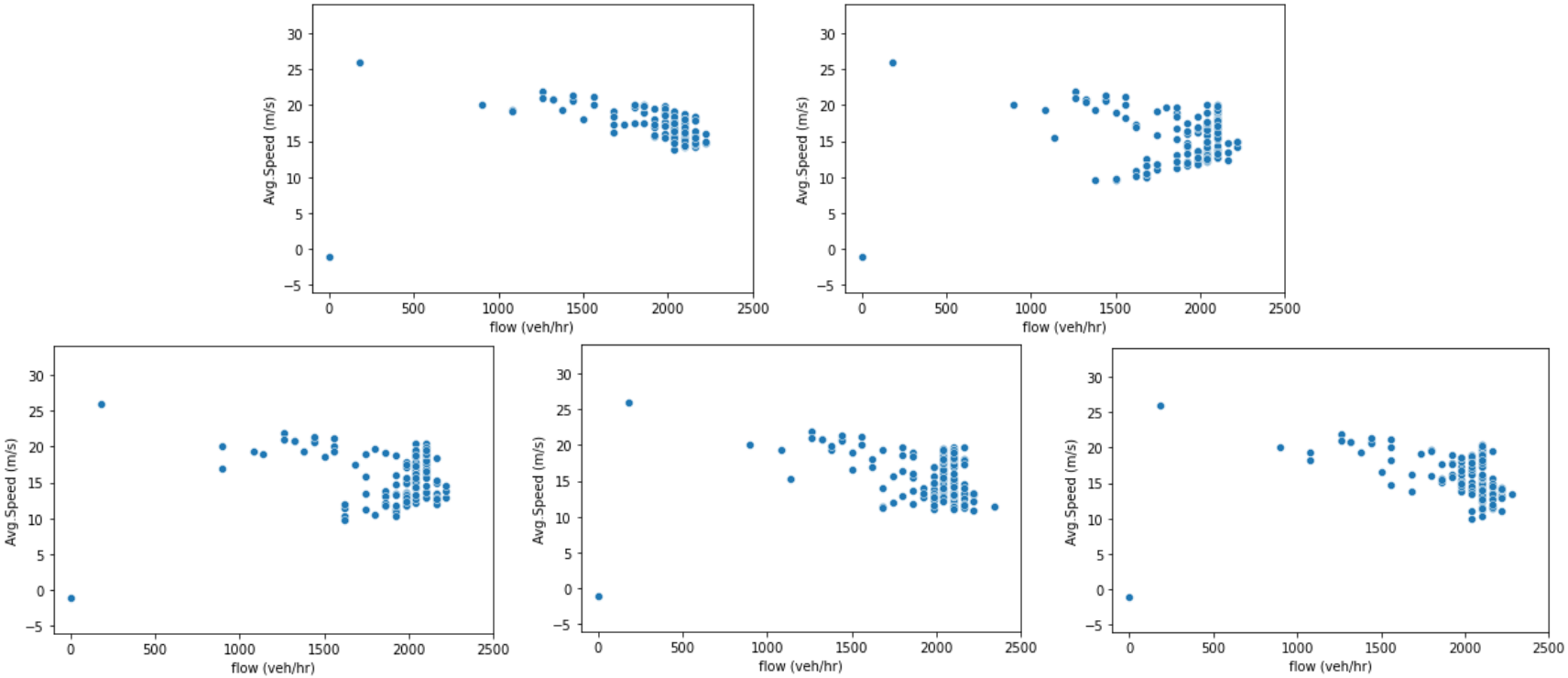

Figure 64. Plot. Speed vs. flow plots at the start of the ramp in experiment 4a (top left – 0%, top right – 25%, bottom left – 50%, bottom middle – 75%, bottom right – 100%).

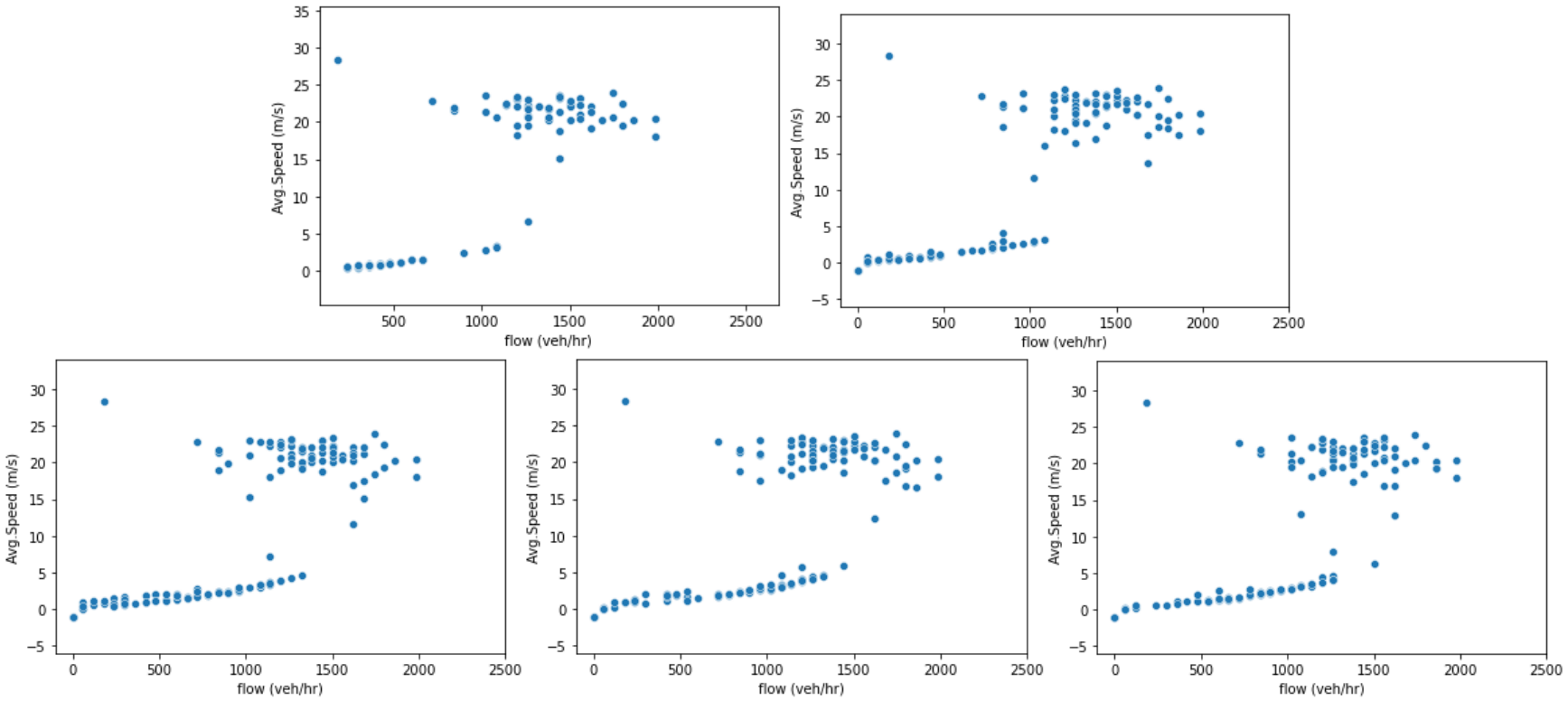

Figure 65. Plot. Speed vs. flow plots at 500 ft before the start of the deceleration lane in experiment 4b (top left – 0%, top right – 25%, bottom left – 50%, bottom middle – 75%, bottom right – 100%).

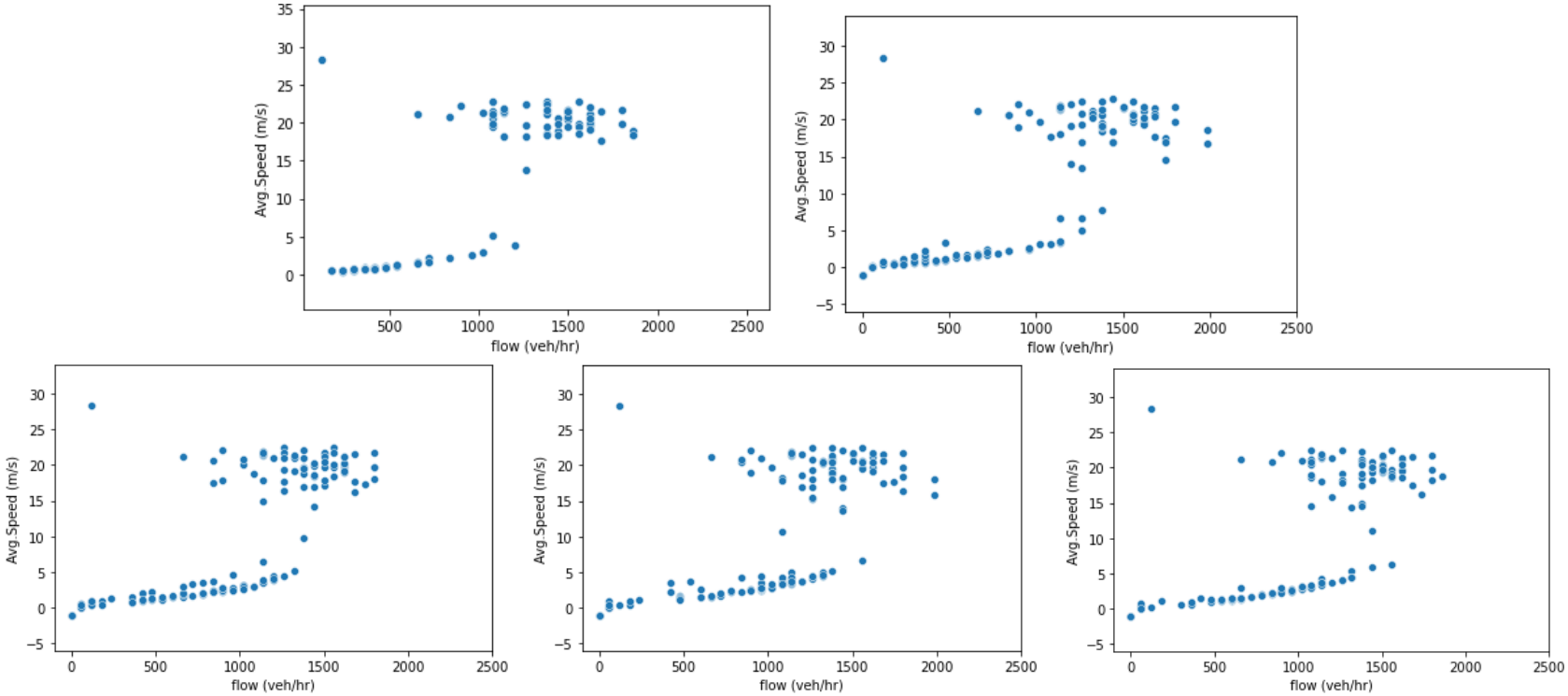

Figure 66. Plot. Speed vs. flow plots at the start of the deceleration lane in experiment 4b (top left – 0%, top right – 25%, bottom left – 50%, bottom middle – 75%, bottom right – 100%).

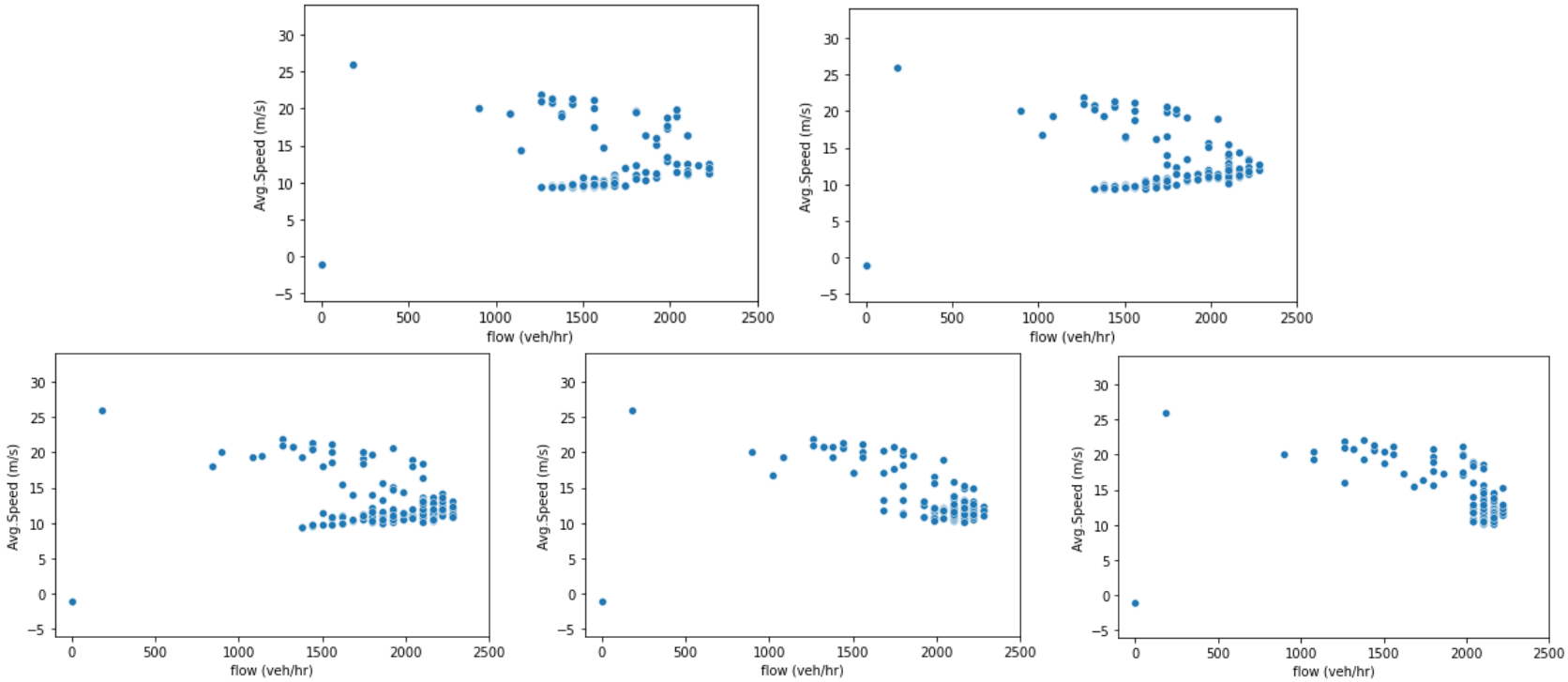

Figure 67. Plot. Speed vs. flow plots at the start of the ramp in experiment 4b (top left – 0%, top right – 25%, bottom left – 50%, bottom middle – 75%, bottom right – 100%).

ACKNOWLEDGMENTS

The information, data, or work presented herein was funded in part by the Georgia Department of Transportation in cooperation with U.S. Department of Transportation Federal Highway Administration as GDOT Research Project 18-23. The authors thank Mr. Alan Davis in the Office of Traffic Operations in GDOT for his support during the project. The views and opinions of the authors expressed herein do not necessarily state or reflect those of the State of Georgia or any agency thereof. This paper does not constitute a standard, specification, or regulation.

REFERENCES

Anagnostopoulos, A. and Kehagia, F. (2019). "CAVs and Roundabouts: Research on Traffic Impacts and Design Elements." 47th European Transport Conference, Dublin, Ireland, October 9–11. Available online: http://dx.doi.org/10.1016/j.trpro.2020.09.008.

Aria, E., Olstam, J., and Schwietering, C. (2016). "Investigation of Automated Vehicle Effects on Driver's Behavior and Traffic Performance." *Transportation Research Procedia, 15*, pp. 761–770. Available online: https://doi.org/10.1016/j.trpro.2016.06.063.

Atkins. (2016). *Research on the Impacts of Connected and Autonomous Vehicles (CAVs) on Traffic Flow: Stage 2: Traffic Modelling and Analysis: Technical Report*. Department for Transport, London, UK. Available online: https://assets.publishing.service.gov.uk/government/uploads/system/uploads/attachment_data/file/530093/impacts-of-connected-and-autonomous-vehicles-on-traffic-flow-technical-report.pdf.

CoEXist. (2021a). "'AV-Ready' Transport Models and Road Infrastructure for the Coexistence of Automated and Conventional Vehicles." CoEXist (website). https://ec.europa.eu/inea/en/horizon-2020/projects/h2020-transport/automated-road-transport/coexist, last accessed December 13, 2021.

CoEXist. (2021b). "Resources." CoEXist (website). Available online: https://www.h2020-coexist.eu/resources/, last accessed December 13, 2021.

DataFromSky. (2021a). "Data From Sky." (website). Czech Republic. Available online: https://datafromsky.com/, last accessed December 13, 2021.

DataFromSky. (2021b). "DataFromSky Viewer." (website). Czech Republic. Available online: https://datafromsky.com/news/datafromsky-viewer-new-version-new-features/, last accessed December 13, 2021.

Eclipse Foundation. (2020). "Simulation of Urban MObility." (website) Available online: https://www.eclipse.org/sumo/.

Elvarsson, A.B. (2017). "Modeling Urban Driving and Stopping Behavior for Automated Vehicles." Semester Project, IVT, ETH, Zürich, Switzerland.

Espinosa, M. (2015). *Safety Evaluation of Signalized Intersections with Automated Vehicles at Various Penetration Levels Based on Conflict Analysis of Simulated Traffic*. Master's thesis, Ryerson University, Toronto, Canada. Available online: https://doi.org/10.32920/ryerson.14652957.

Fernandes, P. and Nunes, U. (2010). “Platooning of Autonomous Vehicles with Intervehicle Communications in SUMO Traffic Simulator.” 13th International IEEE Conference on Intelligent Transportation Systems, Madeira Island, Portugal, September 19–22. Available online: http://dx.doi.org/10.1109/ITSC.2010.5625277.

General Motors. (2015). “General Motors Promotes DSRC for Connected Vehicle (V2X) Technology Development in China.” Corporate Newsroom, November 24. Available online: https://media.gm.com/media/cn/en/gm/news.detail.html/content/Pages/news/cn/en/2015/Nov/1124_v2x.html, last accessed January 10, 2020.

Ghiasi, A., Hussain, O., Qian, S., and Li, X. (2017). “A Mixed Traffic Capacity Analysis and Lane Management Model for Connected and Automated Vehicles: A Markov Chain Method.” *Transportation Research Part B: Methodological*, *106*, pp. 266–292. Available online: https://doi.org/10.1016/j.trb.2017.09.022.

Guo, J., Cheng, S., and Liu, Y. (2020). “Merging and Diverging Impact on Mixed Traffic of Regular and Autonomous Vehicles.” *IEEE Transactions on Intelligent Transportation Systems*, *22*(3), pp. 1639–1649. Available online: http://dx.doi.org/10.1109/TITS.2020.2974291.

Hamilton, I.A. (2019). “Uber Says People Are Bullying Its Self-Driving Cars with Rude Gestures and Road Rage.” *Business Insider*, June 13. Available online: https://www.businessinsider.com/uber-people-bullying-self-driving-cars-2019-6, last accessed January 10, 2020.

Hedlund, J. (2017). *Autonomous Vehicles Meet Human Drivers: Traffic Safety Issues for States*. Governors Highway Safety Association, Washington, DC. Available online: http://www.ghsa.org/sites/default/files/2017-01/AV%202017%20-%20FINAL.pdf.

Hua, X., Yu, W., Wang, W., and Xie, W. (2020). “Influence of Lane Policies on Freeway Traffic Mixed with Manual and Connected and Autonomous Vehicles.” *Journal of Advanced Transportation*, *2020*, [3968625]. Available online: https://doi.org/10.1155/2020/3968625.

Hunter, M. (2021). *Vissim 11 Simulation Guidance*. Final Report, FHWA-GA-11-1833, Georgia Department of Transportation, Atlanta, GA.

INRIA. (2021). “sklearn.mixture.GaussianMixture.” Scikit-learn. (website) Available online: https://scikit-learn.org/stable/modules/generated/sklearn.mixture.GaussianMixture.html, last accessed December 13, 2021.

Kapania, N.R., Govindarajan, V., Borrelli, F., and Gerdes, J.C. (2019). “A Hybrid Control Design for Autonomous Vehicles at Uncontrolled Intersections.” *2019 IEEE Intelligent Vehicles Symposium (IV)*, pp. 1604–1611. Available online: https://doi.org/10.1109/IVS.2019.8814116.

Kesting, A., Treiber, M., Helbing, D. (2010). “Enhanced Intelligent Driver Model to Access the Impact of Driving Strategies on Traffic Capacity.” *Philosophical Transactions of the Royal Society A*, *368*(1928), pp. 4585–4605. Available online: https://doi.org/10.1098/rsta.2010.0084.

Li, D. and Wagner, P. (2019). “Impacts of Gradual Automated Vehicle Penetration on Motorway Operation: A Comprehensive Evaluation.” *European Transport Research Review*, *11*(1), article 36. Available online: http://dx.doi.org/10.1186/s12544-019-0375-3.

Liu, P. and Fan, W. (2020). “Exploring the Impact of Connected and Autonomous Vehicles on Freeway Capacity Using a Revised Intelligent Driver Model.” *Transportation Planning and Technology*, *43*(3), pp. 279–292. Available online: https://doi.org/10.1080/03081060.2020.1735746.

Liu, Y., Guo, J., Taplin, J., and Wang, Y. (2017). “Characteristic Analysis of Mixed Traffic Flow of Regular and Autonomous Vehicles Using Cellular Automata.” *Journal of Advanced Transportation*, *2017*, [8142074]. Available online: https://doi.org/10.1155/2017/8142074.

Liu, H., Kan, X.D., Shladover, S.E., Lu, X.Y., and Ferlis, R.E. (2018a). “Impact of Cooperative Adaptive Cruise Control on Multilane Freeway Merge Capacity.” *Journal of Intelligent Transportation Systems*, *22*(3), pp. 263–275. Available online: http://dx.doi.org/10.1080/15472450.2018.1438275.

Liu, H., Kan, X.D., Shladover, S.E., Lu, X-Y., and Ferlis, R.E. (2018b). “Modeling Impacts of Cooperative Adaptive Cruise Control on Mixed Traffic Flow in Multi-Lane Freeway Facilities.” *Transportation Research Part C Emerging Technologies*, *95*(26), pp. 261–279. Available online: http://dx.doi.org/10.1016/j.trc.2018.07.027.

Lopez, P.A., Behrisch, M., Bieker-Walz, L., Erdmann, J., Flötteröd, Y.P., Hilbrich, R., Lücken, L., Rummel, J., Wagner, P., and Wiebner, E. (2018). “Microscopic Traffic Simulation Using SUMO.” *21st International Conference on Intelligent Transportation Systems (ITSC)*, Maui, HI, November 4–7. Available online: https://elib.dlr.de/127994/1/08569938.pdf.

Lu, Q., Tettamanti, T., Hörcher, D., and Varga, I. (2020). “The Impact of Autonomous Vehicles on Urban Traffic Network Capacity: An Experimental Analysis by Microscopic Traffic Simulation.” *Transportation Letters*, *12*(8), pp. 540–549. Available online: https://doi.org/10.1080/19427867.2019.1662561.

Lu, Q., Tettamanti, T., and Varga, I. (2018). “Impacts of Autonomous Vehicles on the Urban Fundamental Diagram.” 5th International Conference on Road and Rail Infrastructure, CETRA 2018, Zadar, Croatia, May 17–19. Available online: http://real.mtak.hu/id/eprint/83699.

Martin-Gasulla, M.P., Sukennik, P., and Lohmiller, J. (2019). “Investigation of the Impact on Throughput of Connected Autonomous Vehicles with Headway Based on the Leading Vehicle Type.” *Transportation Research Record: Journal of the Transportation Research Board*, *2673*(5), pp. 617–626. Available online: https://doi.org/10.1177%2F0361198119839989.

Mesionis, G., Brackstone, M., and Gravett, N. (2020). “Microscopic Modeling of the Effects of Autonomous Vehicles on Motorway Performance.” *Transportation Research Record: Journal of the Transportation Research Board*, *2674*(11), pp. 697–707. Available online: https://doi.org/10.1177%2F0361198120949243.

Milanes, V. and Shladover, S. (2014). “Modeling Cooperative and Autonomous Adaptive Cruise Control Dynamic Responses using Experimental Data.” *Transportation Research Part C: Emerging Technologies*, *48*, pp. 285–300. Available online: https://doi.org/10.1016/j.trc.2014.09.001.

Morando, M.M., Tian, Q., Truong, L.T., and Vu, H.L. (2018). “Studying the Safety Impact of Autonomous Vehicles Using Simulation-Based Surrogate Safety Measures.” *Journal of Advanced Transportation*, *2018*, [6135183]. Available online: https://doi.org/10.1155/2018/6135183.

Morando, M.M., Truong, L.T., and Vu, H.L. (2017). “Investigating Safety Impacts of Autonomous Vehicles Using Traffic Micro-simulation.” Australasian Transport Research Forum 2017, Auckland, New Zealand, November 27–29. Available online: https://www.australasiantransportresearchforum.org.au/papers/2017.

Müller, L., Risto, M., and Emmenegger, C. (2016). “The Social Behavior of Autonomous Vehicles.” *UbiComp ’16: Proceedings of the 2016 ACM International Joint Conference on Pervasive and Ubiquitous Computing: Adjunct*, *September*, pp. 686–689. Available online: https://doi.org/10.1145/2968219.2968561.

National Academies of Sciences, Engineering, and Medicine. (2017). *Strategies to Advance Automated and Connected Vehicles*. The National Academies Press, Washington, DC. Available online: https://doi.org/10.17226/24873.

National Highway Traffic Safety Administration (NHTSA). (2017). *Automated Driving Systems 2.0: A Vision for Safety*. DOT HS 812 442, U.S. Department of Transportation, Washington, DC. Available online: https://www.nhtsa.gov/sites/nhtsa.gov/files/documents/13069a-ads2.0_090617_v9a_tag.pdf.

Nishimura, Y., Fujita, A., Hiromori, A., Yamaguchi, H., Higashino, T., Suwa, A., Urayama, H., Takeshima, S., and Takai, M. (2019). "A Study on Behavior of Autonomous Vehicles Cooperating with Manually-Driven Vehicles." 2019 IEEE International Conference on Pervasive Computing and Communications (PerCom), Kyoyo, Japan, March 12–14. Available online: http://sig-iss.work/percom2019/papers/p212-nishimura.pdf.

NumPy Steering Council. (2021). "NumPy." (website) Available online: https://numpy.org/, last accessed December 13, 2021.

NumFOCUS. (2021). "pandas." (website) Available online: https://pandas.pydata.org/, last accessed December 13, 2021.

Papadoulis, A., Quddus, M., and Imprialou, M. (2019). "Evaluating the Safety Impact of Connected and Autonomous Vehicles on Motorways." *Accident Analysis & Prevention*, *124*, pp. 12–22. Available online: https://doi.org/10.1016/j.aap.2018.12.019.

PTV Group. (2021). "PTV Vissim." (website) Available online: https://www.ptvgroup.com/en/solutions/products/ptv-vissim/, last accessed December 13, 2021.

Rahman, M.S. and Abdel-Aty, M. (2018). "Longitudinal Safety Evaluation of Connected Vehicles' Platooning on Expressways." *Accident Analysis & Prevention*, *117*, pp. 381–391. Available online: https://doi.org/10.1016/j.aap.2017.12.012.

Randazzo, R. (2018). "A Slashed Tire, a Pointed Gun, Bullies on the Road: Why Do Waymo Self-Driving Cars Get So Much Hate?" *USA Today*, December 13. Available online: https://www.usatoday.com/story/money/cars/2018/12/13/waymo-self-driving-vehicles-face-harassment-road-rage-phoenix-area/2288833002/, last accessed January 10, 2020.

Richter, G., Grohmann, L., Nitsche, P., and Lenz, G. (2019). “Anticipating Automated Vehicle Presence and the Effects on Interactions with Conventional Traffic and Infrastructure.” SUMO User Conference 2019, *EPiC Series in Computing*, *62*, pp. 230–243. Available online: http://dx.doi.org/10.29007/s6m7.

Rothenbucher, D., Li, J., Sirkin, D., Mok, B., and Ju, W. (2016). “Ghost Driver: A Field Study Investigating the Interaction Between Pedestrians and Driverless Vehicles.” 25th IEEE International Symposium on Robot and Human Interactive Communication (RO-MAN), New York, NY, August 26–31, pp. 795–802. Available online: https://doi.org/10.1109/ROMAN.2016.7745210.

Schroeder, B., Morgan, A., Ryus, P., Cesme, B., Bibeka, A., Rodegerts, L., and, Ma, J. (2021). *Capacity Adjustment Factors for Connected and Automated Vehicles in the Highway Capacity Manual*. Draft Phase 1 Report, Pooled Fund Study, Contract #B35967, Oregon DOT, Salem, OR.

Adebisi, A., Guo, Y., Schroeder, B., Ma, J., Cesme, B., Bibeka, A., and Morgan, A. (2021). “*Highway Capacity Manual* Capacity Adjustment Factor Development for Connected and Automated Traffic at Signalized Intersections.” *Journal of Transportation Engineering, Part A: Systems*, *148*(3). Available online: https://doi.org/10.1061/JTEPBS.0000631.

Schwarting, W., Alonso-Mora, J., and Rus, D. (2018). “Planning and Decision-Making for Autonomous Vehicles.” *Annual Review of Control, Robotics, and Autonomous Systems*, *1*, pp. 187–210. Available online: https://doi.org/10.1146/annurev-control-060117-105157.

Seth, D., Cummings, M.L., and Li, S. (2019). “Traffic Efficiency and Safety Impacts of Autonomous Vehicle Aggressiveness.” 99th Annual Transportation Research Board Conference.

Li, S., Seth, D., and Cummings, M.L. (2020). “Traffic Efficiency and Safety Impacts of Autonomous Vehicle Aggressiveness.” 99th Annual Transportation Research Board Meeting, Washington, DC, January. Available online: https://hal.pratt.duke.edu/sites/hal.pratt.duke.edu/files/u36/AV%20Aggressiveness%20TRB%20Paper%20final.pdf.

Shi, L. and Prevedouros, P. (2016). “Autonomous and Connected Cars: HCM Estimates for Freeways with Various Market Penetration Rates.” *Transportation Research Procedia*, *15*, pp. 389–402. Available online: https://doi.org/10.1016/j.trpro.2016.06.033.

Stanek, D., Huang, E., Milam, R.T., and Wang, Y. (2017). "Measuring Autonomous Vehicle Impacts on Congested Networks Using Simulation." *Transportation Research Board 97th Annual Meeting*, Washington, DC, January 7–11.

Sukennik, P. (2018). *Micro-simulation Guide for Automated Vehicles*. Deliverable 2.5 of CoEXist project, October. Available online: https://www.h2020-coexist.eu/wp-content/uploads/2018/11/D2.5-Micro-simulation-guide-for-automated-vehicles.pdf.

Sukennik, P. and Kautzsch, L. (2018). *Default Behavioral Parameter Sets for Automated Vehicles (AVs)*. Deliverable 2.5 of CoEXist project, February. Available online: https://www.h2020-coexist.eu/wp-content/uploads/2018/10/D2.3-default-behavioural-parameter-sets_final.pdf.

Sukennik, P., Lohmiller, J., and Schlaich, J. (2018). "Simulation-Based Forecasting the Impacts of Autonomous Driving." International Symposium of Transport Simulation (ISTS'18) and the International Workshop on Traffic Data Collection and its Standardization (IWTDCS'18), *Transportation Research Procedia*, Elsevier, Amsterdam, The Netherlands.

Tennant, C., Howard, S., Franks, B., and Bauer, M.W. (2016). *Autonomous Vehicles – Negotiating a Place on the Road: A Study on How Drivers Feel about Interacting with Autonomous Vehicles on the Road*. LSE Consulting, London School of Economics and Political Science, City University of London, UK. Executive summary available online: https://www.lse.ac.uk/business/consulting/assets/documents/autonomous-vehicles-executive-summary.pdf.

Tian, R., Li, S., Kolmanovsky, I., Girard, A., and Yildiz, Y. (2018). "Adaptive Game-Theoretic Decision Making for Autonomous Vehicle Control at Roundabouts." *IEEE Conference on Decision and Control (CDC), 2018*, pp. 321–326. Available online: http://dx.doi.org/10.1109/CDC.2018.8619275.

Tiblijaš, D.A., Giuffrè, T., Surdonja, S., and Trubia, S. (2018). "Introduction of Autonomous Vehicles: Roundabouts Design and Safety Performance Evaluation." *Sustainability*, *10*(4), 1060. Available online: http://dx.doi.org/10.3390/su10041060.

Tomás, R.F., Fernandes, P., Macedo, E., Bandeira, J.M., and Coelho, M.C. (2019). "Assessing the Emission Impacts of Autonomous Vehicles on Metropolitan Freeways." *Transportation Research Procedia*, *47*, pp. 617–624. Available online: https://doi.org/10.1016/j.trpro.2020.03.139.

Treiber, M., Hennecke, A., and Helbing, D. (2000). “Congested Traffic States in Empirical Observations and Microscopic Simulations.” *Physical Review E, 62*(2), pp. 1805–1824. Available online: https://arxiv.org/ct?url=https%3A%2F%2Fdx.doi.org%2F10.1103%2FPhysRevE.62.1805&v=cfae6527.

Wagner, P. (2016). “Traffic Control and Traffic Management in a Transportation System with Autonomous Vehicles.” In: Maurer, M., Gerdes, J., Lenz, B., Winner, H. (eds) *Autonomous Driving*, Springer, Berlin, Heidelberg. Available online: http://dx.doi.org/10.1007/978-3-662-48847-8_15.

Wang, Y. and Wang, L. (2017). “Autonomous Vehicles’ Performance on Single Lane Road: A Simulation under VISSIM Environment.” 10th International Congress on Image and Signal Processing, BioMedical Engineering and Informatics (CISP-BMEI), October 14–16. Available online: https://doi.org/10.1109/CISP-BMEI.2017.8302162.

Wei, J., Dolan, J.M., and Litkouhi, B. (2013). “Autonomous Vehicle Social Behavior for Highway Entrance Ramp Management.” *2013 IEEE Intelligent Vehicles Symposium (IV)*, pp. 201–207. Available online: http://dx.doi.org/10.1109/IVS.2013.6629471.

Xu, S. (2021). “How to Use Python to Separate Two Gaussian Curves?” stack overflow, https://stackoverflow.com/questions/51318981/how-to-use-python-to-separate-two-gaussian-curves, last accessed December 13, 2021.

Yeo, H., Skabardonis, A., Halkias, J., Colyar, J., and Alexiadis, V. (2008). “Oversaturated Freeway Flow Algorithm for Use in Next Generation Simulation.” *Transportation Research Record: Journal of the Transportation Research Board, 2088*(1), pp 68–79. Available online: http://dx.doi.org/10.3141/2088-08.

Yu, H., Tak, S., Park, M., and Yeo, H. (2019). “Impact of Autonomous-Vehicle-Only Lanes in Mixed Traffic Conditions.” *Transportation Research Record: Journal of the Transportation Research Board, 2673*(9), pp. 430–439. Available online: https://doi.org/10.1177%2F0361198119847475.

Zhao, C., Wang, W., Li, S., and Gong, J. (2019). “Influence of Cut-In Maneuvers for an Autonomous Car on Surrounding Drivers: Experiment and Analysis.” *IEEE Transactions on Intelligent Transportation Systems, 21*(6), pp. 2266–2276. Available online: http://dx.doi.org/10.1109/TITS.2019.2914795.

Zheng, Y., Ran, B., Qu, X., and Zhang, J. (2019). “Cooperative Lane Changing Strategies to Improve Traffic Operation and Safety Nearby Freeway Off-Ramps in a Connected and Automated Vehicles Environment.” *IEEE Transactions on Intelligent Transportation Systems*, *21*(11), pp. 4605–4614. Available online: http://dx.doi.org/10.1109/TITS.2019.2942050.

Zhou, M., Qu, X., and Jin, S. (2017). “On the Impact of Cooperative Autonomous Vehicles in Improving Freeway Merging: A Modified Intelligent Driver Model-Based Approach.” *IEEE Transactions on Intelligent Transportation Systems*, *18*(6), pp. 1422–1428. Available online: https://doi.org/10.1109/TITS.2016.2606492.